

SFU

UAV Launch System

Final Project Report

Project Group: #3

GROUP MEMBERS:

Erich Deetlefs – Team Lead / Project Manager / Mechanical Engineer

Jakob Kryworuchko – Project Manager / Mechanical Engineer

Prashant Kumar – Stress Analysis Engineer / Materials Engineer



Table of Contents

<i>Table of Contents</i>	<i>i</i>
<i>Table of Figures</i>	<i>iii</i>
<i>Table of Tables</i>	<i>v</i>
I. Introduction	1
Background.....	1
Problem statement	1
Design Objectives.....	1
Design Procedure	1
II. Design Analysis	3
Calculations.....	3
Basic System Kinematics	3
Cradle Stopper	5
Hand Crank Assembly	6
Shaft Design	7
Model	12
Cradle.....	12
Rail	16
Stopper	17
Gearbox	17
Parts.....	19
Bearing.....	19
O-Ring	19
C-Ring.....	19
Draw Latch	19
Quick Release Pin.....	20
Bungee	20
Materials.....	21
Main Structural Material	21
Collision Damper Material	22
Simulations	23
Calculation Comparison: Hand Crank Assembly - Gear and Shaft Design	23
Quick Release Pin Mechanism.....	26
Bottom Elastic Connection	27
End Plate.....	29
III. Final Design Evaluation	31
Design Evaluation.....	31
Cost Evaluation	32
IV. Conclusion	33

V. References	34
VI. Appendix	36
Appendix A: Hand calculations.....	36
Appendix B: Engineering drawings	40
Appendix C: Nickel-chromium alloy - Data Sheet	67
Appendix D: Fluorosilicone - Data Sheet	71
Appendix E: Bill of Materials	80

Table of Figures

Figure 1: Gantt Chart	3
Figure 2: Free body diagram of entire assembly	5
Figure 3: Crank Shaft – horizontal moment and shear force diagrams	8
Figure 4: Crank Shaft - vertical moment and shear force diagrams	8
Figure 5: Intermediate Shaft – horizontal moment and shear force diagrams	10
Figure 6: Intermediate Shaft - vertical moment and shear force diagrams	10
Figure 7: Spool Shaft – horizontal moment and shear force diagrams	11
Figure 8: Spool Shaft – vertical moment and shear force diagrams	11
Figure 9: UAV cradle V1.0	13
Figure 10: UAV cradle V2.0	14
Figure 11: Stress Simulations of the UAV cradle version 2.0	15
Figure 12: UAV cradle V3.0	16
Figure 13: Gym weight stack rubber cushion	17
Figure 14: Gear schematic	18
Figure 15: Granta EduPack structural material results	22
Figure 16: Granta EduPack collision damper material results	23
Figure 17: Hand crack assembly - top view	24
Figure 18: Hand crack assembly maximum stress concentration	24
Figure 19: Hand crack assembly spool shaft - maximum stress concentration	25
Figure 20: Hand crack assembly - isometric view	25
Figure 21: Quick release mechanism - isometric view	26
Figure 22: Quick release mechanism - top view	27
Figure 23: Quick release pin - back isometric view	27
Figure 24: Bottom elastic connector - isometric view	28
Figure 25: Bottom elastic connector - front view	28
Figure 26: Bottom elastic connector high stress concentrations -isometric view	29
Figure 27: Endplate side peg geometry - side view	30
Figure 28: Endplate greatest stress concentrations – isometric view	30
Figure 29: Endplate fixed geometry – front view	31
Figure 30: Final assembly	40
Figure 31: Exploded view final assembly	41
Figure 32: Hand crack	42
Figure 33: Cradle impact stopper	43
Figure 34: Endplate	44

Figure 35: Cradle Barrier	45
Figure 36: Bearing holders for cradle	46
Figure 37: Bottom rail bungee connection	47
Figure 38: Bungee connection for cradle	48
Figure 39: Bearing holders for cradle	49
Figure 40: Center body for cradle	50
Figure 41: Combo gear	51
Figure 42: Cradle impact stopper	52
Figure 43: UAV cradle	53
Figure 44: Input gear	54
Figure 45: Lower tripod section	55
Figure 46: Rail	56
Figure 47: Rail winch connection	57
Figure 48: Rear tripod stand	58
Figure 49: Side bracket for cradle	59
Figure 50: Spool holder	60
Figure 51: Stand plate	61
Figure 52: UAV holder for cradle	62
Figure 53: UAV holder for cradle	63
Figure 54: Winch handle	64
Figure 55: Winch plate	65
Figure 56: Wire spool	66

Table of Tables

Table 1: Project Design Phases	2
Table 2: Project evaluation criteria and goals.....	32
Table 3: Bill of Materials	32

I. Introduction

Background

The project outlined in this report involves the research, design, and optimization of a system to launch a UAV into the air, for use in remote areas where the use of a runway may not be possible. This system will allow for UAVs to carry heavier loads further distances with the same sized batteries since none of the UAVs battery capacity will go towards the energy-intensive process of achieving takeoff velocity. UAVs, like all other aircrafts, require a minimum controllable airspeed before they can take off. One benefit of UAVs, however, due to their lightweight construction, is that they can reach these takeoff speeds in just a few seconds with the use of a launching system. There are many different methods for a launcher to achieve this, such as bungee assisted slides, pneumatic propulsion, or a belt driven system. However, when considering the design of such a system, additional materials to drive these methods should be considered. For example, with a pneumatic and even a hydraulic launcher, a compressor is required to pressurize the gas and a power supply is required to power that compressor. This adds additional weight to the system, reducing portability and ease of use in remote areas, and should be considered in the design process. To build this system, a variety of goals have been set which would match up with existing systems. These include the ability to launch a variety of UAV systems. For this project, we will be using specifications from the following UAVs: the Skywalker X8, and the ScanEagle 3.

Problem statement

The increased use of Unmanned Aerial Vehicles (UAV's) in many industries, such as military, agriculture, Search and Rescue, and even product deliveries in recent times has called for ways to help UAVs perform their duty more effectively, the target of this project is to successfully design an Unmanned Aerial Vehicle (UAV) Launch System, with the aim of propelling a UAV into flight with the necessary launch velocity, departure angle, and associated design parameters. The system is to be designed using an elastic bungee propulsion mechanism to accelerate the UAV into flight. The final design should be transportable by no more than three personnel.

Design Objectives

- Goal 1: Design a launch system to send a UAV into flight with appropriate launch velocity, and at an optimal departure angle
- Goal 2: Design a cradle to hold a variety of UAV systems such as a Skywalker X8 or a ScanEagle 3 and release it at the correct angle without causing any damage to the propelled object
- Goal 3: Stop cradle without causing damage, extending lifecycle as long as possible and reducing chances of fatigue failure over time
- Goal 4: Minimize the size and weight of the launch system to make it easily transportable

Design Procedure

The Design Procedure of the UAV Launch System was broken up into four phases: Research, Prototype, Simulation and Optimization, Documentation. These phases allowed us to pay attention to fundamental prerequisites of the project and avoid having to backtrack later.

Phase	Description	Dates
Research	The focus of this phase is to research the real-world applications of the UAV launch system. We will also be compiling several parameters of interest to best complete the next phase.	Start: Sept. 25, 2021 End: Oct. 12, 2021
Prototype	This phase of the project is in prototyping. Using information gathered in phase one, the initial design for the UAV Launch System is put together. Following design objectives, this phase allows us to get an initial idea of what the final product will look like.	Start: Oct. 13, 2021 End: Nov. 11, 2021
Simulation and Optimization	This next and arguably the most important phase of our project is where the design created in the previous phase is further refined into its final form. Through various FEA studies and simulations, we can assure our design will be sufficient to withstand all loading cases it will be subject to in its use.	Start: Nov. 12, 2021 End: Nov. 27, 2021
Documentation	The last phase of our design project is documentation. This will include putting together all the deliverables for the project so that it is ready to be presented.	Start: Nov. 28, 2021 End: Dec. 05, 2021

Table 1: Project Design Phases

Thanks to the rigorous simulation and optimization phase we undertook after the initial prototyping phase, we were able to find a flaw in our initial design. The motor and belt system are far too large and heavy for use in a portable format. To achieve the necessary launch velocity to propel the UAV into flight, the motor would have had to produce 30 kilowatts, which would require more external components than initially expected. Therefore, to achieve all our initial design objectives we have pivoted our design to use an elastic bungee propulsion system to propel the UAV into flight, with a crank system to retract the cradle. Another benefit of our phase-based approach to this design project was leaving some buffer period between the end of our timeline and the submission dates for the final deliverables. Additional setbacks occurred due to licensing issues with Solidworks, which saw only one of our group members able to finish the design and simulation work. This pre-scheduled buffer time allowed the team to pull together and adapt to unforeseen circumstances and still deliver on our objectives.

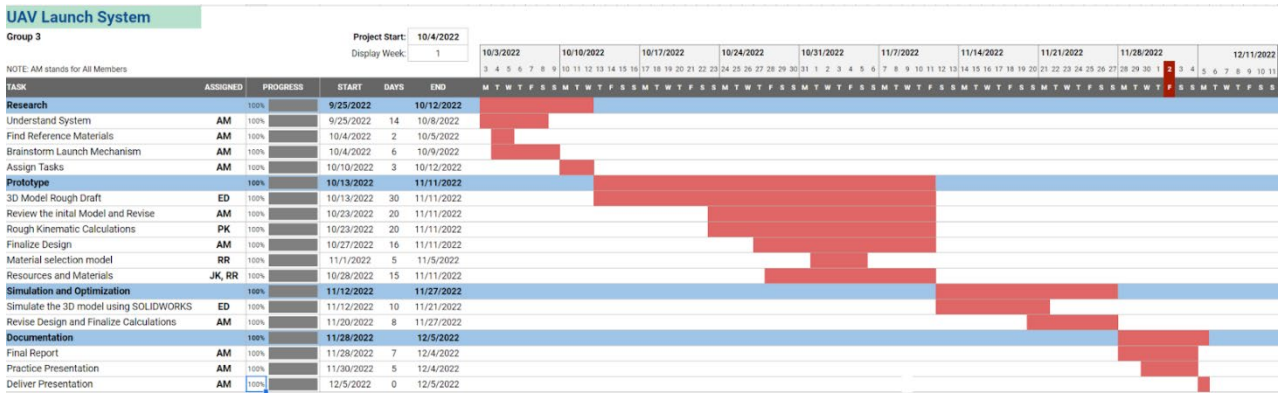


Figure 1: Gantt Chart

II. Design Analysis

Calculations

Here we will be laying out the important parameters of interests and hand calculations conducted on them. This will ensure the final project meets our design objectives and most importantly is able to perform its task of propelling a UAV into flight. Full hand calculations are available in the appendix.

From our research, we have concluded that the ideal launch angle will be designed to be about 30 degrees. This will provide enough total momentum to the UAV to successfully launch it and also have enough upwards velocity to continue climbing, without it being too steep such that a stall may occur. This also provides a sufficient initial launch angle such that there will be less space needed in front of the launcher for the UAV to have to “pull up” and climb after being released from the launcher.

From our originally proposed goals, we want the launcher to be able to launch an approximately 25 kg UAV at a velocity of 20 m/s or more in order to surpass our project goals. However, through our research phase, we have concluded that the ScanEagle UAV, which will be our reference UAV for the majority of the project, has a max takeoff weight of about 22 kg and a cruising speed of about 26 m/s [1]. Also, the launching mechanism designed for the ScanEagle actually launches with a velocity of 25 m/s [2]. Thus, we revised our project goals to launch a 20kg UAV at a velocity of 25 m/s.

Naturally, this means that all calculations involving the launching mechanism will aim to surpass these design goals. The launch speed will be sufficient to overcome drag and generate enough lift to be able to climb in altitude. Once all kinematics parameters are addressed, stress and design factor analysis can take place in order to further optimize the design of the project as a whole, in order to ensure surpassing or at least meeting the design goals.

Basic System Kinematics

From the 30-degree launch angle and a track length of 3 meters, the basic kinematic calculations of the UAV Launcher can be accomplished. Assuming negligible friction force between the cradle and the rail due to the bearings, a simple “ramp” kinematic analysis was completed. Using initial velocity as 0m/s and final velocity of 25m/s over a distance of 3m, a necessary acceleration of 104m/s² is needed. The UAV has a mass of 20kg and the cradle has a mass of 2kg, so the total launch force will be applied to 22kg.

Fighting against gravity at a 30-degree angle, the applied force must be 2395.91N. Note that this is constant. Elastics apply force in a linear manner. Using kinematics, the time for the launch displacement to occur is calculated as about 0.24 seconds. The total work which is equivalent to the energy change was then found to be about 7200 J, with the power needed about 30kW. This was checked by using a simple energy conservation analysis of the sum of the changes in potential and kinetic energy.

Assuming the elastic bands function as an ideal spring, the total potential energy stored in them must be enough to supply the necessary change in energy of the launched load. Assuming a 90% efficiency of energy conversion, due to friction, drag, and a bit of slack at the end of the rail, the total stored elastic potential energy was designed to be about 8000 J. From here, over a displacement of 3m, the spring constant of the elastics was determined to be 1778 N/m.

Thus, at the fully stretched length of 3m, the maximum force that must be exerted on the crank mechanism and on the quick release pin was $1778 \times 3 = 5334$ N.

$$V_i = \frac{0m}{s}, V_f = \frac{25m}{s}$$

For Drone mass = 20kg and cradle = 2kg, negligible friction force on rail due to bearings

$$m = 20kg + 2kg = 22kg$$

$$\text{Rail length } L = 3m$$

$$d = 3m \quad V_f^2 = V_i^2 + 2ad$$

$$\rightarrow (25m/s)^2 = 2a(3m)$$

$$\rightarrow a = 10.4m/s^2$$

$$F_A - F_{ig} = F_A - (m_{parallel} * g) = F_A - (22kg)(\sin(30))(9.81m/s^2) = ma$$

$$\rightarrow F_A = 2395.91N$$

$$d = \frac{1}{2}at^2 + v_0t + d_0 = 3 = \frac{1}{2}10.4m/s^2t^2$$

$$\rightarrow t = 0.24s$$

$$W = F(\Delta d) = 2395.91N(3m) = 7187J$$

$$P = \frac{\Delta E}{\Delta t} = \frac{7187}{0.24} = 29949 W$$

Check if $W = \Delta E \rightarrow 0.15\%$ error, negligible

$$\Delta KE = \frac{1}{2}MV^2 = \frac{1}{2}(22kg)(25)^2 = 6875J$$

$$\Delta PE = mg\Delta h = (22kg)(9.8m/s^2)(\sin 30)(3m) = 323.73J$$

$$\Delta KE + \Delta PE = \Delta E = W = 6875J + 323.73J = 7198.73J \approx 7187J$$

Assume elastic bungees act as an ideal spring

$$PE_{Stored} = U = \frac{1}{2}K(\Delta x)^2$$

Where Δx = is the length of the rail = 3m

Assuming 90% efficiency of energy conservation

Due to friction losses, some slack at the end of the rope, etc.

$$U = \frac{7198.73J}{0.9} = 7998J \approx 8000J = \frac{1}{2}K(3m)^2$$

$$\rightarrow k = 1778N/m$$

At 3m fully stretched length, max force on crank and quick release pin:

$$F = k\Delta x = 1778 * 3 = 5334N$$

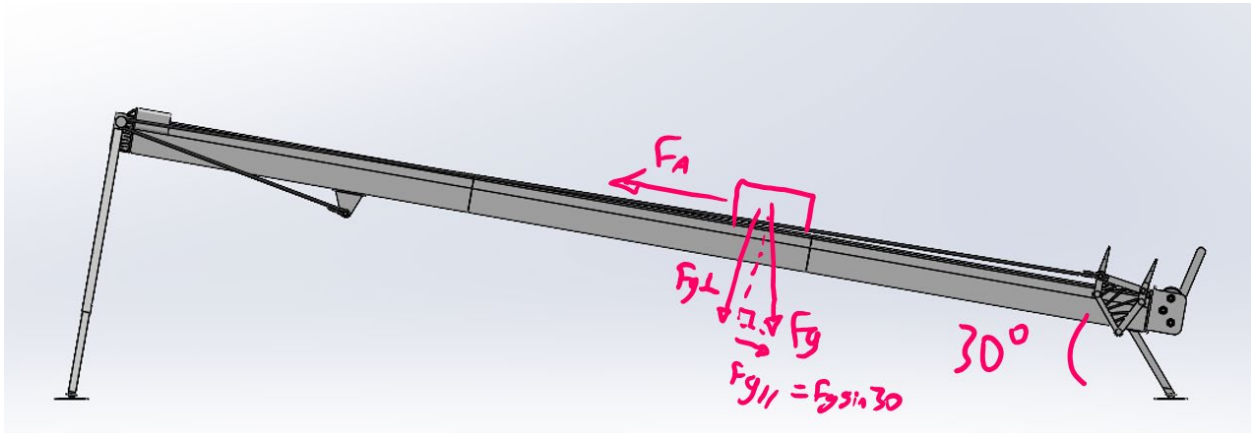


Figure 2: Free body diagram of entire assembly

Cradle Stopper

The next component of the project to be analyzed was the cradle stopper at the end of the rail. This part must be designed to absorb and withstand the large impact force of the cradle at full velocity. Starting with a simple momentum calculation, the 2kg cradle with 20kg UAV load striking the cradle stopper at 25 m/s has a momentum of 550kgm/s. Since the cradle goes from this speed to a stop, the change in kinetic energy will be 6875 J. The change in potential energy is assumed to be negligible due to the relatively tiny displacement this occurs over. Assuming a 2cm deflection of the stopper, the necessary deceleration was found to be 15625 m/s² with an impact force of 31250 N, considering that only the 2kg cradle will be stopped, but not the 20kg UAV. The stress was then calculated as force over area, yielding 16.2MPa. The thickness of the stopper is 10cm. Checking the assumption for a 2cm deflection using stress over strain, and the Young's Modulus of the originally selected material for the stopper (SBR rubber, E = 5171KPa), the necessary Young's Modulus would need to be much higher at 81MPa. The displacement with SBR rubber under these conditions, was about 8cm, which is way too much.

Selecting a stiffer material (FUMQ Fluorosilicone, E = 50MPa), the displacement was found to be about 2.5cm, which is more reasonable and desired. The impact force is then 25000 N and the peak stress is 12.95MPa. This is under the yield stress for FUMQ, which ensures that the material is only elastically deformed and will spring back to its original state after the impact is absorbed, rather than permanently deforming, guaranteeing that the stopper will be able to undergo many cycles of this compression without change. Additionally, this material is very rugged and is able to withstand nearly all conditions with negligible change in performance or properties. This is exactly the desired performance that was needed for the cradle stopper.

$$mv = (25m/s^2)(22kg) = 550kg * m/s^2$$

$$\Delta KE = \frac{1}{2}mv^2 = \frac{1}{2}(22kg)(25)^2 = 6875J$$

Assume 2 cm deflection

$$v^2 = 2a\Delta d = (25m/s)^2 = 2a(0.02)$$

Deceleration: $a = -15625 \text{m/s}^2$

$$M_{cArdle} a = 2\text{kg}(15625\text{m/s}^2) \Rightarrow 31250\text{N impact force}$$

A = impact area

$$\frac{F}{A} = \frac{31250}{(350 + 490 * 2 + 600)\text{mm}^2 * 10^{-6}} = 16.2 \text{MPa}$$

Check 0.02m deflection assumption

$$\delta = \frac{\Delta L}{L} = \frac{0.02\text{m}}{0.1\text{m}} = 0.2$$

Youngs Modulus = $E = 5171 \text{ KPa SBR rubber}$

$$E = \frac{\sigma}{\delta} = \frac{FL}{A\Delta L} = \frac{16.2 * 10^6 \text{ MPa}}{0.2} = 81 \text{ MPa}$$

$81 \text{ MPa} \neq 5.17 \text{ MPa}$

$$E = 5.17 \text{ MPa} = \frac{FL}{A(\Delta L)^2}$$

$$\rightarrow \Delta L = 0.08$$

$$0.08 > 0.02$$

Deflection is too high, stiffer material is needed

Hand Crank Assembly

The hand crank assembly is one of the most important mechanical assemblies in the project. Involving gears, shafts, torques, and the most human interaction during operation, as well as being under the highest stresses, the hand crank assembly must be designed well.

Firstly, the length of spooling and the resulting diameter on the spool at the maximum tension force must be found. This is done using the diameter of the wire rope, at $\frac{1}{4}$ inch, which is 6.35mm. From here, we take the length of the spool and calculate that about 8 full wraps of the rope can fit on one layer of the spool. Then, using cylindrical geometry and a sum involving the changing diameter per each additional layer of spool, it is found that 5 spool layers are needed to wind up all 3m of wire rope. At 5 layers, the distance from the center axis is 40.6mm, and the tension on the rope at this point would be the maximum of 5334N. Thus, the torque is found to be 216.4Nm.

Sourced from NASA, the average person can generate about 120N of cranking force [3]

Using a 25cm handle, the maximum torque generated would be 30Nm. Using about 80% human effort, the torque generated is 24Nm. Thus, the torque reduction ratio needed for the gearbox to achieve 216Nm is 9.

Using Table 8-7 in the textbook, the teeth numbers can be 15 for the small gear and 45 for the bigger gear, to avoid interference for 20-degree full depth pinion spur gears. This provides a gear reduction of 3, and thus two sets of these gears will be needed. 3 shafts will then be needed: crank shaft, intermediate shaft, and spool shaft. Using 10.5mm for the small gear radius, the large gear radius is 31.5mm. The gear width is 6mm, the plate thickness is 3mm, and the handle gap distance is 6mm.

Thus, the final design parameters are:

- Large gear: 45 teeth, 63mm diameter
- Small gear: 15 teeth, 21mm diameter

$$E = 50 \text{ MPa} = \frac{FL}{A\Delta L} = \frac{25^2 L}{A\Delta L}$$

For L = 0.10m, A = impact area = $1930 \times 10^{-6} \text{ m}^2$

$$\rightarrow \Delta L = 0.025 \text{ m}$$

$$F = ma, \quad m = 2 \text{ kg} \rightarrow 2a = \frac{(25 \text{ m/s})^2}{0.025 \text{ m}} = 25000 \text{ N}$$

Using $V_f^2 = V_i^2 + 2ad$ if $V_i = 25 \text{ m/s}$, $v_f = 0 \text{ m/s}$

$$\text{Thus, deceleration } a = \frac{25000}{2} = 12500 \frac{\text{m}}{\text{s}^2}$$

$$\sigma = \frac{25000 \text{ N}}{1930 \times 10^{-6} \text{ m}^2} = 12.95 \text{ MPa}$$

Which is just under the Yield stress from FVMQ ensuring that there is only elastic deformation

12.95 MPa = Max stress on cradle and stopper with:

25000N impact force @ impact, 0.025m = 2.5cm compression deflection of stopper

Shaft Design

The three shafts within the hand crank assembly must be checked to make sure the diameters are thick enough to withstand the loads. The first shaft will be the crank shaft. The torque of 24Nm is applied by the hand crank, and the 21mm diameter gear provides a tangential force of 2290N and a radial force of 830N. When the human force applied on the hand crank (96N) is parallel to the tangential force, the load on the shaft is greatest. Thus, using the shaft design procedure, finding reaction, and shearing forces, and bending moments for both planes relating to the gears. The peak moment will be 16.03Nm. Assuming $K_t=2$ due to gear key seats, safety factor $N=3$, reliability of 0.99, and a shape factor of 0.9 (since small diameter), the minimum diameter must be 1.48mm. However, due to the small distances between force applications, the bending moments may be less than the pure shear stress. Thus, the maximum shear force of 2290N was used in the max shear stress formula for a circle, and compared to the shear strength, which is approximated as 0.75 times the yield stress. The minimum diameter from this calculation must be 3.85mm.

Using the same procedure, the intermediate shaft minimum diameter was found. This shaft has two gears, and a torque applied to it of 72Nm. For the smaller gear, the tangential force was 6857N, and radial force was 2495N. The larger gear had tangential force of 2290N, and radial force was 830N. The maximum bending moment was 76.6Nm, and the minimum diameter was found to be 2.49mm. From the maximum shear stress of 8158N, the minimum diameter was found to be 7.26mm.

Repeating the procedure yet again, the spool shaft was designed. This shaft had the wire rope attached to it under tension with a force of 5334N. The torque on the shaft is 216Nm, and from the one large gear on it, the tangential force is 6857N, and the radial force is 2495. The gearbox assembly is perpendicular to the launcher rail, so all 5334N of tension force will be in the horizontal plane of the shaft. The maximum bending moment was 150.1Nm, and the minimum diameter was found to be 3.12mm. The max shear stress of 8738N yielded a minimum diameter of 7.51mm.

Note that all shafts were designed with a diameter of 12mm, to ensure consistency and an appropriate safety factor for the various loads that occur in this relatively complex assembly mechanism. This leaves the safety factors in the double-digit ranges, which will ensure that no failures occur over time.

Crank Shaft

$$T = 24 \text{ Nm}$$

$$W_{TB} = \frac{T}{R_s} = \frac{24 \text{ Nm}}{10.5/1000} = 2290 \text{ N}$$

$$W_{\text{ebb}} = 2.90 \cdot \tan(20) = 830 \text{ N}$$

Most Force when the human force on the crank is parallel to $W_{\text{TB}} \rightarrow 96 \text{ N} = 120 \cdot 0.8$

Horizontal



Figure 3: Crank Shaft – horizontal moment and shear force diagrams

Vertical

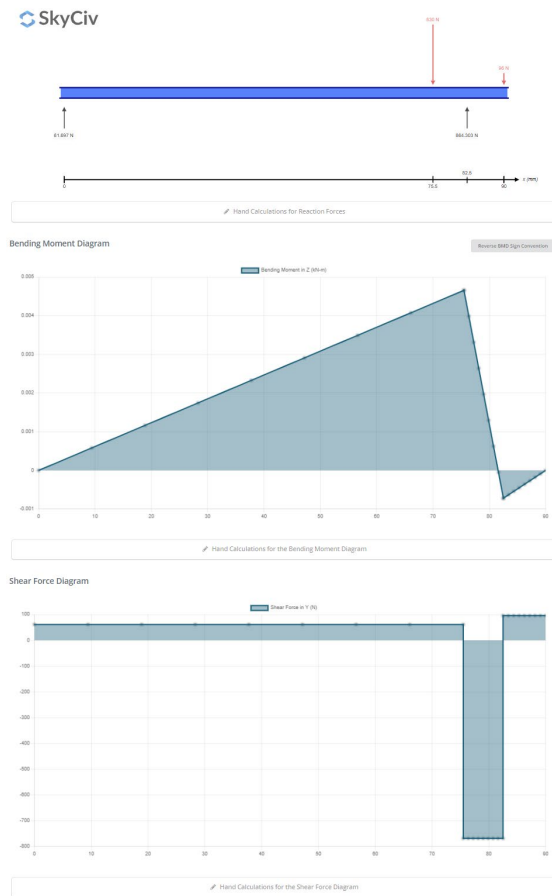


Figure 4: Crank Shaft - vertical moment and shear force diagrams

$$R_A + R_s = 2194 \text{ N}$$

$$2290 \text{ N}(75.5 \text{ mm}) = R_c(82.5 \text{ mm}) + 96 \text{ N}(90 \text{ mm})$$

$$R_c = 1991 \text{ N}$$

$$R_A = 203 \text{ N}$$

$$M = \sqrt{(15.33 \text{ Nm})^2 + (4.681 \text{ Nm})^2} = 16.03 \text{ Nm}$$

$$R_A + R_s = 926 \text{ N}$$

$$R_c(82.5 \text{ mm}) = 830 \text{ N}(75.5 \text{ mm}) + 96 \text{ N}(90 \text{ mm})$$

$$R_c = 864 \text{ N}$$

$$R_A = 62 \text{ N}$$

Assume $K_t = 2.0$ & $N = 3$

$$U_s = 1250 \text{ MPa}$$

$$S_Y = 1050 \text{ MPa}$$

$$S_n = 420 \text{ MPa}$$

$$S'_n = (0.81)(0.9)(420 \text{ MPa}) = 306.2 \text{ MPa} \rightarrow \text{assuming 0.99 reliability, \& } C_s = 0.9$$

$$D = \left[\frac{32(3)}{\pi} \sqrt{\left(\frac{2(16.03Nm)}{306.2MPa} \right)^2 + \frac{3}{4} \left(\frac{24}{1050MPa} \right)^2} \right]^{1/3} = 1.48mm \text{ minimum!}$$

Check Cs: $C_s = 1 \approx 0.9$, negligible difference.

$$\tau \text{ shear stress? Max shear} = 2290N \quad \tau_{\max} \text{ for a circle} = \frac{4V}{3A}$$

$$\tau_{\max} \approx 0.75S_y = 0.75(1050MPa) = 788MPa \quad \tau_a = \frac{788}{3} = 263MPa, \text{ for } N = 3$$

$$A = \frac{4(2290MPa)}{3(263*10^6)} = 1.2 * 10^{-5} = \pi r^2 \rightarrow r = 1.92mm$$

For shear, minimum diameter = 3.85mm

Intermediate Shaft

$$T = 72Nm$$

$$W_{Tc} = \frac{T}{R_s} = \frac{72Nm}{31.5/1000} = 2290N$$

$$W_{rc} = 830N$$

$$W_{TB} = \frac{72Nm}{10.5/1000} = 6857N$$

$$W_{rB} = 6857Nm * \tan 20^\circ = 2495N$$

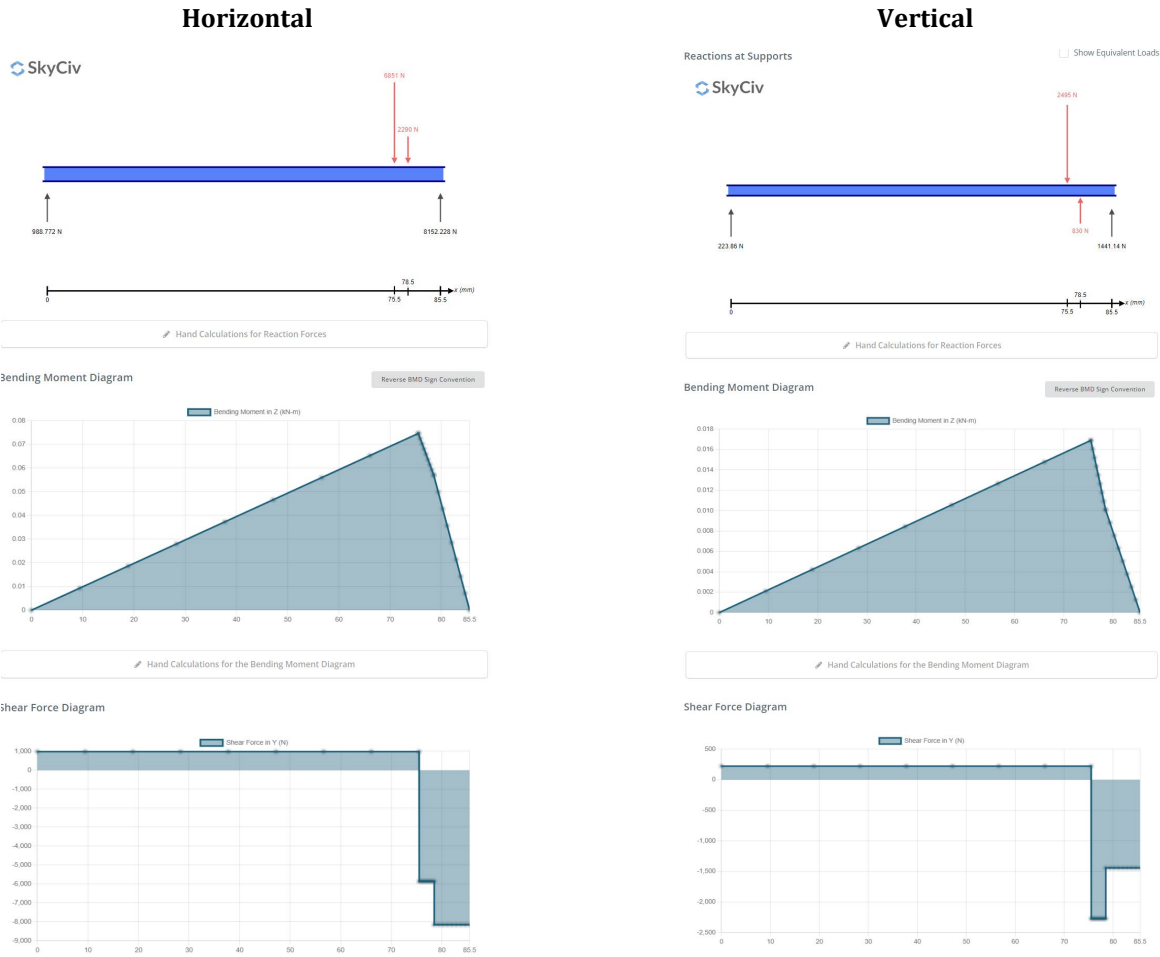


Figure 5: Intermediate Shaft – horizontal moment and shear force diagrams

Figure 6: Intermediate Shaft - vertical moment and shear force diagrams

$$R_D = 8158 \text{ N}$$

$$R_A = 989 \text{ N}$$

$$M = \sqrt{(74.67 \text{ Nm})^2 + (16.9 \text{ Nm})^2} = 76.6 \text{ Nm}$$

$$R_D = 1441 \text{ N}$$

$$R_A = 224 \text{ N}$$

$$D = \left[\frac{32(3)}{\pi} \sqrt{\left(\frac{2(76.6 \text{ Nm})}{306.2 \text{ MPa}} \right)^2 + \frac{3}{4} \left(\frac{72}{1050 \text{ MPa}} \right)^2} \right] = 2.49 \text{ mm}$$

Check Cs: $C_s = 1 \approx 0.9$, negligible difference.

τ shear stress? Max shear = 8158 N

$$\tau_{\max} \text{ for a circle} = \frac{4V}{3A} = \frac{4(8158 \text{ N})}{3(263 \cdot 10^{-5} \text{ m}^2)} = 4.1 \cdot 10^{-5} \text{ m}$$

$$A = \pi r^2 \rightarrow r = 3.63 \text{ mm}$$

$$D_{min} = 7.26 \text{ mm}$$

Spool Shaft

$$T = 216 \text{ Nm}$$

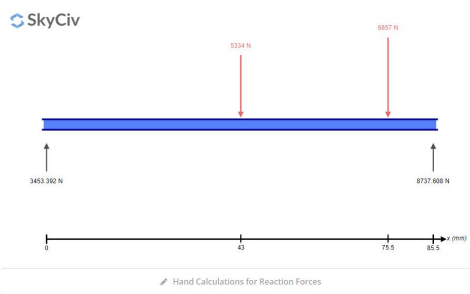
Assuming the wire rope ends its final wrap around the spool near the center of the spool $\rightarrow 5334\text{N}$.

$$W_T = \frac{T}{R_s} = \frac{216\text{Nm}}{31.5/1000} = 6857\text{N}$$

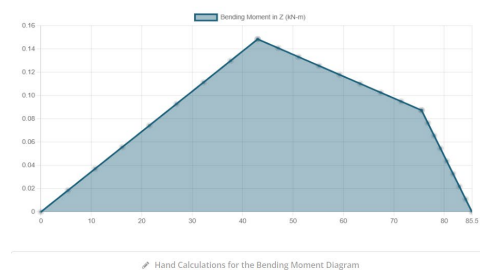
$$W_r = 2495\text{N}$$

Gear box is perpendicular to the rail, so the full component of 5334N is in the horizontal plane

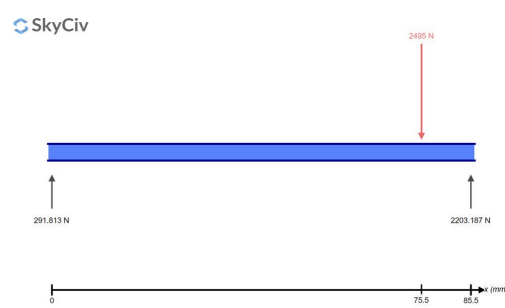
Horizontal



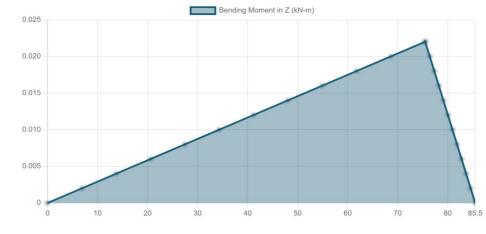
Bending Moment Diagram



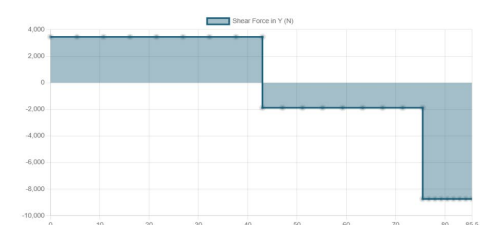
Vertical



Bending Moment Diagram



Shear Force Diagram



Shear Force Diagram

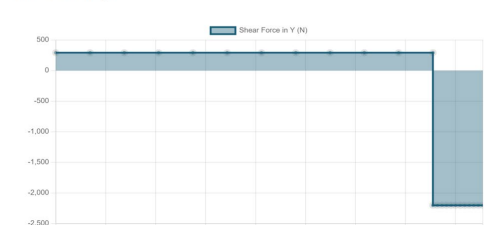


Figure 7: Spool Shaft – horizontal moment and shear force diagrams

Figure 8: Spool Shaft – vertical moment and shear force diagrams

$$R_D = 8737.6\text{N}$$

$$R_A = 3453.4\text{N}$$

$$R_D = 2203.2\text{N}$$

$$R_A = 291.8\text{N}$$

$$M = \sqrt{(148.5 Nm)^2 + (22.05 Nm)^2} = 150.1 Nm$$

$$D = \left[\frac{32(3)}{\pi} \sqrt{\left(\frac{2(150.1 Nm)}{306.2 Mpa} \right)^2 + \frac{3}{4} \left(\frac{216}{1050 MPa} \right)^2} \right] = 3.12 mm$$

Check Cs: $C_s = 1 \approx 0.9$, negligible difference.

$$\text{Max shear} = 8738 N \quad \tau_{\max} \text{ for a circle} = \frac{4V}{3A} = \frac{4(8738N)}{3(263 \cdot 10^{-5})} = 4.1 \cdot 10^{-5} m$$

$$A = \pi r^2 \rightarrow r = 3.76 mm$$

$$D_{min} = 7.51 mm$$

From the calculations done by hand, it is clear that the design of the components have a much larger than necessary safety factor. This will help the endurance and lifetime of our design and will allow the UAV Launcher to have an exceptionally low failure rate. From the stresses seen on the shafts in the crank assembly, to the elasticity and strength of the cradle stopper, it is clear that these components are well designed. Accounting for safety factors, fatigue and endurance limits, and ultimate/yield strengths, the apparatus should easily be able to achieve over 1000 use cycles before a failure occurs. This claim is further proved by the results shown in the simulation section below.

Model

This section of the report will go over the changes and the progress of the design model for a UAV launch system over the course of this project. The system contains 3 important parts that were optimized and changed the most over the design period. Those being the rail system, the cradle, and the impact stopper. The changes for these were due to changes in the method of launching. Initially the cradle was to be propelled by a motor and belt system, however, as stated previously, this was an issue since the required motor would need to produce 30 kilowatts, requiring more external components and overall causing a failure in the initially set parameters. Various other propulsion mechanisms were discussed, such as tension gas spring, pneumatic piston, and magnets however none of them offered the same capabilities as a bungee system. The implementation of the bungee system allowed us to stay within the initially set parameters and were simple enough to implement into the already designed system without having to fully redesign. The bungee system did not come without difficulties though. Due to the large amount of stress that such a system undergoes it was important to create well designed connections points. The following subsections discuss the key components of the launch system, starting with the design of the cradle.

Cradle

The UAV cradle is built from several parts and has gone through several iterations. The first iteration consisted of a box shape that wrapped around the entire rail, the model of which can be seen in Figure 9. The issue with this design was its weight, bulky nature, and overall unaesthetic design. This design also required a rail system that had rollers on it since the cradle did not contain any bearings itself.

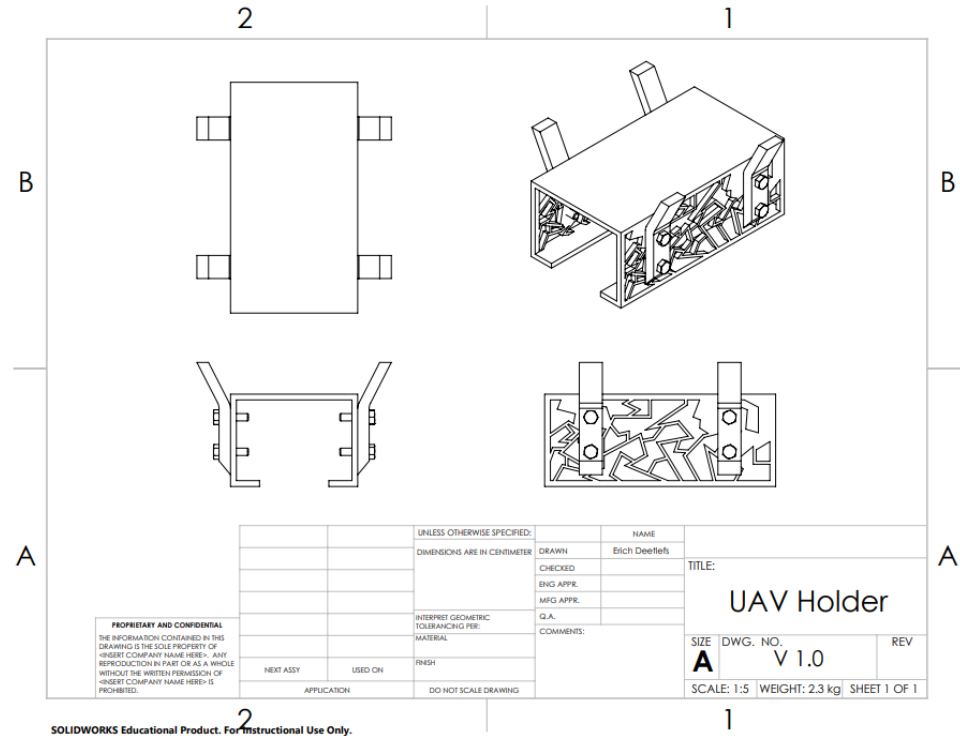


Figure 9: UAV cradle V1.0

Another downfall of this design was that it was hard to manufacture as well as it was unnecessarily strong, being able to withstand weights that were not required in a UAV launch system. In the end this design was quickly scraped and replaced by Cradle Version 2.0. After sketching a few designs and referencing some similar systems on the internet, a new and improved cradle was modeled. In the updated version, as seen in Figure 10, the cradle is now built using many more parts than its predecessor. This version also included the use of bearings on the cradle itself rather than on the rail, as well as the use of well-designed rotating brackets that fit the mounting specifications of a ScanEagle 3 UAV.

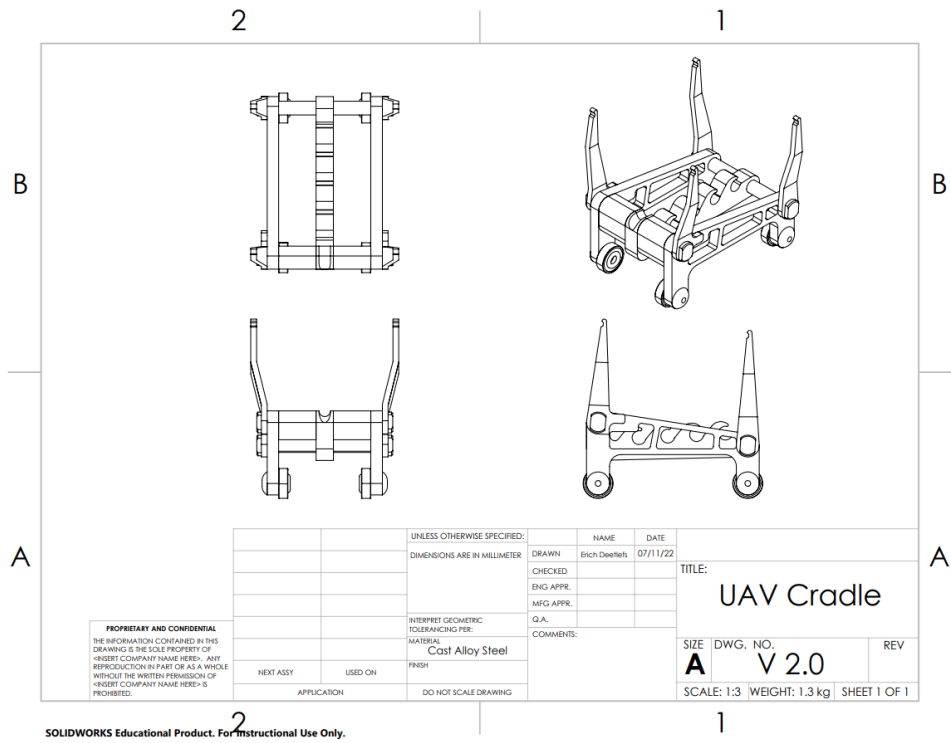


Figure 10: UAV cradle V2.0

This new cradle consists of several parts that are attached together through rivets, screws, and pins. While this adds to the complexity of the system, it allows for a much lighter part as well as the ability to replace individual parts, if damaged, rather than the entire cradle. The design is also a lot simpler to manufacture than the previous version due to it being made of several parts rather than a single block. While the weight that it can bear is less than Version 1, Version 2 holds more than enough weight than would be required, which is proved in a static simulation as seen in Figure 11.

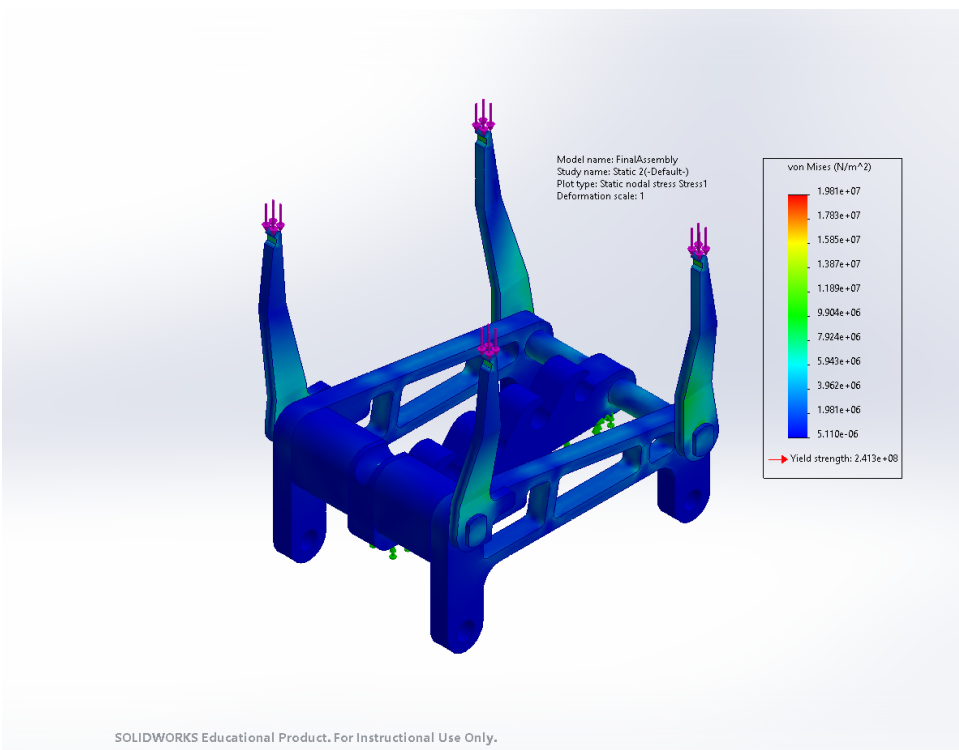


Figure 11: Stress Simulations of the UAV cradle version 2.0

However, the design for the second cradle version was built around the use of a motor and belt system. When the propulsions system was changed to a bungee propulsion method, a few changes had to be made to the design of the cradle. The most notable of which are the addition of the bungee connection and the third bearing. These changes can be seen in Figure 12.

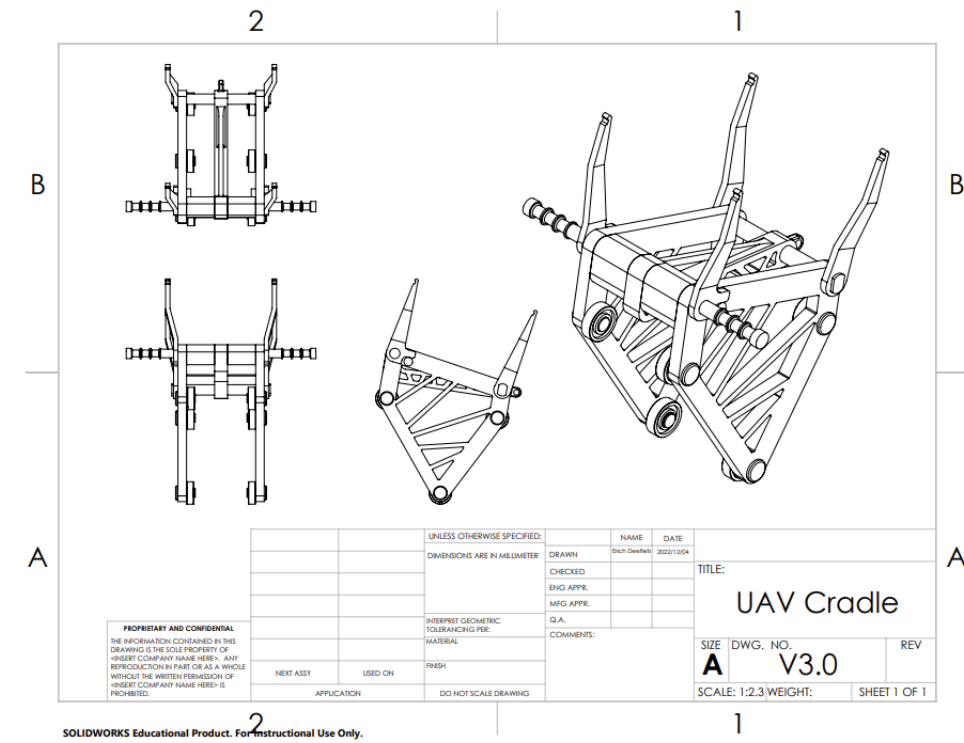


Figure 12: UAV cradle V3.0

The addition for the third bearing was so that the load on the upper two bearings could be more evenly distributed in order to reduce the friction as the cradle moves along the rail. The bungee connection included three slotted sections so that up to three bungee cords could be connected to it at once. All the parts that make up the cradle are easily manufacturable using methods such as CNC milling or using a lathe for the bungee attachment. The simulation in Figure 11 still partially applies to version 3.0 since the only section that was changed that applies to the simulation is the side bracket. Another notable change that cannot be seen in this version was replacing the rivets that hold the bearings to a pin and c-ring clip. This allows the bearings to be easily swapped out since they are the part that will be undergoing the most use and will fatigue the quickest. Overall, the final design of the UAV cradle fits the parameters that were initially set and allows for the part to be easily manufactured and tested in a real-world environment.

Rail

The rail system was designed with the idea that it could be split up into smaller sections, the drawings of which can be seen in Appendix B, Figure 46. The total length for a singular section was initially set to be 1.5 [m] but was later changed to 1.0 [m]. Each of the rail sections had their centers cut out to allow for the passthrough of wires, and belt for the belt and wire system. Since this system was changed to a bungee system this passthrough could have been changed and deleted. However due to time constraints, the initial rail design was kept as it and this passthrough was used to not only lighten the overall mass of the system but allowed as somewhat of a storage area for other components when the launcher was collapsed. Each section is also to be connected using a set of pins for alignment and a R5 Draw Latch to lock them together. The sections would be fitted together with O rings to allow for a better fitment as well as reduce the amount of noise in the system. In total up to 3 of these rail sections would be used in the final rail system which would result in a total length of 3 [m] which the UAV could use to build up speed. In the future a topology study could be run on this rail system in order to lighten the mass of the entire launcher, since the rail makes up a majority of its weight.

Stopper

The only part that was not previously considered in past models was the cradle stopper. This was once again a part that had gone through different iterations when designing it, due to the findings in the calculations. Initially a piston damper was considered since it could easily be bought from any manufacturing company, however it would add complications to the design as well as required external parts to run, in turn increasing the weight of the launcher. The next idea was to use some form of a bellow damper or compression pad. The latter offered the advantage of being lightweight however would not have been able to withstand the impact forces that were required. In the end inspiration was taken straight from a gym weight stack rubber cushion as seen in Figure 13.



Figure 13: Gym weight stack rubber cushion

This design is perfectly suited to withstand the impacts when made with the Silicon Rubber material found in the materials section below. The design for the stopper used in our launcher system can be seen in Appendix B, Figure 33.

Gearbox

The most intricate section of the launcher system is the gearbox system, which is used to wind the UAV cradle to the bottom of the rail, stretching the bungees. As seen in the calculations, the required gear ratio was found to be 9:1. To implement such a gear ratio, it is required that a system be built using multiple gears, and in the case of this system we used a total of 4 gears all using a gear module of 1.4. The main input gear, the drawings for which are seen in Appendix B, Figure 44, has a diameter of 21mm and a total tooth count of 15. It is then attached to a combo gear that consists of a larger 63mm gear with a tooth count of 45 placed alongside another “input gear” on the same axis. This would then bring the ratio to 3:1 when all placed together. Finally, adding another 63mm diameter, 45 toothed gear to the gearbox and attaching it to the spool allows for that 9:1 gear ratio system. In Figure 14, a rough sketch of this designed gearbox is shown. The chain was used to illustrate the connection between the small intermediate gear and the large spool gear, without obstructing the view of the larger intermediate gear. Note that in the real assembly, this chain is not included. The gears are meshed together.

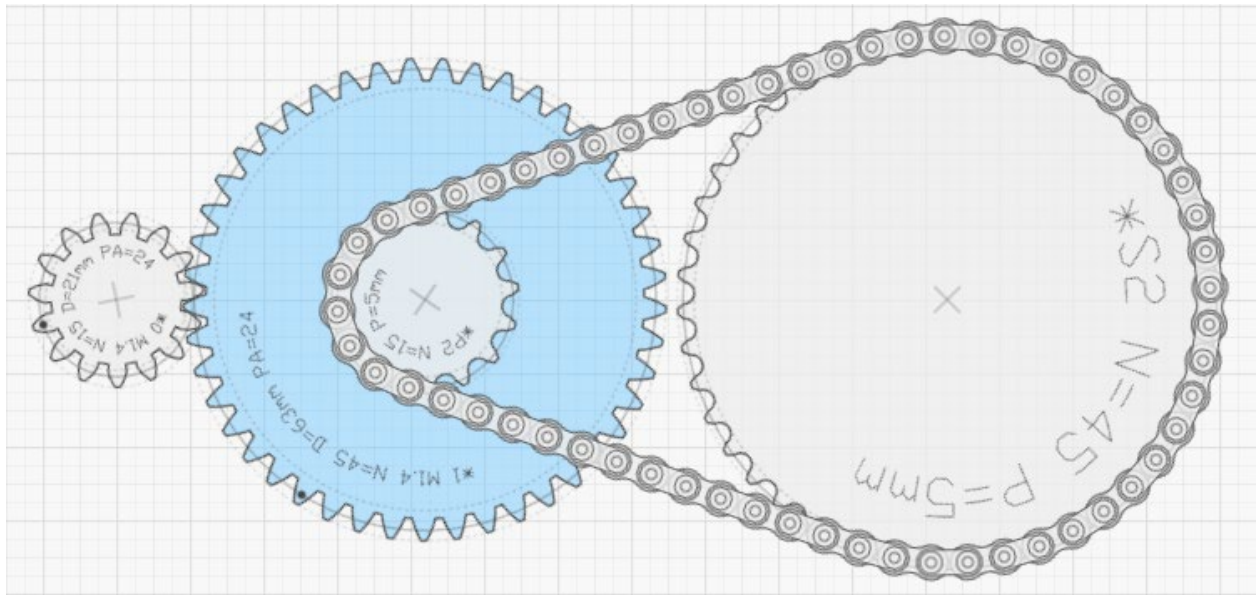


Figure 14: Gear schematic

This entire gearbox system was contained within a frame that was made using a single 3mm thick piece of sheet metal. The choice of using a sheet metal was to allow for simple manufacturing capabilities. As seen in Appendix B, Figure 55, this part can easily be stamped or cut using a plasma cutter and then bent to the required angle. Overall, this gearbox is a robust system that can withstand the required forces in order to pull the cradle back to its launch position while under tension from the bungee cords.

In the end, the design for this UAV launcher far surpassed our personal requirements as well as taught us a lot about the modeling of such a system. The final weight of the entire system came out to be a total of 93.4 kg, which was well below the goals we had previously set. As previously stated, there are definitely upgrades and changes that could be made such as optimizing the rail system, which would reduce the overall weight, and the functionality of the quick release system. Additionally other features could be added to extend the life of the bearings as well as decrease the difficulty of manufacturing some components. That being said, this design is definitely a well-designed launcher and could be manufactured and tested against real-world scenarios.

Parts

As with any complex design, there are many smaller components which must be taken into account. This section of our final report will outline these components, and their purpose within the design of our UAV Launch System.

Bearing

Bearings are a key component when an object is required to rotate or slide along another rotating or static object. These are used in a wide range of industries and are a common part found on many types of machinery, whether a common drawer or devices found in the aerospace industry. Bearings serve three main purposes, to carry a load, reduce friction and position moving machine parts [4]. Bearings are composed of 3 main pieces, the inner raceway, outer raceway and rolling element, which allows rotation. The first big decision to tackle when selecting a bearing is whether to choose a roller bearing or a ball bearing, each has its own unique strengths and weaknesses. A roller bearing has a larger contact patch between the roller and the raceways and therefore is ideal for use at lower speeds and when it must support a large load. Ball bearings, on the other hand, have very small contact patches and are mainly used in applications where the forces are lower, but rotation speeds need to be much higher [5]. For our application, the force exerted on the bearing by the rail or cradle is not expected to be outside the range of use for a ball bearing. Furthermore, the launch speeds needed to achieve by the system to propel the UAV are quite high. As such, a ball bearing is best suited to our needs. For our purpose, the NSK 6000zz bearing is selected from Mi Motion [6] as it is available for use in Solidworks, and it is sufficient for the speeds achieved during the launch of a UAV from our launch system. The price breakdown for this component can be seen in the Bill of Materials shown in Table 3 and Appendix E.

O-Ring

Another important component in industry is the O-Ring. O-Rings are used to seal the connections between pipes or tubes. They allow a tight fit between components not allowing air, water, or any other fluids to penetrate the seal [7]. They also allow a slight amount of movement in the junction of two parts, reducing the risk of damage from contact. The biggest selection criterion, in this case, is the material of the O-ring. These differences in the material allow for different rigidities, temperature ranges and amount of pressure it will need to resist. In our application, the O-ring will sit in the junction between each segment of the rail. The O-ring will not be subjected to high temperatures outside the ambient temperature at its location of use; we've selected a range of -20 to +40 degrees centigrade. Furthermore, it is not expected that they will need to withstand any hydraulic pressure. As such, there are many O-rings which will easily be able to meet these criteria. The price breakdown for this component can be seen in the Bill of Materials shown in Table 3 and Appendix E.

C-Ring

Another important part which allows the ceiling of the interface between two components is the c-ring, they are seated in a groove in the part and compressed by the mating surface. Similar to an O-Ring, they provide a seal between these components, though as opposed to O-rings they are made of a metal and will not provide any movement in the mating area. The price breakdown for this component can be seen in the Bill of Materials shown in Table 3 and Appendix E.

Draw Latch

Draw latches are another important component for the function of the UAV Launch System. They will allow temporary joining of the individual rail segments together, allowing the deconstruction of the launch system for ease of transportation. As such, it is important for the latch to be able to securely fasten the segments together, as the failure of any latch could result in the separation of the segments during a launch which could cause a number of compounding failures. For our purpose, two latches positioned on either side of the rail are preferred. This will allow an even distribution of forces on each latch, and not interfere with the prescribed motion cradle or UAV. The price breakdown for this component can be seen in the Bill of Materials shown in Table 3 and Appendix E.

Quick Release Pin

For use on the UAV Launch System, four quick release pins are needed. One on each of 3 legs of the launch system, allowing for articulation of the feet for placement on rough surfaces and adjustment of the launch angle, as well as one for the release of the cradle, propelling the UAV into flight. This fourth and final pin will be under the most stress and must withstand again the shear forces caused by the elastics used to propel the system. As such, an FEA study is completed to ensure it will not fail under these loading conditions; further analysis on this is in the Simulations section of this report. The price breakdown for this component can be seen in the Bill of Materials shown in Table 3 and Appendix E.

Bungee

A main and very important component for our UAV launcher are the bungees. This replaces the belt and motor system theorized in our midterm report, which we have since moved away from as it adds too much weight to the system, causing it to no longer be easily transportable. Bungee elastics are our main propulsion system for the UAV and are what imparts the majority of the forces on our assembly. For our purpose, it was determined that we would need six bungees with a spring constant of 296.3 N/m, and a length of approximately two meters which would be cut to the specific length needed with securing loops made. For the procurement of the bungee, we would be ordering a custom-made bungee to suit the needs outlined above. The price breakdown for this component can be seen in the Bill of Materials shown in Table 3 and Appendix E.

Materials

This section of the report will outline the material selection methods through the use of a Granta EduPack Study. Material characteristics are chosen and placed on the x and y axis to determine which materials best suit these criteria. Limiting factors are also selected to ensure the final material best meets all of our design objectives.

Main Structural Material

From initial research and modelling, we were able to determine that the main structural components would need to be strong enough to withstand repeated use but also light enough to meet our design goals. As such, they needed to meet the following criteria: high yield strength, low young's modulus, high toughness, and low density. Additionally, we defined multiple limiting factors to narrow down the candidate materials and ensure they best suit our application. These include picking a metal with high acid and saltwater corrosion and UV resistance. The material parameters were selected such that the entire design will resist repeated impacts while remaining lightweight enough to be transported easily. To find this material, a level 3 material study was conducted using Granta EduPack. For this study, we must select material characteristics to be placed on the x and y-axis. For the y-axis, we selected the tensile strength and young's modulus. This term is important as the design must withstand high-force impacts. Yield strength is defined as the maximum force a material can withstand without excessive plastic deformation [7]. Young's modulus is a material property which tells us how easily it can be stretched or deformed. It is the ratio of tensile stress (σ) to tensile strain (ϵ) and, therefore, the slope of the stress vs strain graph [8]. Hence the larger this combined value is, the stronger the material chosen will be. The next parameters chosen for the x-axis of the Granta study were hardness and density. In this case, we wanted to minimize the weight and, thus, the density of the material while simultaneously achieving the highest toughness value possible. Toughness is the energy a material can absorb before failure [9]. Finally, the material in the upper right corner will be the best suited for our application as it will meet all the criteria set out above.

Additionally, limiting factors are set in place in order to limit the materials which are able to operate in the harsh environment the launcher will operate in. The limiting factors selected for our purpose are corrosion resistance which includes saltwater corrosion resistance for maritime use, as well as UV-resistant properties for use in arid, sunny environments. We also limit our study to materials with good acid and oil durability for use around heavy machinery. Furthermore, a metal filter was added to filter out carbon composites and other brittle materials, which despite performing well on the graph, could lead to potentially dangerous situations as catastrophic failure would be near impossible to detect beforehand [10]. The final result of this in Figure 15 below shows stainless steel alloys in teal and ferromagnetic metals in red.

With this study now complete, the materials of choice are Stainless Steel, austenitic AISI 302, HT, Grade D, Stainless Steel, austenitic AISI 304 ½ hard and Nickel-Chromium alloy, INCONEL 718 solution and aged. Ultimately Nickel-Chromium alloy, INCONEL 718 solution and aged, is chosen because it has the lowest density, relatively low cost, highest toughness, and very high yield strength. The combination of these factors makes it a common material choice for marine architecture and chemical processing.

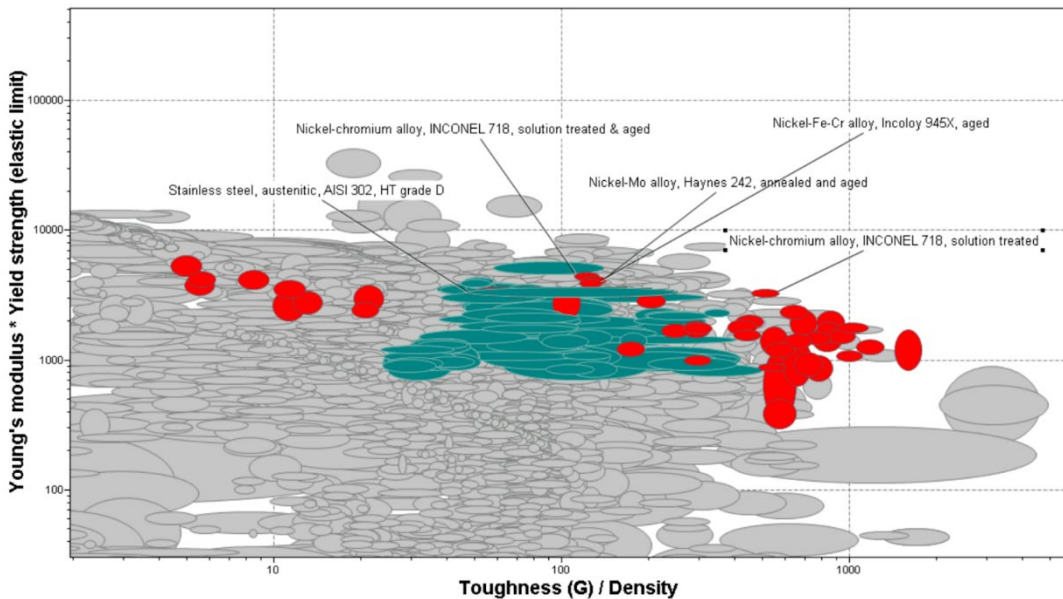


Figure 15: Granta EduPack structural material results

Collision Damper Material

The second required material is a collision damping material to protect the stopper at the end of the rail and the cradle from permanent deformation due to the repeated high impact forces, which the launcher will be subject to in its use. As such, from preliminary research, it was determined that an elastomer with a low Young's Modulus and high yield strength would be ideal. To find the optimal material for this part, another level 3 Granta EduPack study is conducted. To run this study, material constraints are placed along the x and y-axis. For the x-axis, the inverse of Young's Modulus is chosen as a way to minimize its value and thus maximize the deformation capabilities of the bumper, allowing it to achieve its goal of deforming while slowing down the UAV holder over a distance and reducing stress concentrations. With that being said, we must select a material that provides enough resistance to stop the cradle within a reasonable amount of space. To pick this Young's Modulus value, we iterated through multiple rubbers to find the one which would perform as needed. Furthermore, optimizing the material for this parameter will allow the UAV to take off smoothly. The next parameter selected for the y-axis is the yield strength which is defined as the point at which plastic deformation occurs [7]. This value was placed along the y-axis and is essential to the design as the stopper must be able to withstand a high number of repeated forces without plastically deforming. Plastic deformation is defined as the point at which permanent deformation occurs due to stress [11]. The combination of these axis will mean that the best material will appear furthest up and graph and towards the right, as seen in Figure 16.

With the axis of the graph defined, limiting values are selected to limit candidate materials to elastomers and have to material with specific material properties such as seawater resistance, high thermal operating region and UV resistance. The first of these limiting parameters is that the material must be an elastomer which is a polymer able to withstand high deformations and return to its original shape with little to no damage or plastic deformation [12]. The elastomers in Figure 10 can be seen in red and light blue.

Additionally, materials are filtered for different material properties. Starting with excellent UV resistance as the launcher will be exposed to sunlight, and the rubber cannot break down. As well as seawater resistance which enables this device to be used in maritime regions. With this study now complete and iterative calculations on Young's Modulus completed, the optimal candidate material is Fluorosilicone (FVMQ, heat cured, 10-30% fumed silica). This is due to its balanced Young's Modulus and high yield strength. Furthermore, the properties it possesses make it an ideal material for a wide range of environments with a high temperature range from -57°C to 250°C, with the material showing relatively little shrinkage over that range. Due to these properties, it is commonly used in naval aircraft, gaskets, and mounts.

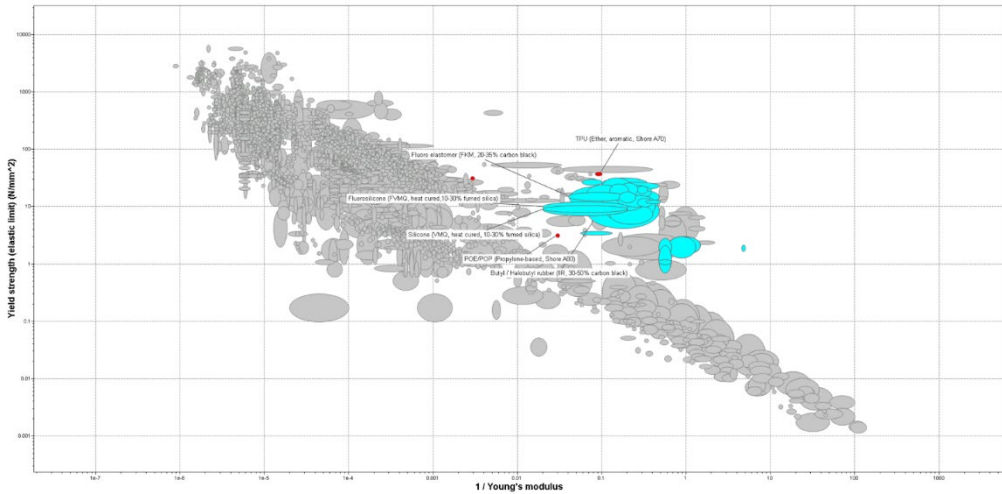


Figure 16: Granta EduPack collision damper material results

Simulations

Several simulations were conducted for this project, such as Static Studies, Design Studies, Topology Studies, and Motion Studies. Through these studies, we are able to analyze the various loads acting on the model as well as the motion of its parts and optimize them to best suit our design objectives. This section of the report will outline the individual parts designed and the studies ran on them.

Calculation Comparison: Hand Crank Assembly - Gear and Shaft Design

In this simulation, the handle and structural plate are kept fixed, and the maximum torque of 216Nm is applied on the wire rope spool. This allows the simulation to calculate the stresses on the gears and shafts within the gear assembly. From the hand calculations, it was clear that the design was quite over-engineered, with large safety factors and the dimensions being multiples larger than necessary. Thus, it is no surprise that the simulation study also showed very low values of stress concentrations, and the maximum stress in the whole assembly is nowhere near the yield strength of the material used. The only difference between the simulations and the calculations would be in the stress concentrations observed in the more intricate geometries in the model, while the calculations assumed more simplified geometries. Shown below, the highest stresses occur where there are fillets or changes of shaft diameter, which were not accounted for in such a detailed manner in the hand calculations. However, the results between the simulation and the hand calculations are comparable and yield the same results, both concluding that this assembly is very much able to handle the maximum loads it will encounter, and the level of safety factor within the whole assembly is much higher than necessary. This simulation further supports the claim initially posed by the calculations, showing that this assembly, being so far from any stress limits, should easily be able to surpass over 1000 use cycles before any failure occurs.

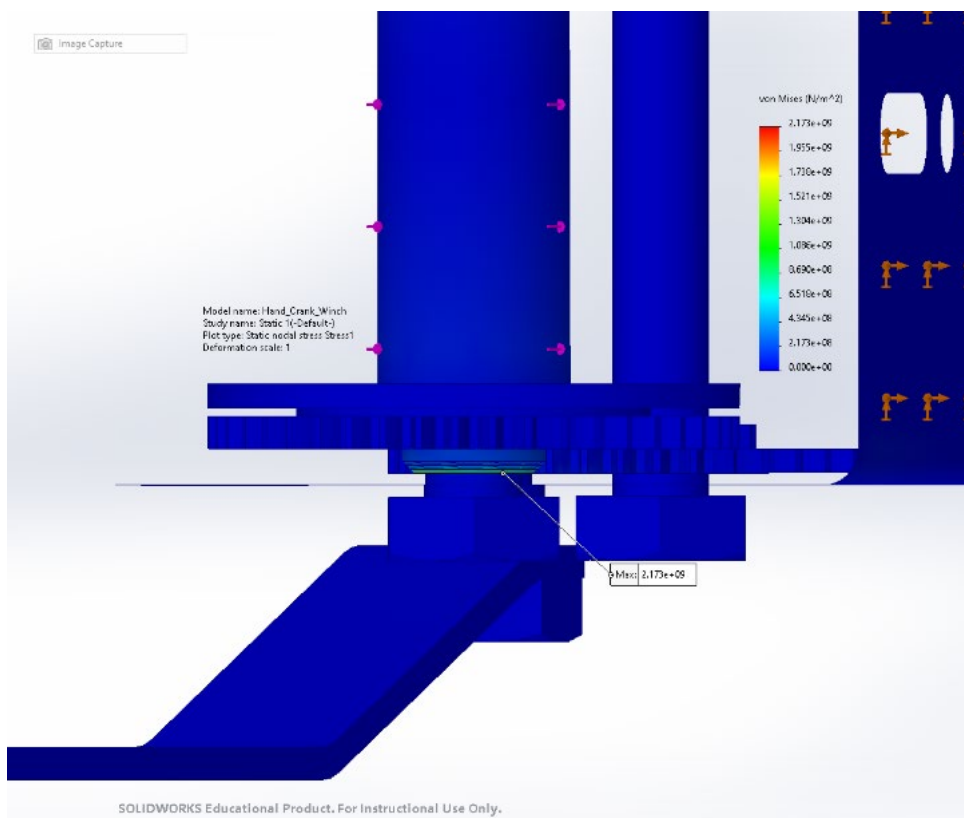


Figure 17: Hand crack assembly - top view

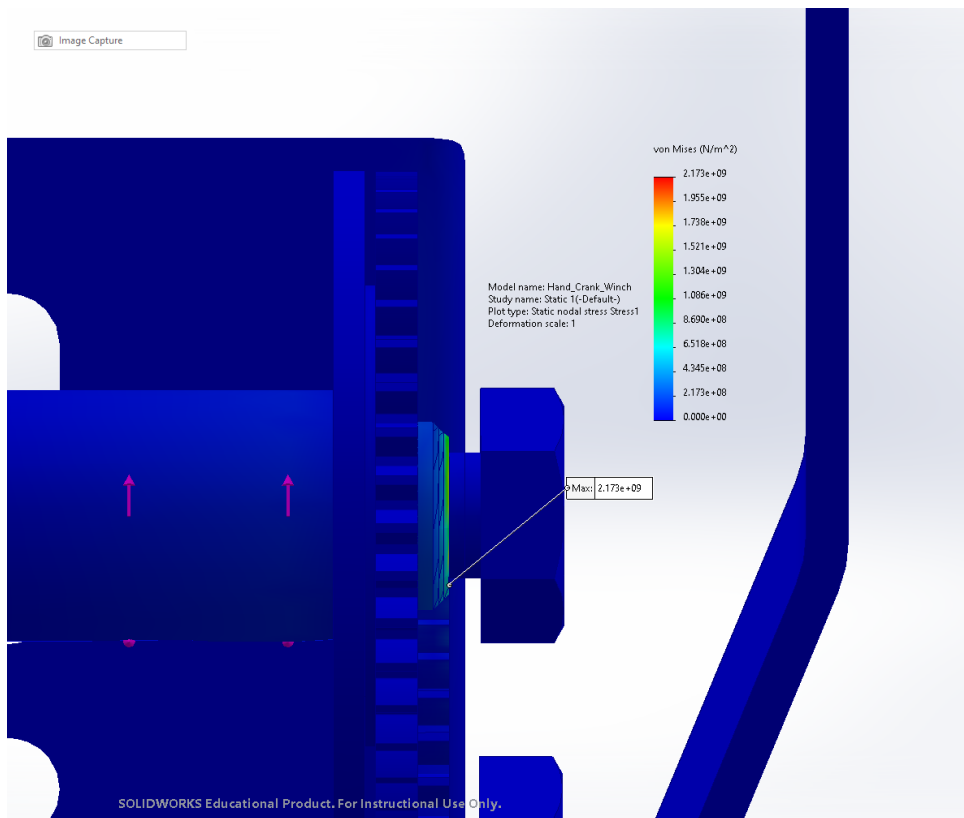


Figure 18: Hand crack assembly maximum stress concentration

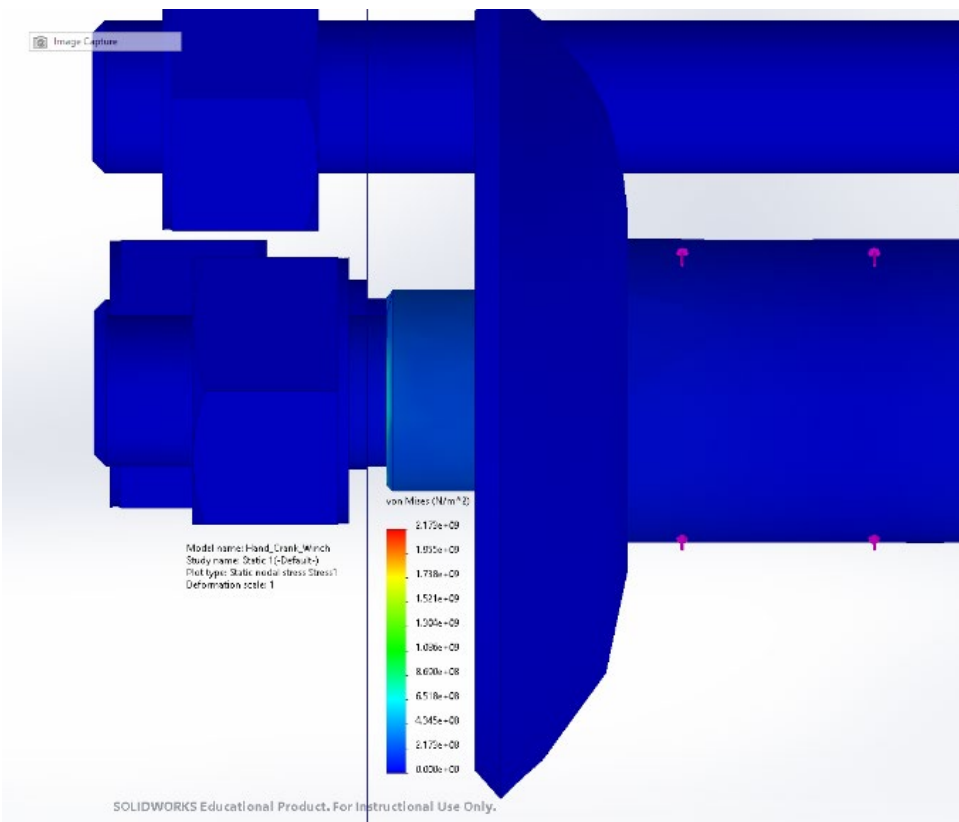


Figure 19: Hand crack assembly spool shaft - maximum stress concentration

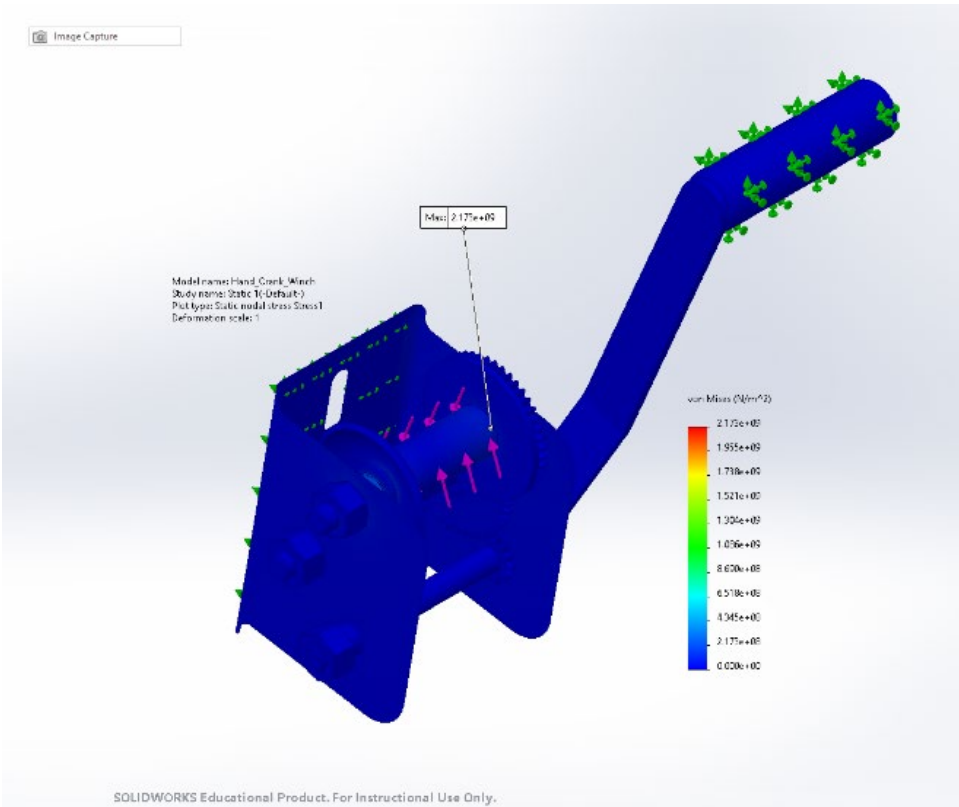


Figure 20: Hand crack assembly - isometric view

Quick Release Pin Mechanism

The quick release pin mechanism is an essential part of the design connecting the UAV cradle to the crank frame. It is required to withstand 5334 N without deforming, so the simulation was done with 5867 N to be safe. To ensure this design goal is met, we ran an FEA static simulation on the mechanism. To simulate the maximum stress, a force of 5867N is applied, pulling the cradle away from the crank, and the crank mechanism is fixed in place with the pin mated concentrically between them. Reviewing the results in figures 21, 22, and 23, we can see that the pin is subjected to shearing forces from the two holding mechanisms pulling apart, with the maximum stress in this mechanism occurring in the pin at 3.931×10^2 MPa. This verifies the strength of our design as it is well below the yield strength value of 1.11×10^9 MPa.

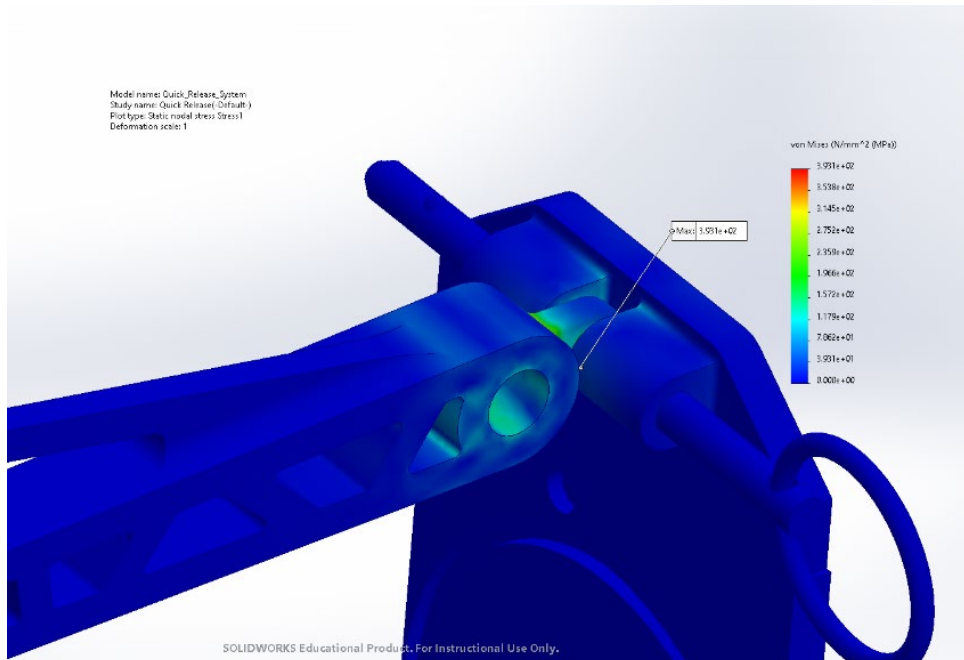


Figure 21: Quick release mechanism - isometric view

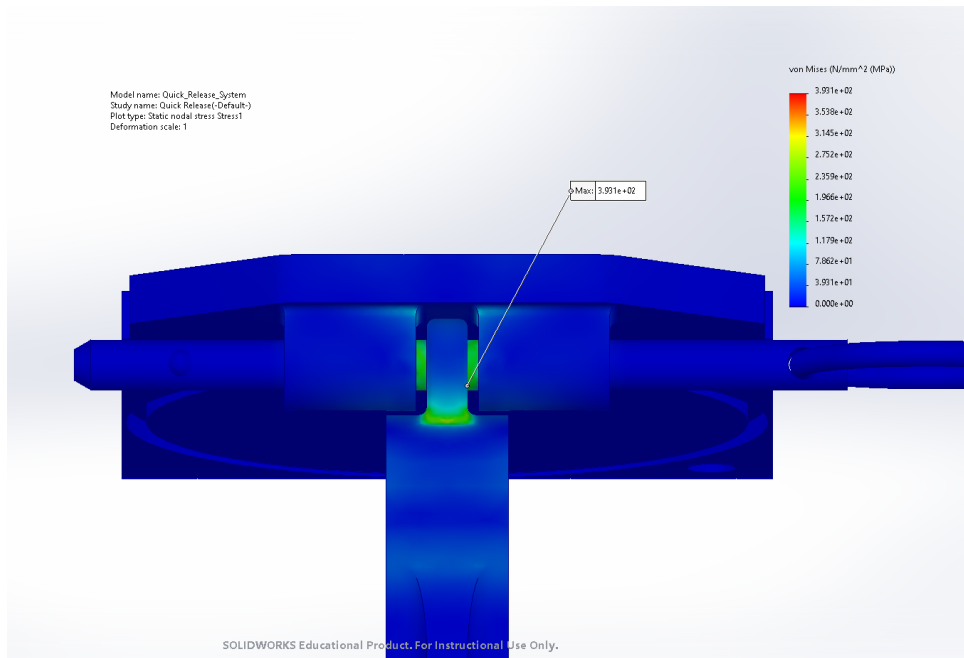


Figure 22: Quick release mechanism - top view

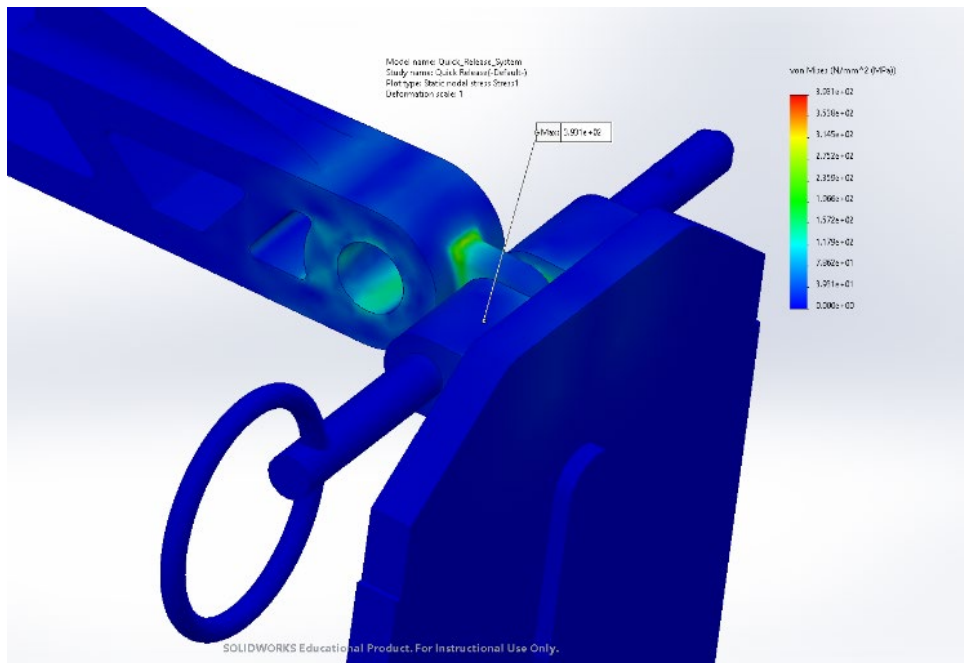


Figure 23: Quick release pin - back isometric view

Bottom Elastic Connection

The elastic band used to propel the UAV exerts a massive amount of force on different components. Hence, it is essential to study the stress concentrations on the part. To do so, we utilized the Solidworks FEA simulation, simulating a static load on an assembly. This study is done to account for the worst possible case where the pegs on the bottom have the highest stress concentrations. This occurs when the cradle is furthest from the stopper, with the bungees fully stretched. At this distance, the bungees will be generating 2667 N of force on either side of the holder, for a total of 5334 N of elastic force generated by the bungees. Reviewing the results of the Solidworks FEA static test in figures 24, 25, and 26, it is easy to see that the elastic connector design is more

than sufficient. The maximum stress concentration of 3.219×10^8 MPa is well below the material yield strength value of 1.1×10^9 MPa. On additional inspection, we can see that the most significant stress concentrations are found furthest from the point of application of the bands and closest to the holder. This concentration occurs as expected as the change in geometry causes a shearing force and bending moment on the fixed support rod from the holder.

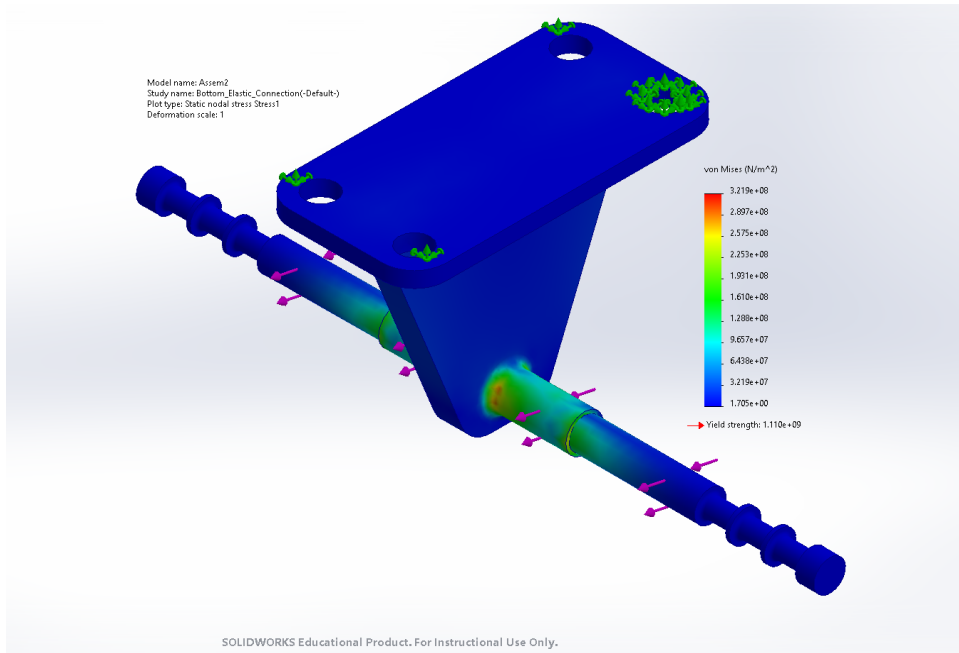


Figure 24: Bottom elastic connector - isometric view

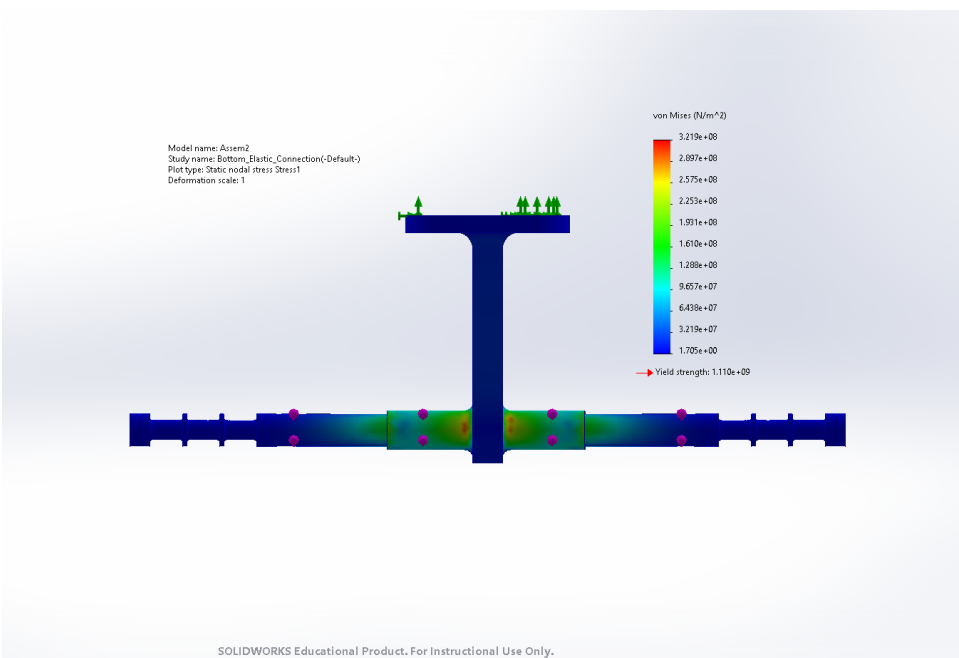


Figure 25: Bottom elastic connector - front view

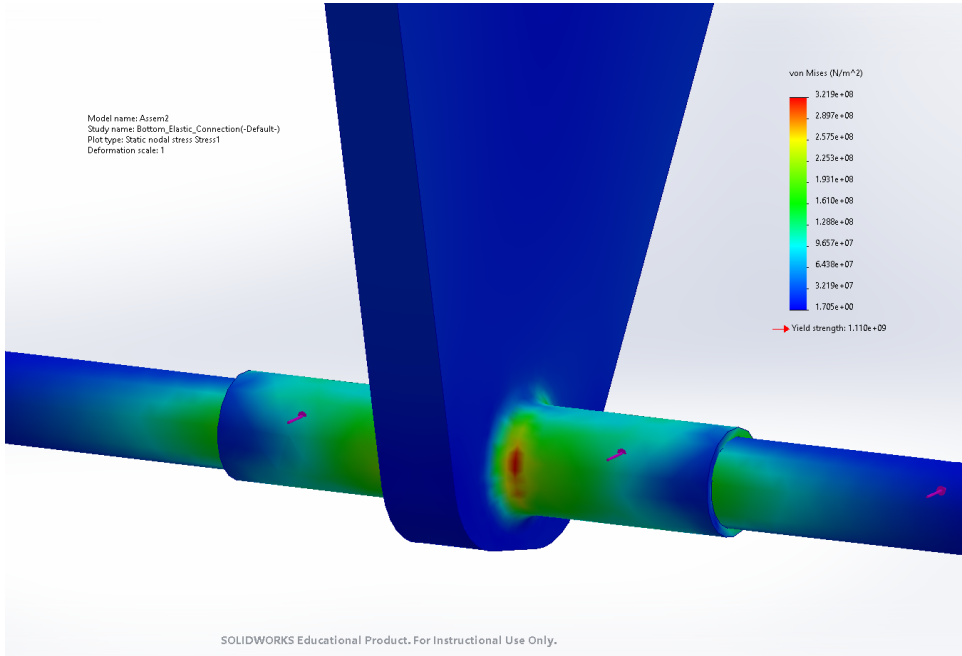


Figure 26: Bottom elastic connector high stress concentrations –isometric view

End Plate

The End Plate is responsible for withstanding two different forces: impact force and the static force caused by the elastic band. For this simulation, we chose to focus on the static case where the elastic exerts the total maximum force of 5334 N on each of the two pegs shown in Figure 28 below, due to the elastic wrapping around the peg and applying double the tension force. To simulate the static force, a Solidworks FEA simulation was used with the fixed end in Figure 29 attached to the rail and a 5867 N force (to be safe) simulating the elastic pulling the pegs towards the crank. Examining the results of the FEA, the pegs withstand the force well, with a maximum stress concentration of 4.493×10^8 MPa occurring closest to the main structure (fixed support) due to the shearing force and bending moment created by the elastic. Comparing the maximum stress with the yield strength of 1.110×10^9 MPa, this design is quite safe and allows for a high factor of safety, suggesting that the end plate is over-designed and will hold up to repeated launches.

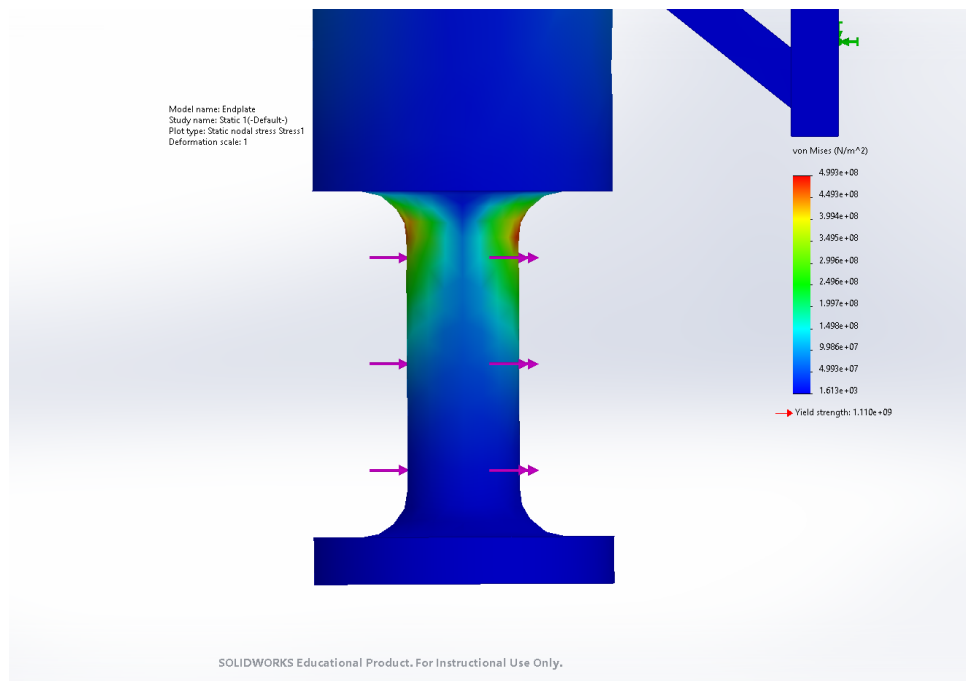


Figure 27: Endplate side peg geometry - side view

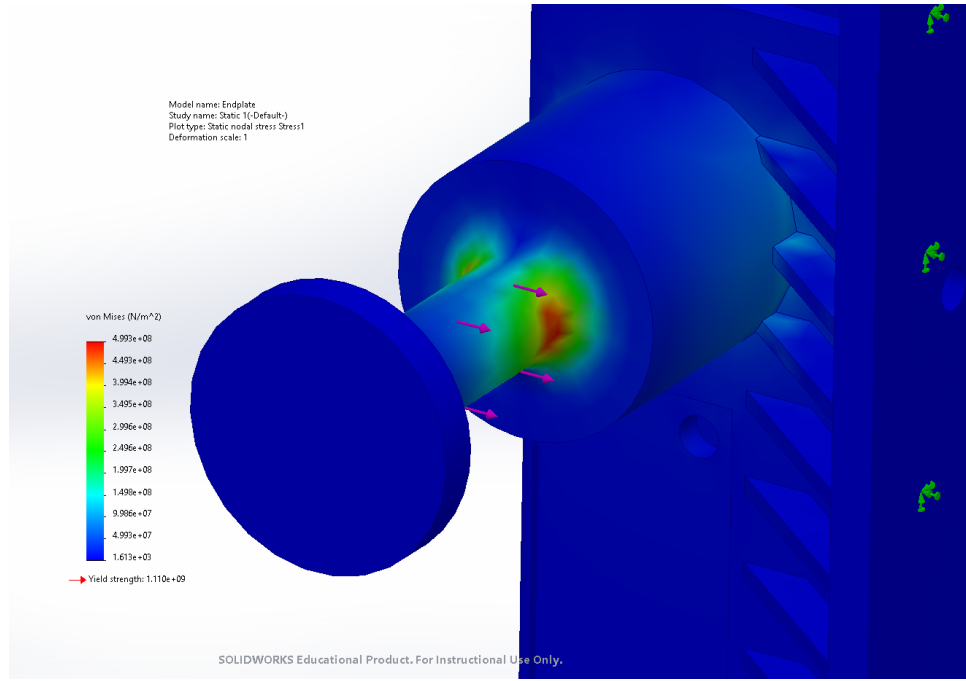


Figure 28: Endplate greatest stress concentrations – isometric view

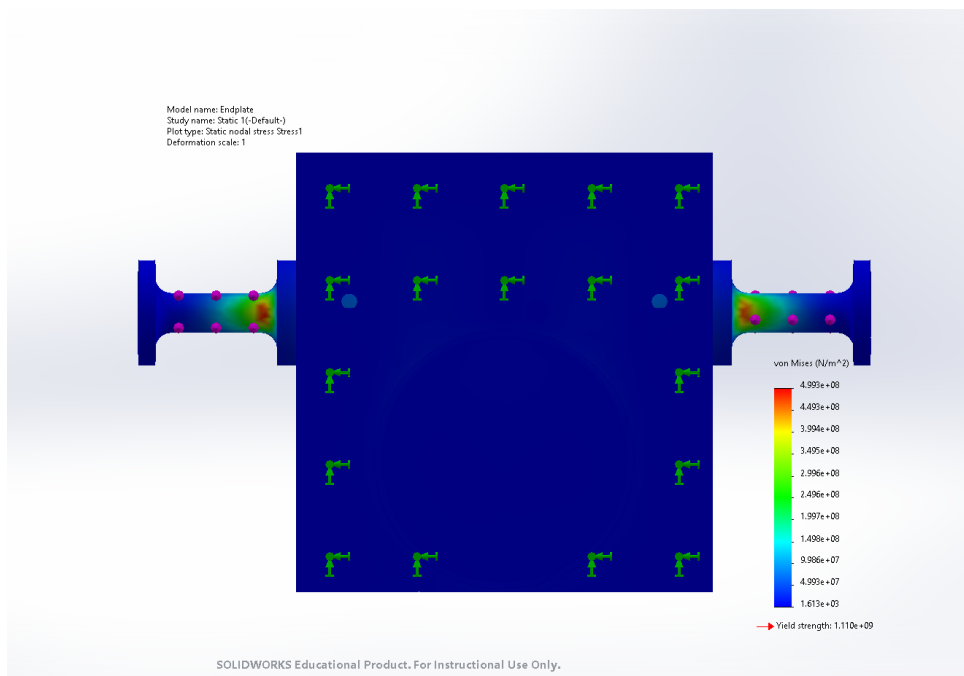


Figure 29: Endplate fixed geometry – front view

III. Final Design Evaluation

Design Evaluation

To assess the overall performance of the UAV launcher an initial criterion was generated based on the design objective set out in the initial stages of this project. These include:

- The design of a launch system to send a UAV into flight with appropriate launch velocity, and at an optimal departure angle.
- The design of a cradle to hold a variety of UAV systems such as a Skywalker X8 or a ScanEagle 3 and release it at the correct angle without causing any damage to the propelled object.
- To stop the cradle without causing damage, extending the lifecycle as long as possible and reducing chances of fatigue failure over time.
- To minimize the size and weight of the launch system to make it easily transportable.

These criteria have been further defined to include the ability to launch an 18kg UAV at 25m/s, have a failure rate below 1000 failures in time and weigh less than 150 kg.

We can now assess our project based on the goals laid out above and in Table 2 below. We can confidently say that we have achieved and surpassed all of our goals, with the project capable of launching a UAV weighing up to 20 kg at a speed of 25m/s, with an overall weight of just 94.3 kg, making it easily transportable and set up by three people. Additionally, if a drone weighing less than 20kg is used, a launch velocity greater than 25m/s can be achieved, thus exceeding the project goals. Essentially, the launchable load and speed goals are interchangeable and are each surpassed, given the other is constant and met. As shown in the calculations and simulations sections, the UAV Launcher should easily be able to perform over 1000 use cycles before a failure.

Criteria	1 - Project Goals Far Below Expected	2 - Project Goals Marginally Met	3 - Project Goals Met	4 - Project Goals Surpassed
Launchable load [kg]	10	15	18	20+
Launch Speed [m/s]	10	18	25	25+
Failure Rate (Uses until Failure)	10	100	1000	10000
Weight of Launcher [kg]	1000	500	150	75
Portability	Heavy Machinery Required	Pick up Truck/Van Required	Three People required to Transport	Single Person required to Transport

Table 2: Project evaluation criteria and goals

Cost Evaluation

Our initial budget for this project was \$10 000. As shown in Table 3, and Appendix E, the Bill of Materials (BOM) depicts all material and part costs associated with turning this design project into a real product. The total cost in the BOM is \$2,353.85, this comes out significantly below our initial budget but there are some caveats. A very significant cost not taken into consideration in this BOM is manufacturing, seeing as all the main components of this design would require custom fabrication, we would have to order the materials listed in items number 009 and 010, and have it fabricated in such a way that it fit our design, using methods such as CNC milling. Some estimates put this cost at 80-200 dollars an hour depending on the quality of the machine [13], but to achieve a more accurate figure we would have to work with a CNC milling company to get a quote. Despite this we believe we would still be able to come in under \$10 000, at final cost.

Item Number	Item	Supplier	Supplier Part Number	Material Description	Price	Quantity	Cost
001	Ball Bearing	MIMOTION	7408907	10 mm ID, 26 mm OD, 8 mm Width, Double Sealed, C3 Internal Clearance	\$ 28.54	6	\$ 171.24
002	Assorted O-Rings	KEWAYO	KEWAYO01	225 pieces included	\$ 16.47	1	\$ 16.47
003	C-Ring	Huyett	7318240000	ANSI B27.7-3CM1 (min order 7)	\$ 0.32	7	\$ 2.25
004	Draw Latch	D.B. Roberts Inc	R5-0074-07, R5-0079-07	Steel, zinc plated	\$ 39.97	4	\$ 159.88
005	Quick Release Pin	VTurboWay	B07RJBGHNP	316 Stainless Steel: 3"x1/4" (Full Length 3.75")	\$ 13.99	2	\$ 27.98
006	Bungee	Primeline Industries	Custom	2m x 1": 296.3 N/m	Quote	6	Quote
007	Heavy Hex Bolt	ASMC Industrial	0000-124212	M12 x 1.75 x 110 (30N) (min order 10)	\$ 3.46	10	\$ 34.64
008	Heavy Hex Nut	ASMC Industrial	0000-251292	M12 x 1.75 (min order 50)	\$ 1.47	50	\$ 73.60
009	Damper Material	Polycomp UK	Mil-DTL-25988C	CAD/kg	\$ 9.81	0.7	\$ 6.87
010	Structural Metal	ALTEMP USA	UNS N07718 nickel alloy inconel 718	CAD/kg	\$ 20.01	93	\$ 1,860.93
							Total: \$ 2,353.85

Table 3: Bill of Materials

IV. Conclusion

The initial goals and metrics set at the start of the design process for the UAV Launcher have all been met, allowing our primary aim of propelling a UAV into flight with appropriate departure angle, velocity, and associated design parameters, without sacrificing safety. Attaining the desired launcher performance while maintaining an acceptable safety factor in all loaded components was crucial to the success of our design. The components of the system with the greatest loads, such as the hand crank assembly, exceeded the desired safety factors, which was verified using hand calculations as well as FEA analysis in SolidWorks. By achieving these metrics, the project is an effective and versatile tool for the launching of standard UAV systems.

This design can be improved to make the manufacturing process of our product more feasible. The large safety factors may contribute to additional cost as they can be seen as “over-engineering” and hence use more material than necessary. We decided to implement large safety factors as our goals could be met and surpassed while keeping costs and weights low, and higher safety factors ensure the longevity, durability, and dependability of our system. More optimization would allow us to reduce the weight and cost of the system by using less material and more easily manufactured geometries.

The materials used in the case of this project were meticulously chosen, using Granta EduPack, based on various different parameters that were set such as the impact that the rubber had to withstand and the forces the metal would be put under. Other parameters that were considered in our case were the environment in which the launcher would be used. This helped narrow down the precise material required for all the parts in our design. Through this extensive research, we were also able to roughly estimate the material cost for each of the parts, helping us find an approximation for the total price of the entire system. Additionally, the goal of system mass being under 150 kg was exceeded, with the final weight coming out at 93.4kg. This weight could have been decreased with a more optimized rail design using a topology study, however due to a time constraint, this was not possible.

Overall, the design of our UAV Launcher system met or exceeded all the design goals and objectives with no issues. The system is light, portable, cheaper than anticipated, over-engineered, safe, dependable and is able to perform exactly what is expected of it. There are no real disadvantages or cons in our design or any characteristics that are not necessarily desired. Our UAV Launcher system checks all the boxes and more than achieves everything it was designed to accomplish.

V. References

- [1] Boeing, [Online]. Available: <https://www.boeing.com/farnborough2014/pdf/BDS/ScanEagle%20Backgrounder%200114.pdf>. [Accessed 4 December 2022].
- [2] Naval Technology, [Online]. Available: <https://www.naval-technology.com/projects/scaneagle-uav/>. [Accessed 4 December 2022].
- [3] NASA, [Online]. Available: https://msis.jsc.nasa.gov/sections/section04.htm#_4.6_KINESTHESIA.
- [4] OGGB, [Online]. Available: <https://www.ggbearings.com/en/why-choose-ggb/faq/bearings-faq/what-ball-bearing#:~:text=A%20ball%20bearing%20is%20a,and%20friction%20across%20moving%20planes>. [Accessed 4 December 2022].
- [5] 3. Insider. [Online]. Available: <https://3dinsider.com/ball-vs-roller-bearings/>. [Accessed 4 December 2022].
- [6] MiMotion, [Online]. Available: <https://www.motion.com/products/sku/07408907>.
- [7] Corosionpedia, [Online]. Available: <https://www.corrosionpedia.com/definition/1193/yield-strength>.
- [8] Birmingham, University of, [Online]. Available: [https://www.birmingham.ac.uk/teachers/study-resources/stem/Physics/youngs-modulus.aspx#:~:text=The%20Young%27s%20modulus%20\(E\)%20is,%CE%B5%20%3D%20dl%2Fl](https://www.birmingham.ac.uk/teachers/study-resources/stem/Physics/youngs-modulus.aspx#:~:text=The%20Young%27s%20modulus%20(E)%20is,%CE%B5%20%3D%20dl%2Fl). [Accessed 4 December 2022].
- [9] University, Iowa State, [Online]. Available: <https://www.nde-ed.org/Physics/Materials/Mechanical/Toughness.xhtml>.
- [10] Shapes., [Online]. Available: <https://www.shapesbyhydro.com/en/material-properties/why-structural-projects-need-ductile-metals-like-aluminium/#:~:text=Ductility%20allows%20structures%20to%20bend,So%20are%20most%20aluminium%20alloys>. [Accessed 4 December 2022].
- [11] Vedantu, [Online]. Available: <https://www.vedantu.com/physics/plastic-deformation>. [Accessed 4 December 2022].
- [12] MDPI, [Online]. Available: <https://www.mdpi.com/2073-4360/14/6/1186/htm#:~:text=Elastomer%20insulators%20are%20able%20to,damage%20or%20change%20of%20shape>. [Accessed 4 December 2022].
- [13] 3ERP, [Online]. Available: <https://www.3erp.com/blog/cnc-milling-cost/#:~:text=The%20average%20CNC%20machining%20cost,sophisticated%20CNC%20machines%20cost%20more..> [Accessed 4 December 2022].

- [14] The Hope Group, [Online]. Available: <https://www.thehopegroup.com/blog/2020/08/o-ring-material-guide/>. [Accessed 4 December 2022].

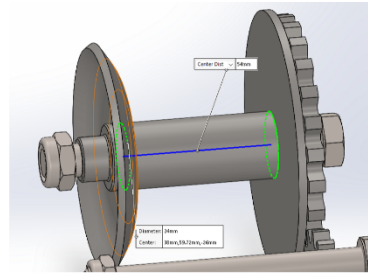
VI. Appendix

Appendix A: Hand calculations

Wind/Crank

assuming $\frac{1}{8}$ inch wire rope diameter = 6.35 mm

$$\frac{54}{6.35} = 8.5 \Rightarrow 8 \text{ wraps per spool layer}$$



$$OD = n(2y) = 75.4 \text{ mm} + \frac{6.35}{2} = \text{wrap diameter} = 78.6 \text{ mm}$$

Needed spool length = 3m = 3000 mm

$$3000 = \sum_{i=0}^n (78.6 \text{ mm} + 6.35i) \cdot 8, \quad n+1 = \text{spool layers.}$$

$$n \approx 3.2 \Rightarrow \text{round up to } 4 \Rightarrow n+1 = 5$$

@ 5th spool layer, distance from center axis = $\frac{2y}{2} + 6.35 \times 5 - \frac{6.35}{2}$

\Rightarrow spool radius + 5 wire diameters - $\frac{1}{2}$ diameter (for centroid) = 90.6 mm.

Tension on rope @ this point = max tension of elastis stretched to 3m. = $\boxed{5334 \text{ N}}$

$$470.6 \text{ mm} = 0.4706 \text{ m.} \quad T = Fr = 5334 \times 0.04706 = \boxed{216.4 \text{ Nm}}$$

Design shaft: 54 mm diameter enough?

Gear ratio? from NASA ^{average} 1 person can generate about 120N cranking force. MAX.

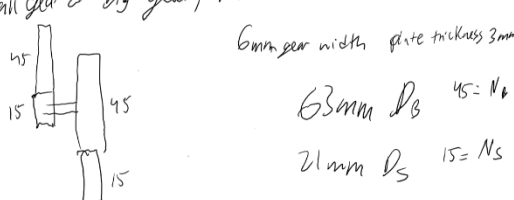
$$25 \text{ cm handle} \Rightarrow 0.25 \times 120 = \boxed{30 \text{ Nm}}$$

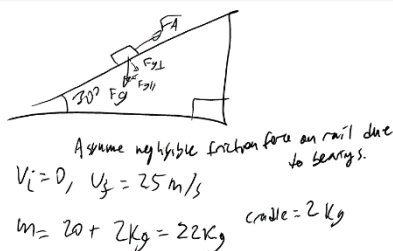
$$\text{using 80% effort} \Rightarrow \boxed{24 \text{ Nm}} \quad \frac{216.4}{24} = 9 \times \text{torque reduction.}$$

Using table 8-7: can use $\boxed{N_s = 15} \quad \boxed{N_B = 45}$
for No interference. Using 200 full depth pinion spur gears.

$$\text{Using } R_{s_{\text{min}}} = \boxed{10.5 \text{ mm}}, \quad R_{B_{\text{max}}} = 9 \times 10.5 = \boxed{31.5 \text{ mm}} \\ \text{Small gear & big gear, need 2 sets & 3 shafts: } \frac{45}{15} \times \frac{45}{15} = 9 \checkmark$$

6mm gear width plate thickness 3mm handle 6mm.





Assume rail length $\approx 3 \text{ m}$.

$$d = 3 \text{ m}, \quad V_f^2 = V_i^2 + 2ad$$

$$\Rightarrow 25^2 = 2a(3)$$

$$\Rightarrow a = 104 \text{ m/s}^2$$

$$F_A - F_{g\parallel} = F_A - 22(\sin 30)(9.81) = 72(104) = m_a$$

$$\Rightarrow F_A = 2395.91 \text{ N}$$

$$d = V_i t + \frac{1}{2} a t^2 \Rightarrow 3 = \frac{1}{2}(104)t^2 \Rightarrow t = 0.24 \text{ sec.}$$

$$W = \Delta E = 2396 \times 3 = F_d = 7187.73 \text{ J}$$

$$P = \frac{\Delta E}{\Delta t} = \frac{7187.73}{0.24} = 29918.88 \text{ W}$$

$$\text{Check: } \Delta KE = \frac{1}{2} (22)(25)^2 = 6875 \text{ J}$$

$$\Delta PE = mgh = 22(9.81)(\sin 30)(3) = 323.73 \text{ J}$$

$$\Delta PE + \Delta KE = \Delta E = W = 6875 + 323.73 = 7198.73 \text{ J}$$

0.15% error rounding.

Assume elastic bands acts as ideal spring:

$$PE_{\text{stored}} = U = \frac{1}{2} K(\Delta x)^2 \Rightarrow \Delta x = \text{rail length} = 3 \text{ m}$$

Assuming 90% efficiency of energy conversion
(due to friction, some slack @ end of rail, etc.)

$$\frac{7198.73}{0.9} = U = 7998 \approx 8000 \text{ J} = \frac{1}{2} K(3)^2$$

$$\Rightarrow K = 1778 \text{ N/m}$$

② 3m stretched length:

$$F = Kx = 1778 \times 3 = 5334 \text{ N}$$

\Rightarrow Max force on crank & quick release pin.

Cradle stopper

$$(25 \text{ m/s}) (22 \text{ kg}) = 550 \text{ kg m/s momentum}$$

$$\Delta KE = \frac{1}{2} (22)(25)^2 = 6875 \text{ J.}$$

Assume 2 cm deflection: 0.02 m.

$$25^2 = 2a(0.02) \Rightarrow a = 15625$$

$$m_{cradle} a = 2(15625) \approx 31250 \text{ N impact force}$$

$$\frac{F}{A} = \frac{31250}{(350+490 \times 2 + 600) \text{ mm}^2 \times 10^{-6}} = \frac{31250}{1930 \times 10^{-6}} = 16.2 \text{ MPa.}$$

Check 0.02 m deflection assumption:

$$S = \frac{\Delta L}{L} = \frac{0.02}{0.1} = 0.2.$$

Young's Modulus = 750 MPa $\Rightarrow 5171 \text{ kPa SBR rubber}$

$$E = \frac{\sigma}{\epsilon} = \frac{FL}{ADL} = \frac{16.2 \times 10^6}{0.2} = 81 \text{ MPa. } \neq 5.17 \text{ MPa.}$$

$$\therefore F = \frac{25^2 L}{A(L)^2} = 25000 \text{ N from } (v_s^2 - v_i^2) = 2ad$$

$$\therefore E = 5.17 \text{ MPa} = \frac{FL}{ADL} = \frac{25^2 L}{A(L)^2} = \Delta L = 0.08 \neq 0.02$$

Too high! need stiffer material:

use FVMQ flangosilicone.

$$E = 50 \text{ MPa} = \frac{(25^2)L}{A(L)^2} @ L = 0.10 \text{ m} \Rightarrow \Delta L = 0.025 \text{ m} \checkmark$$

$$\therefore F = ma, m = 2 \Rightarrow 2a = \frac{25^2}{0.025} = 25000 \text{ N from } (v_s^2 - v_i^2) = 2ad$$

$$\therefore \sigma = \frac{25000}{(1930 \times 10^{-6})} = 12.95 \text{ MPa}$$

\Rightarrow just under yield stress
for FVMQ, ensures elastic deformation

12.95 MPa \Rightarrow Max stress on cradle & stopper contact area,

(@ 25000 N impulse force @ impact)

(@ 0.025 m = 2.5 cm compression deflection of stopper.)

Appendix B: Engineering drawings

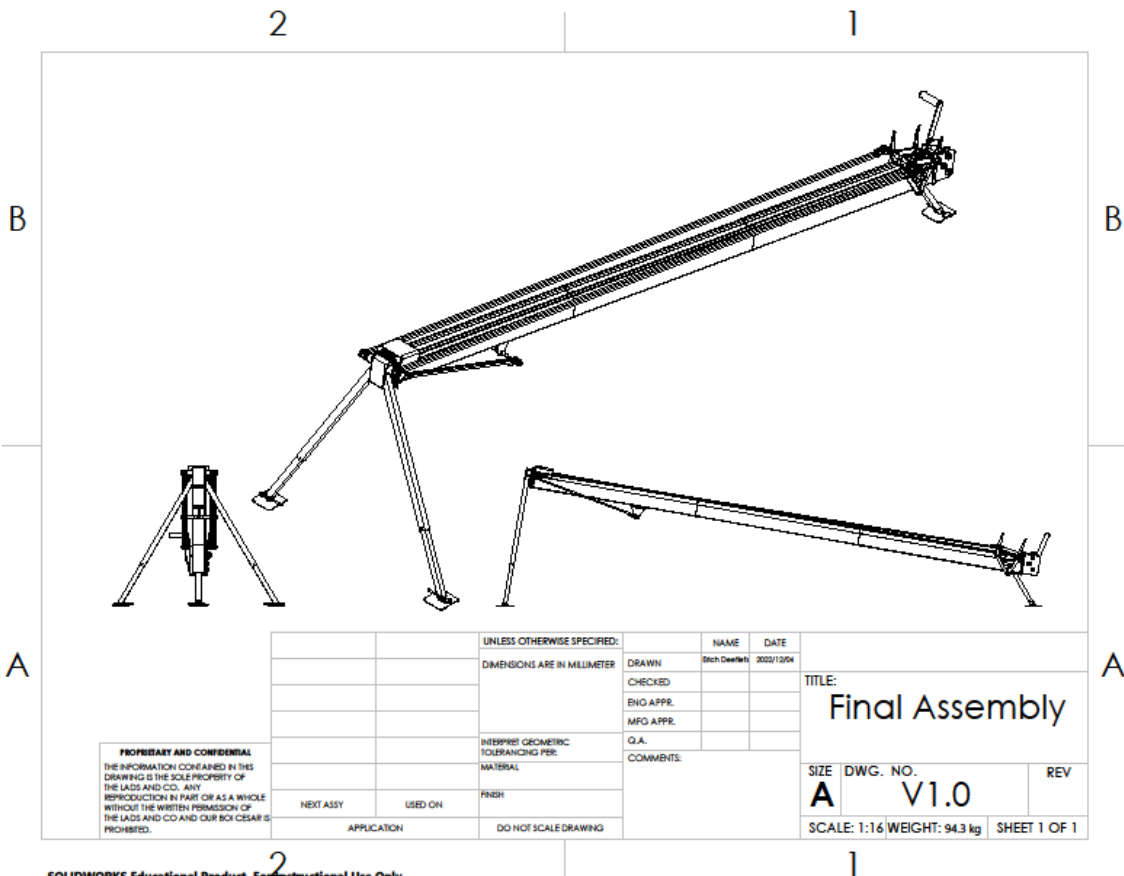


Figure 30: Final assembly

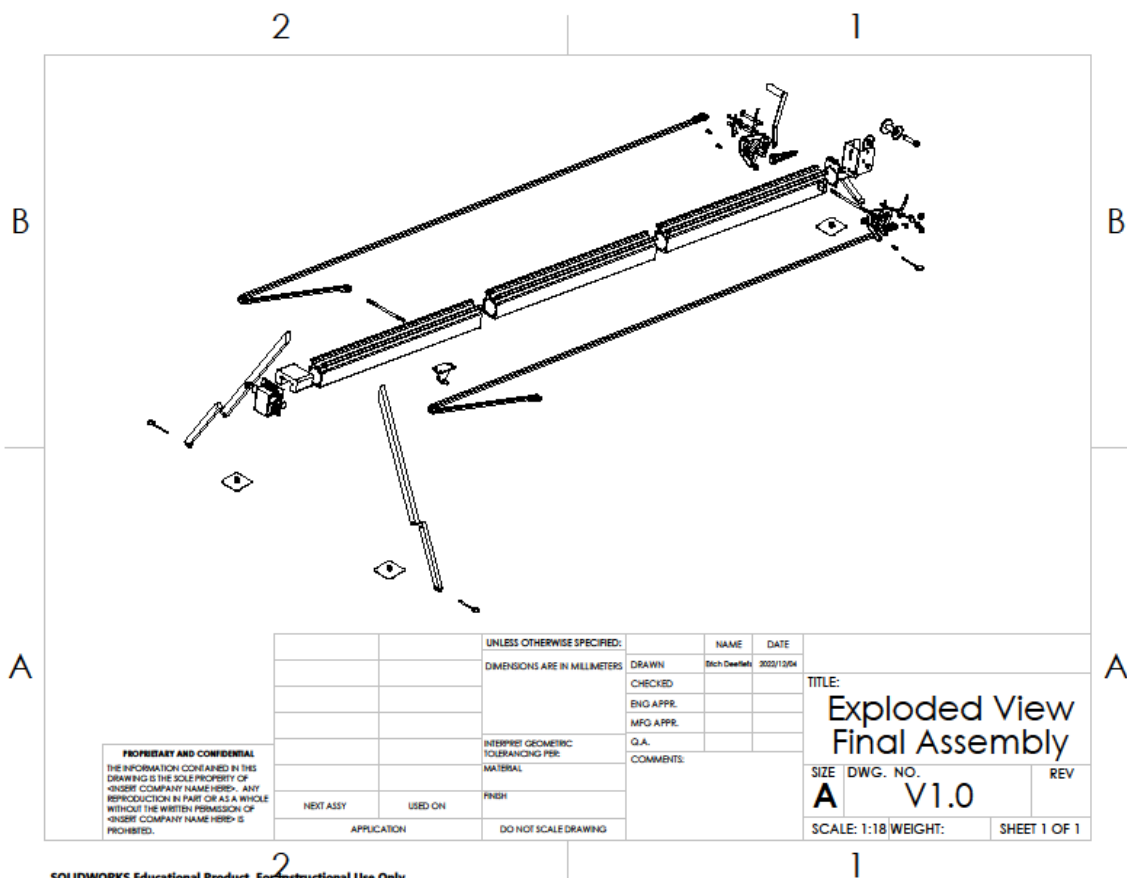


Figure 31: Exploded view final assembly

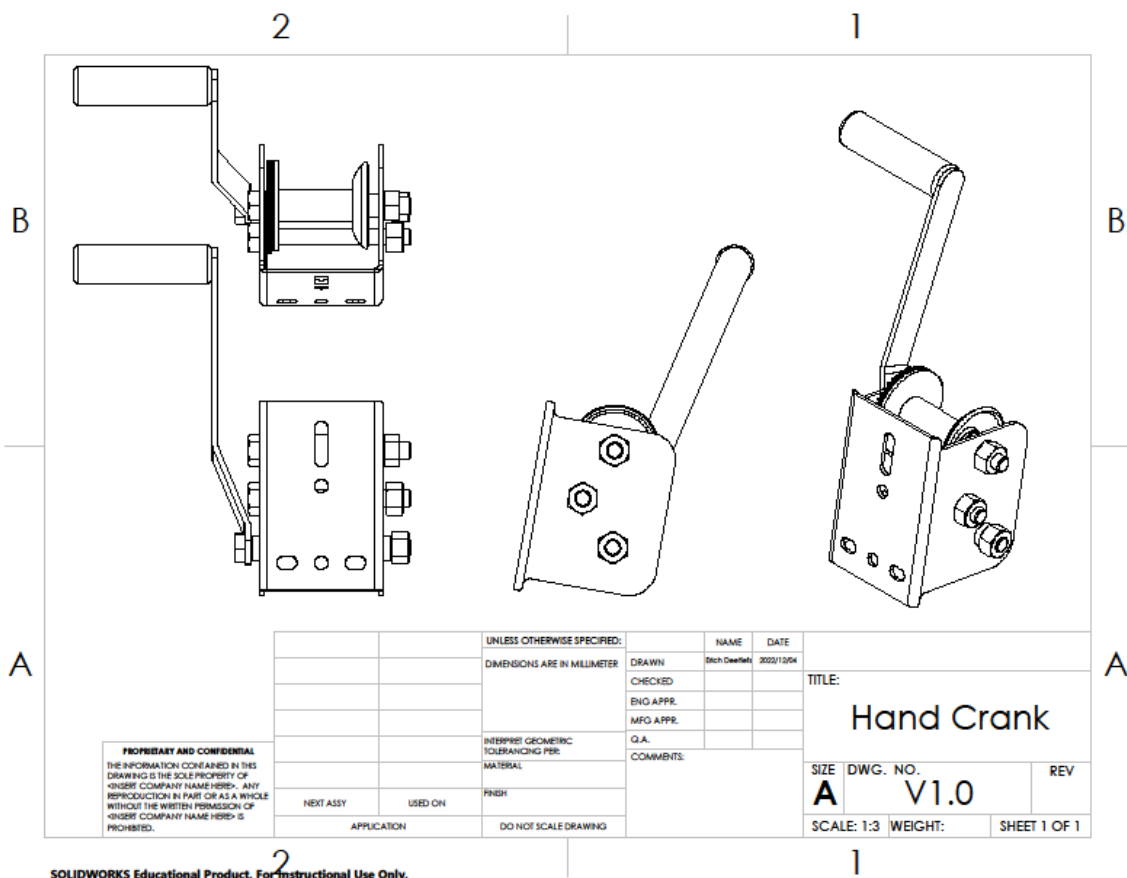


Figure 32: Hand crack

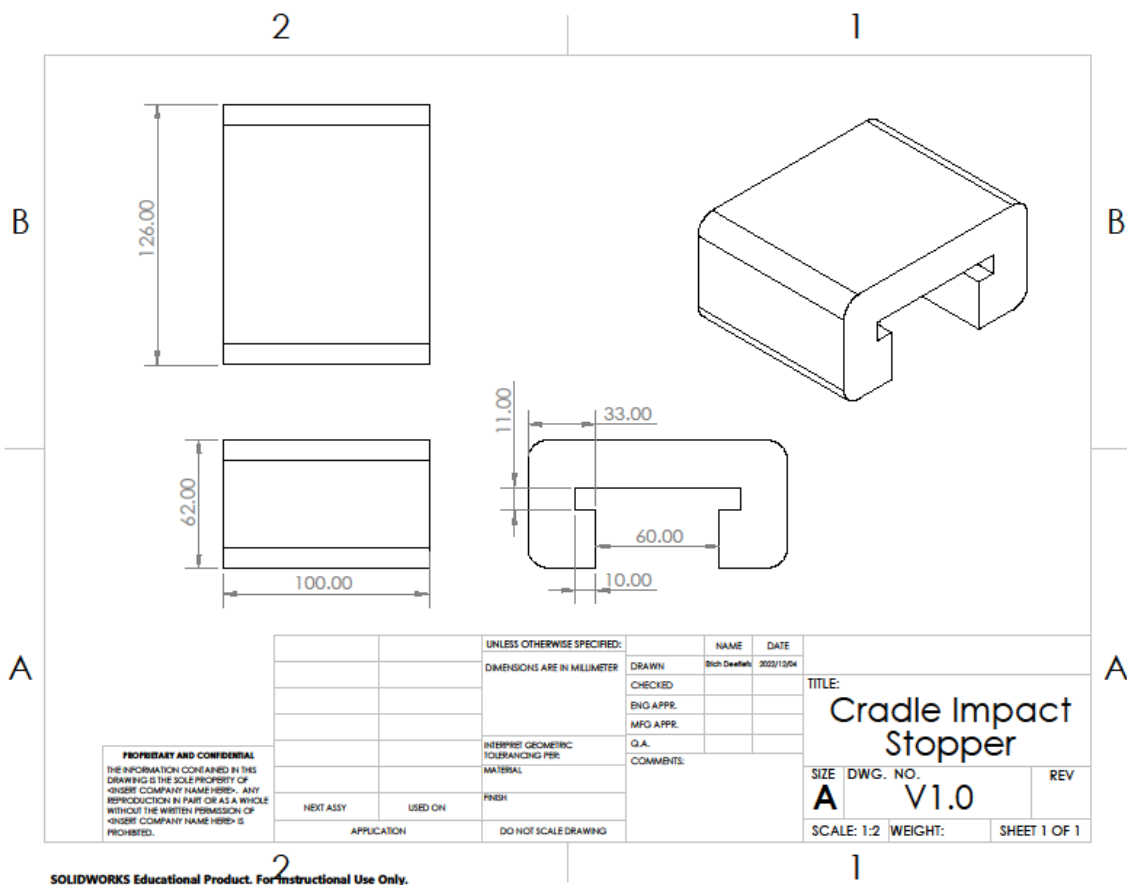


Figure 33: Cradle impact stopper

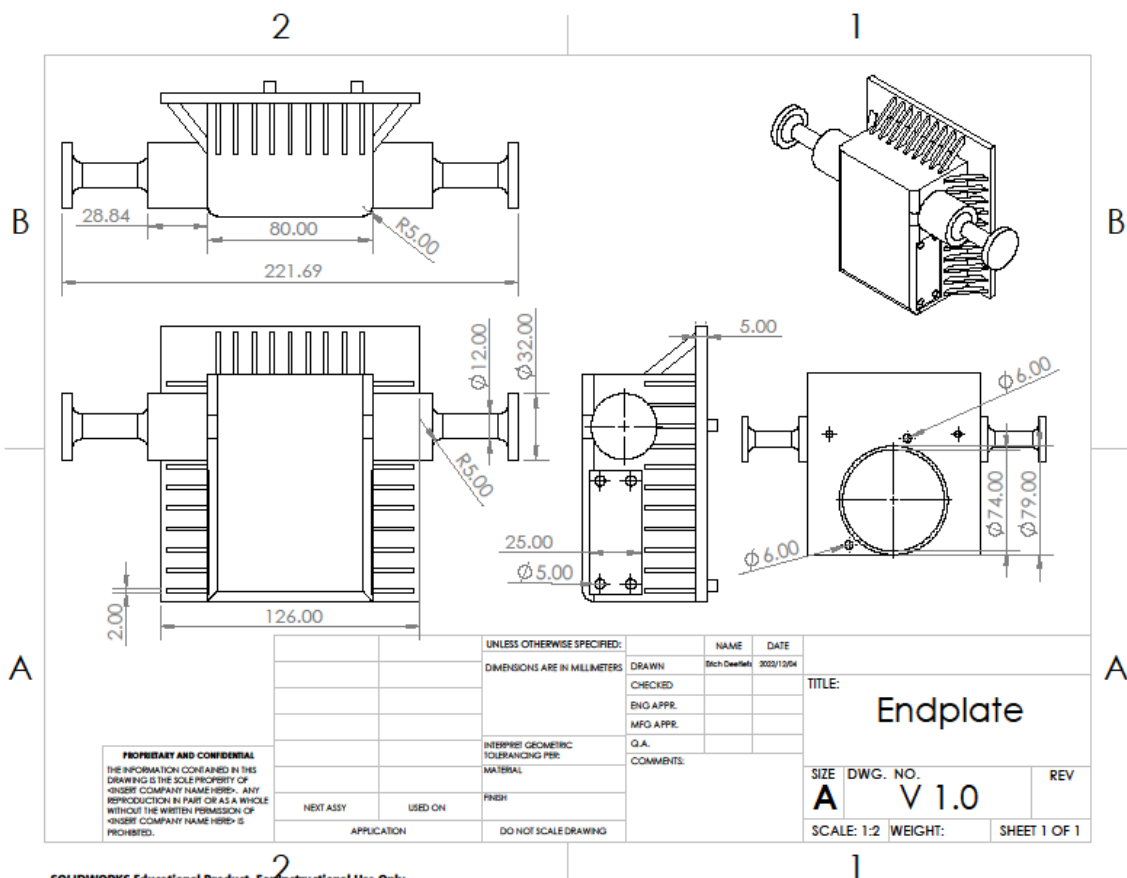


Figure 34: Endplate

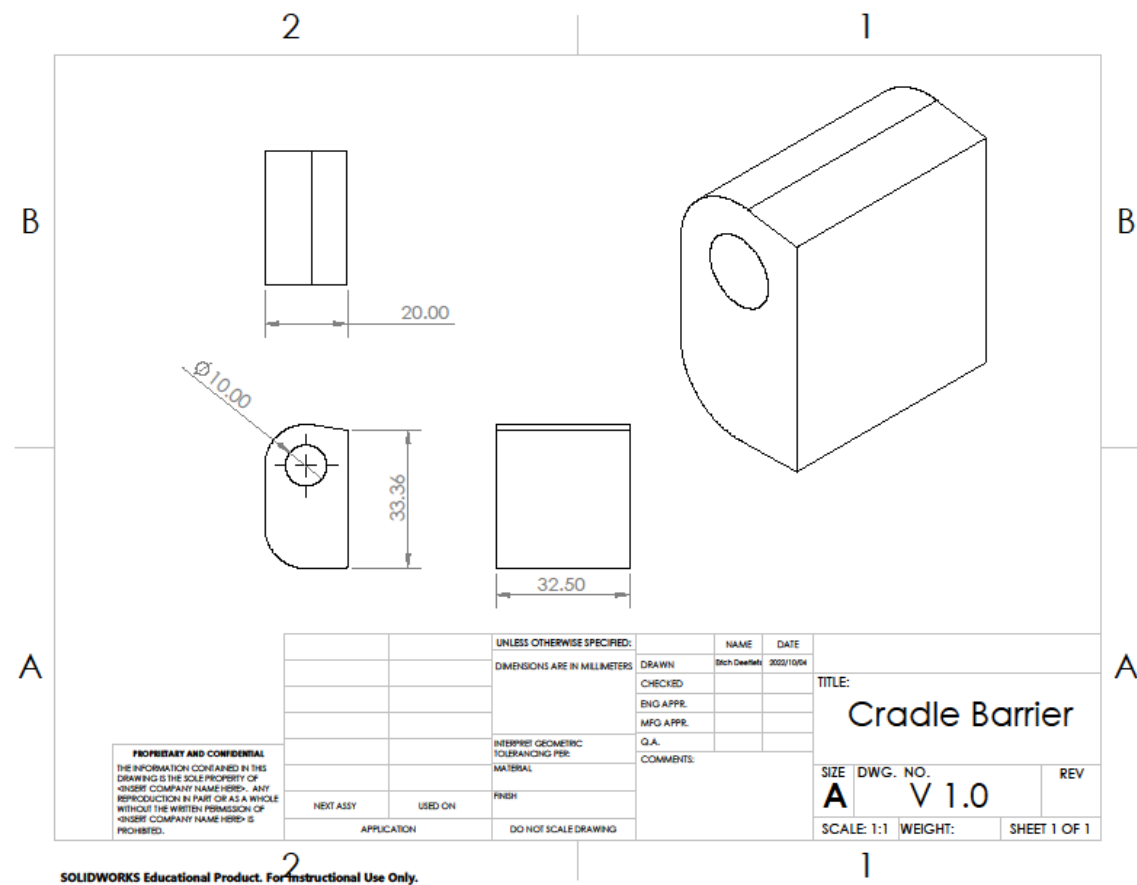


Figure 35: Cradle Barrier

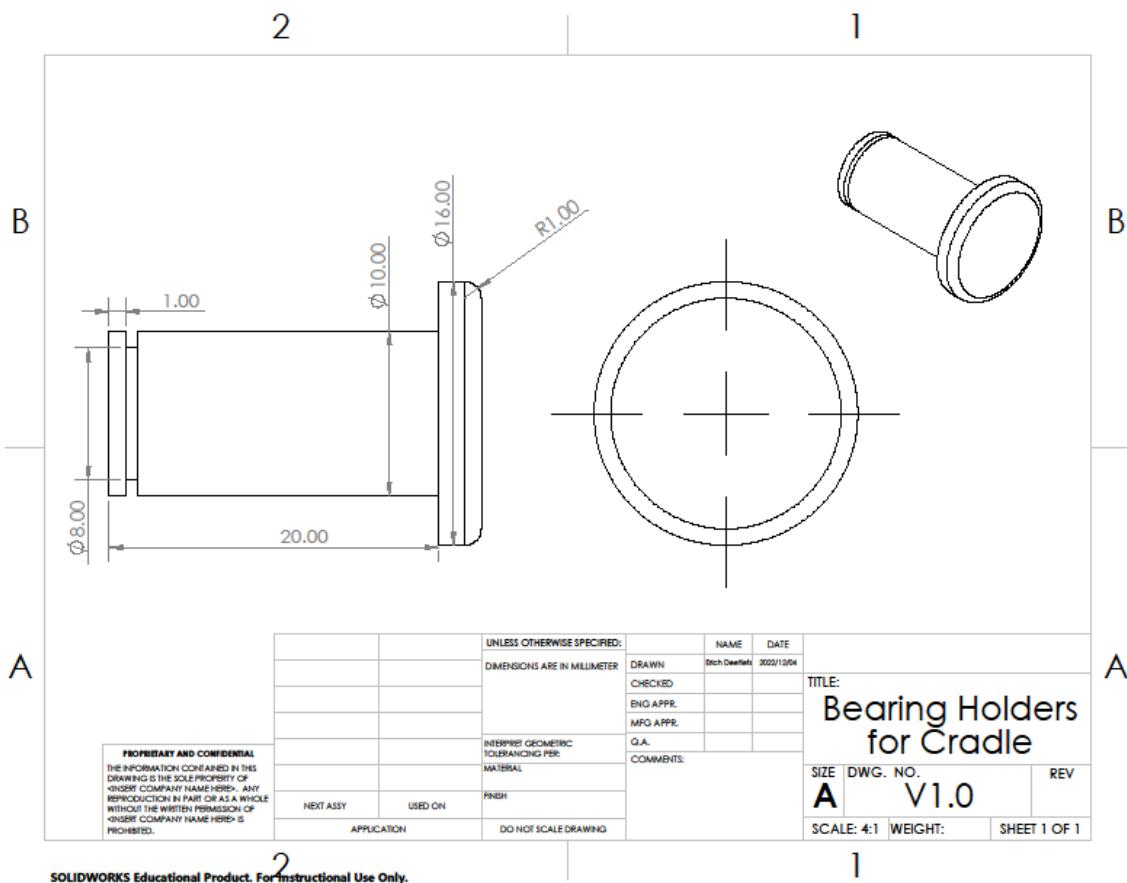


Figure 36: Bearing holders for cradle

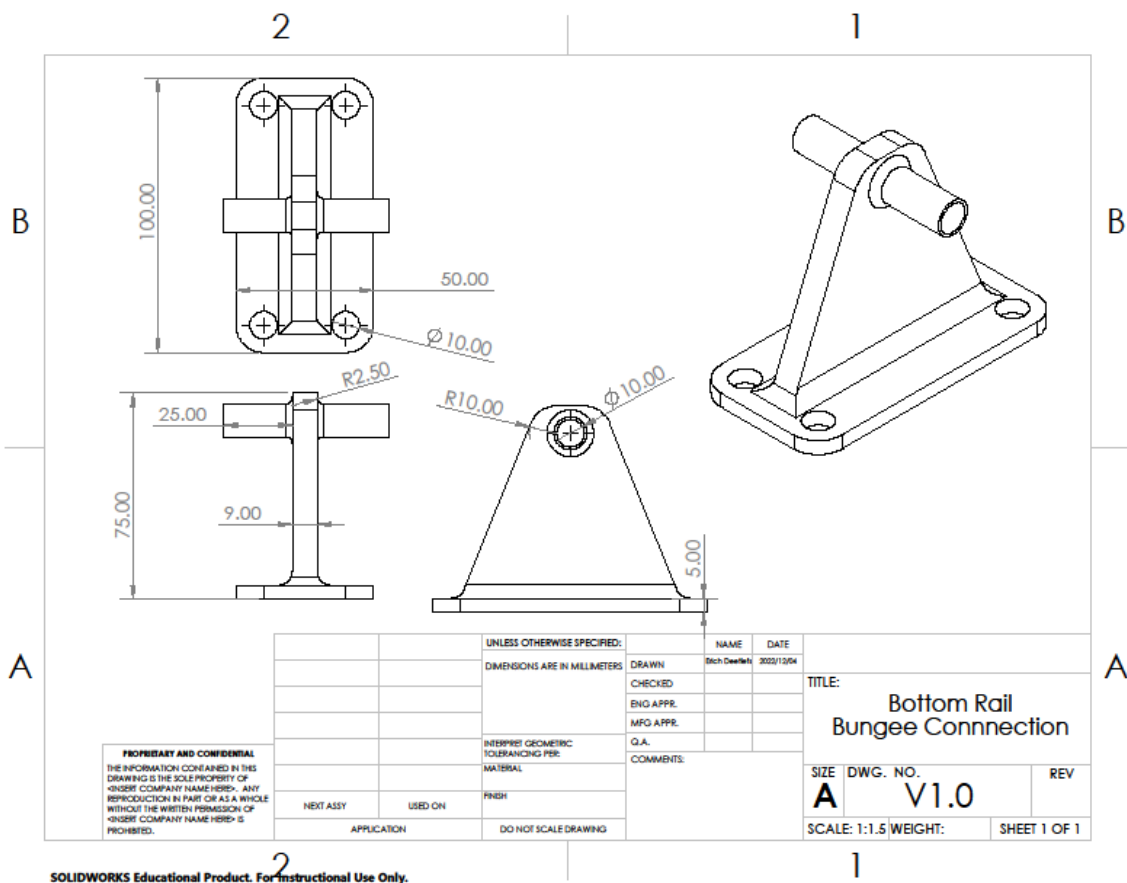


Figure 37: Bottom rail bungee connection

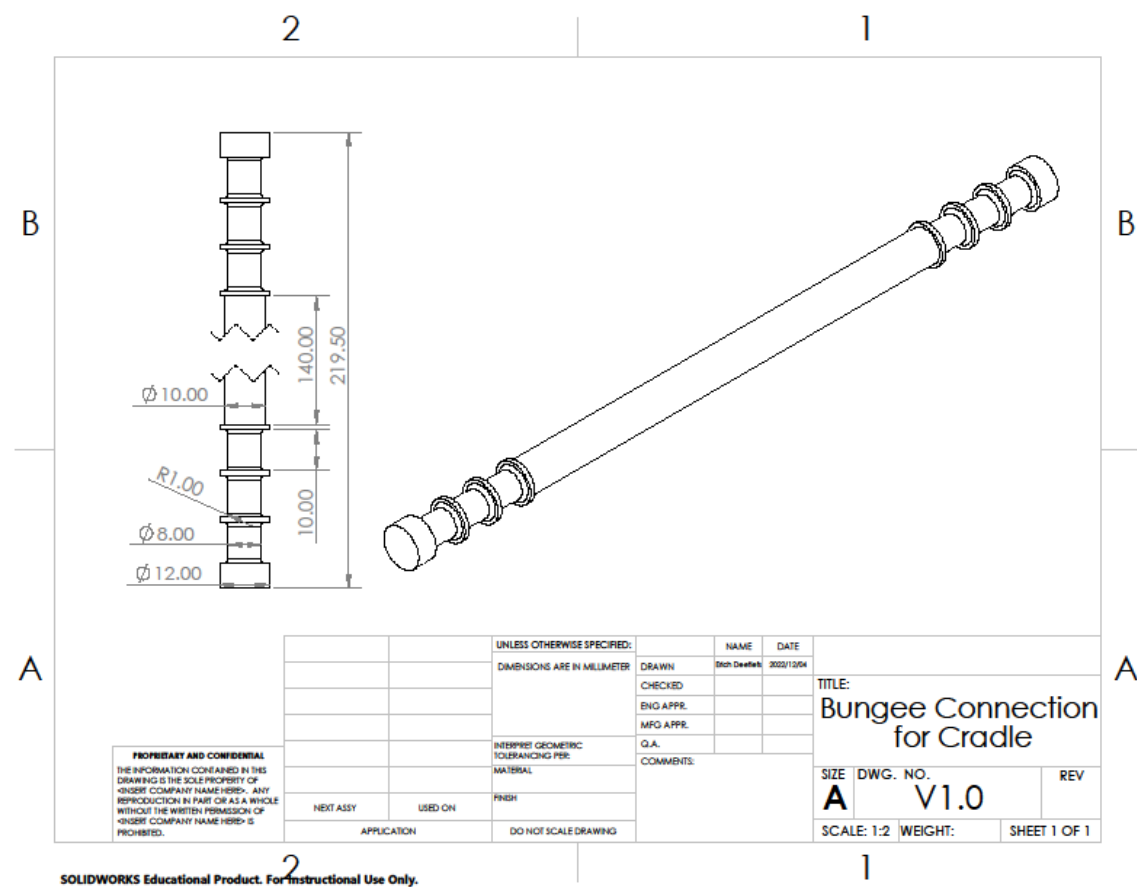


Figure 38: Bungee connection for cradle

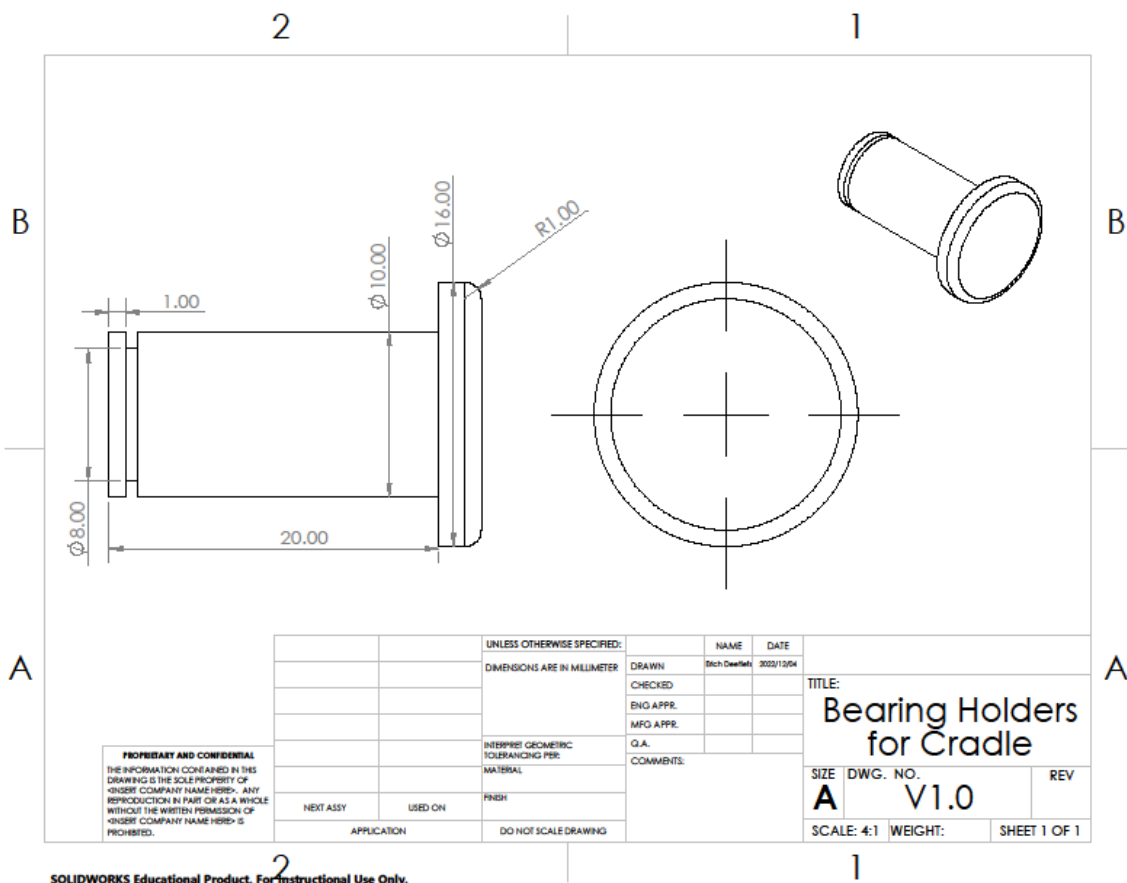


Figure 39: Bearing holders for cradle

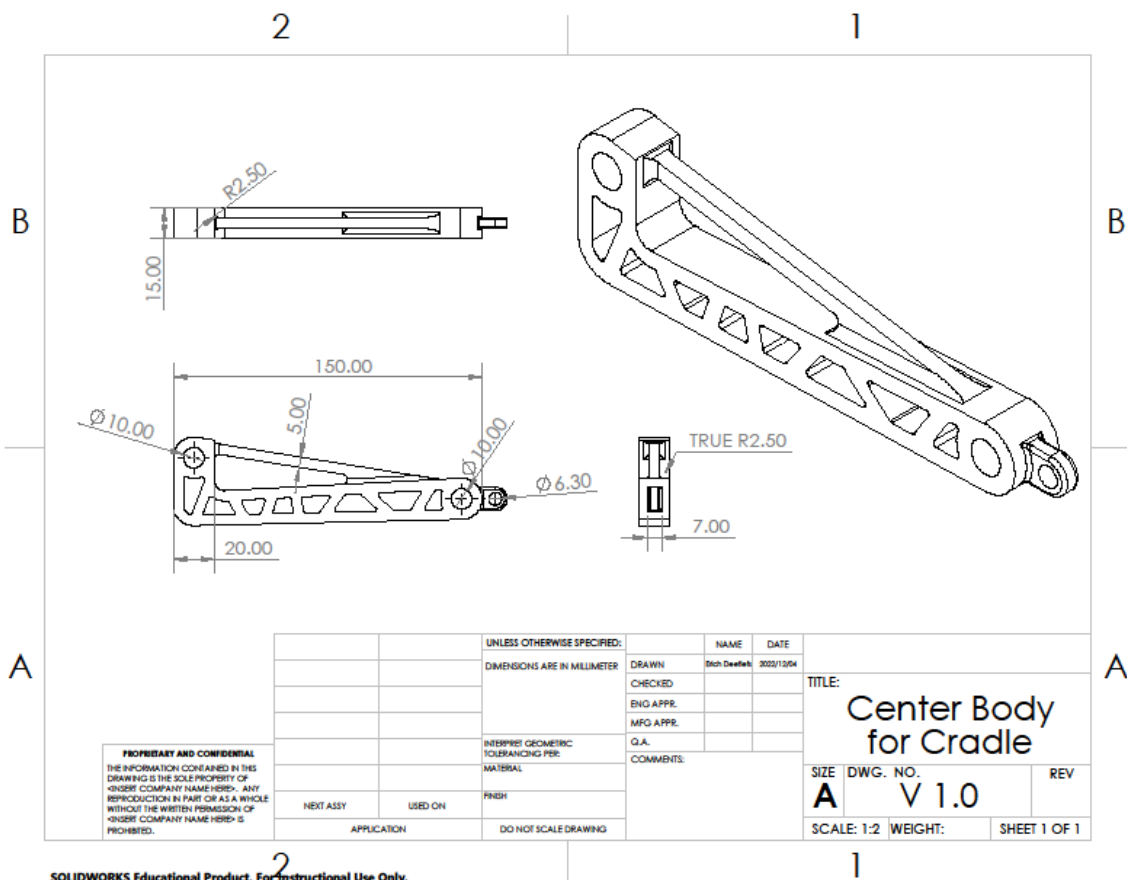


Figure 40: Center body for cradle

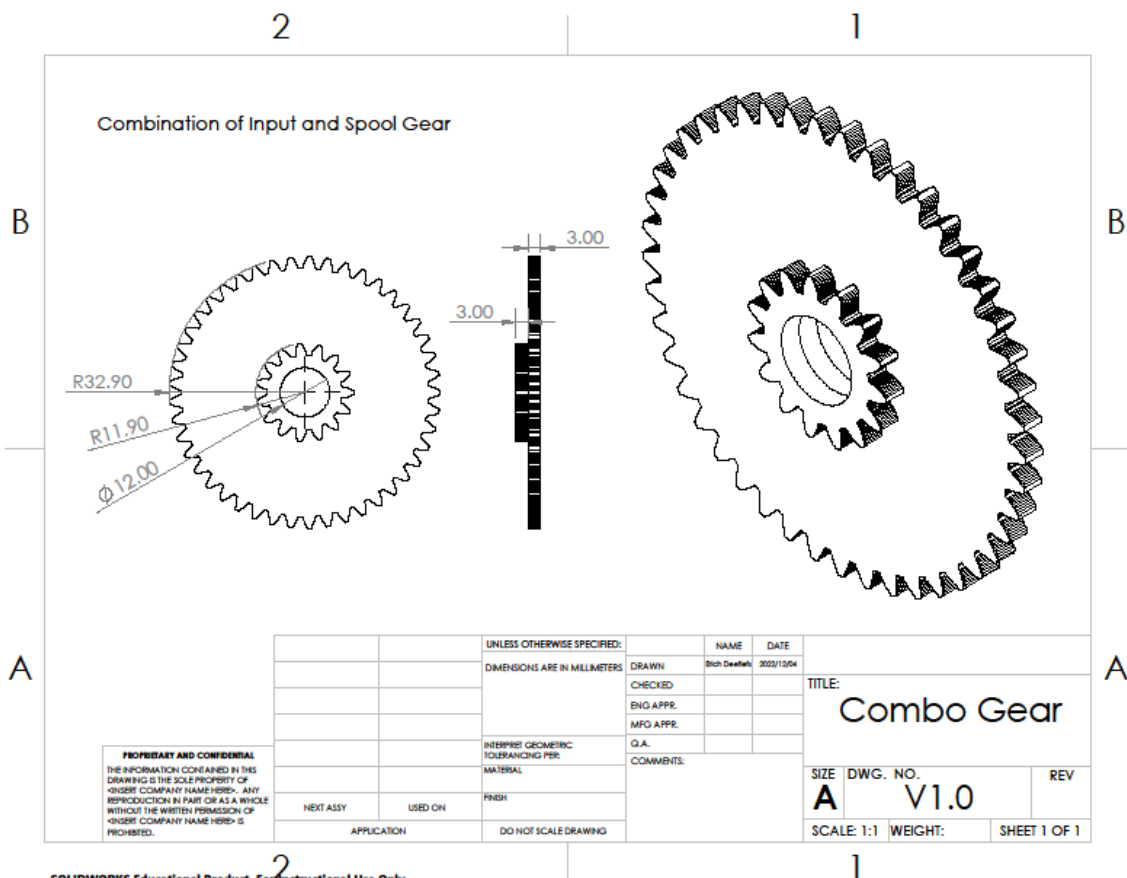


Figure 41: Combo gear

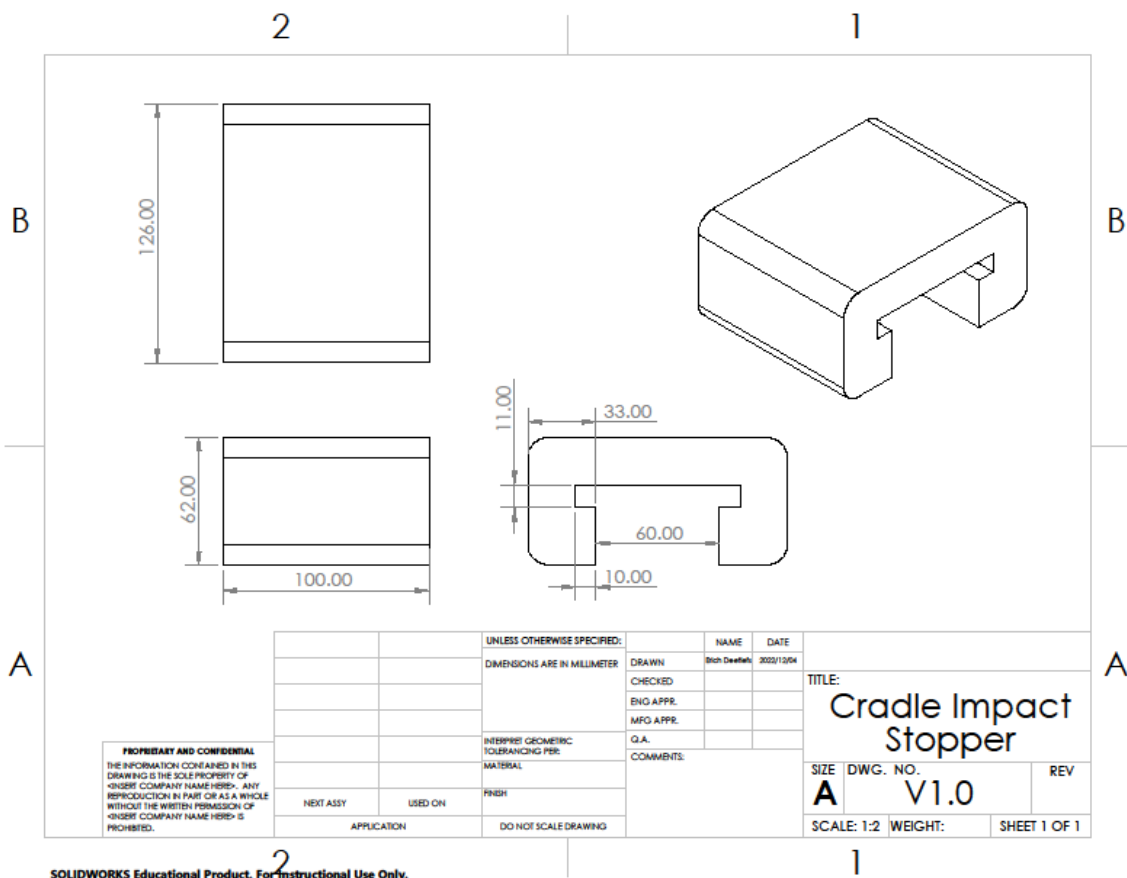


Figure 42: Cradle impact stopper

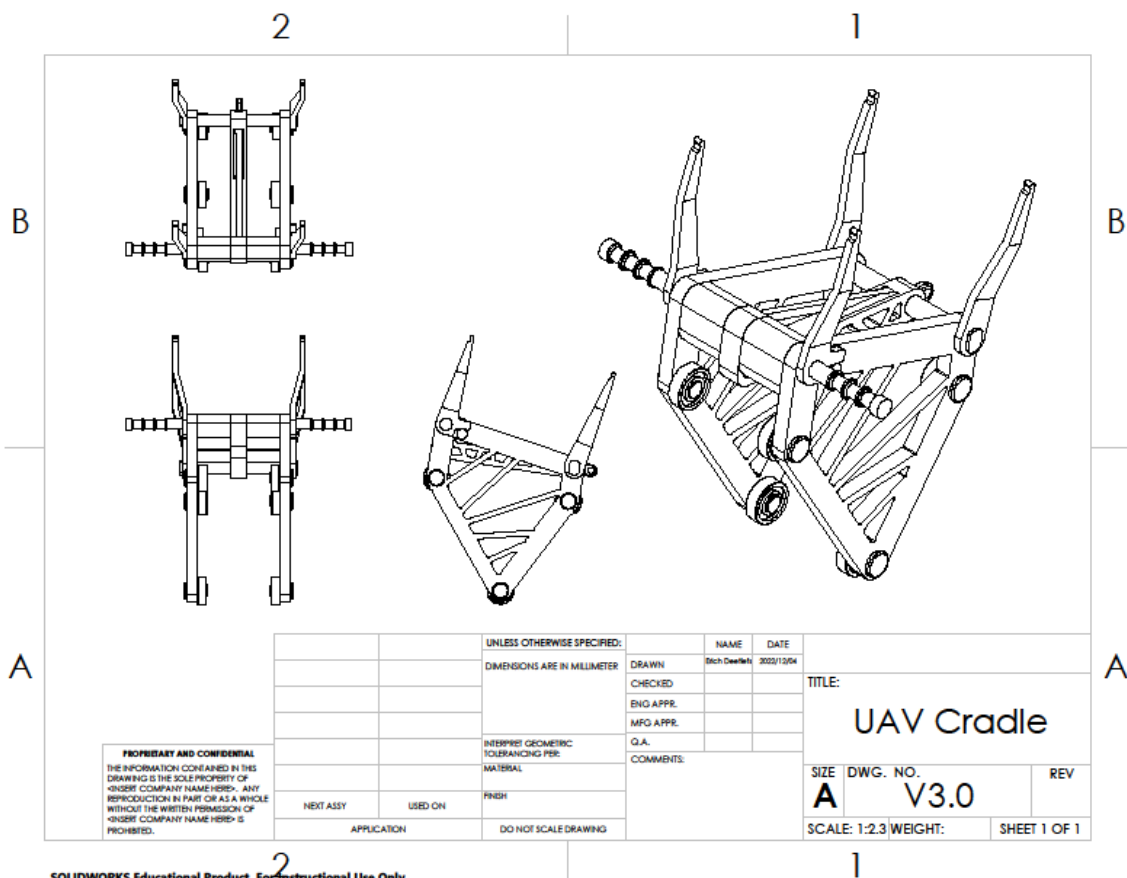


Figure 43: UAV cradle

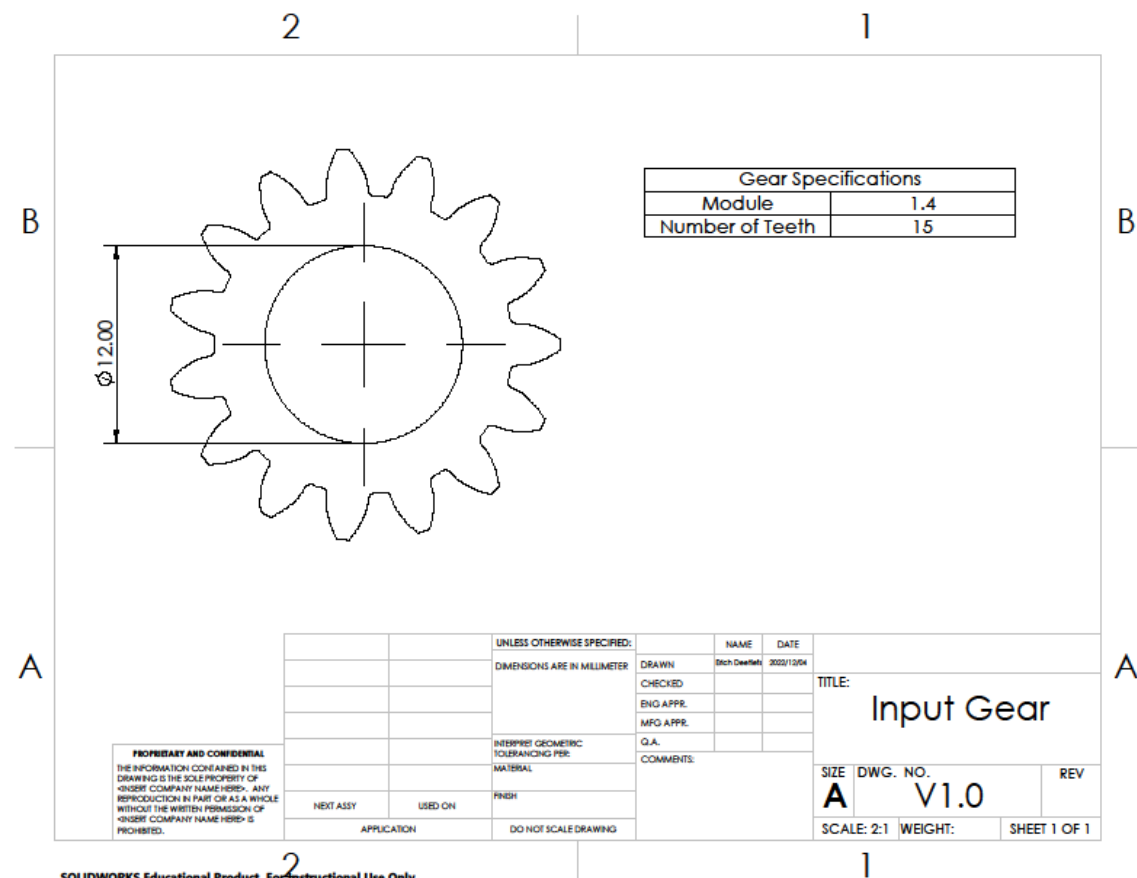


Figure 44: Input gear

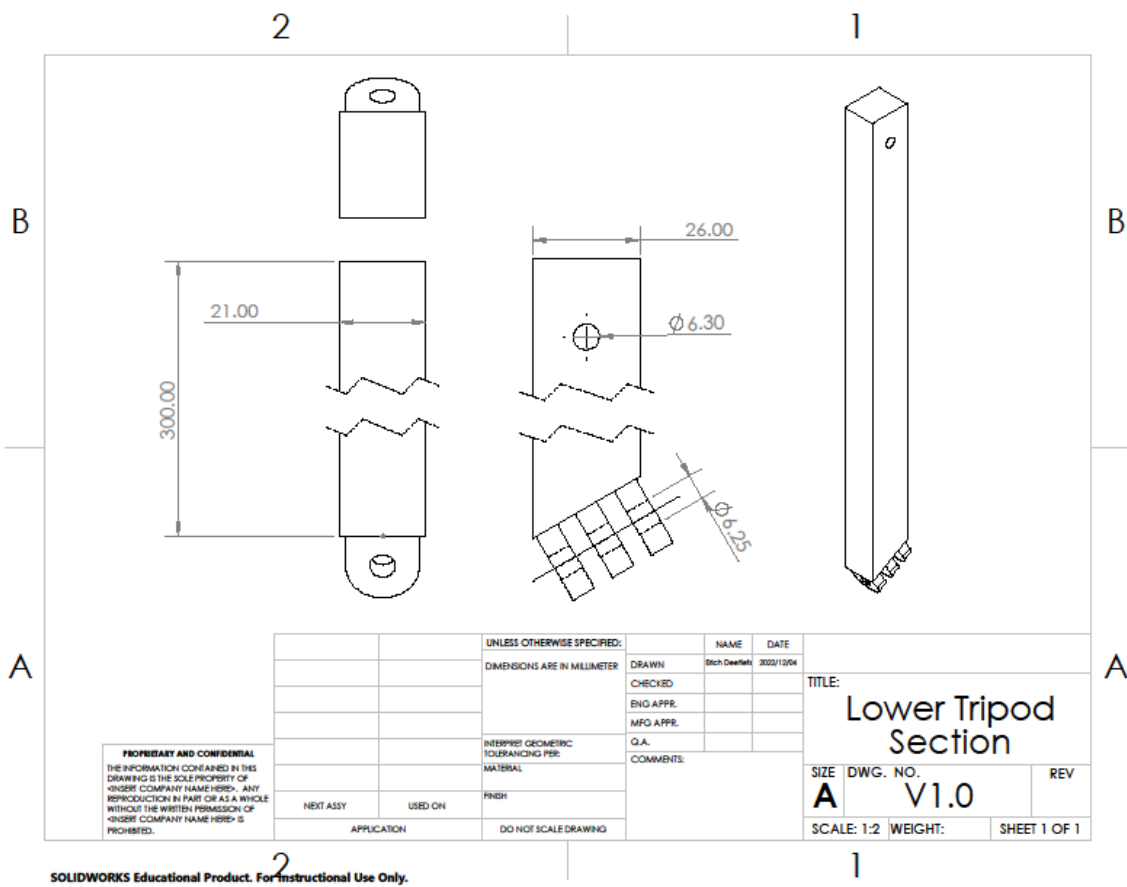


Figure 45: Lower tripod section

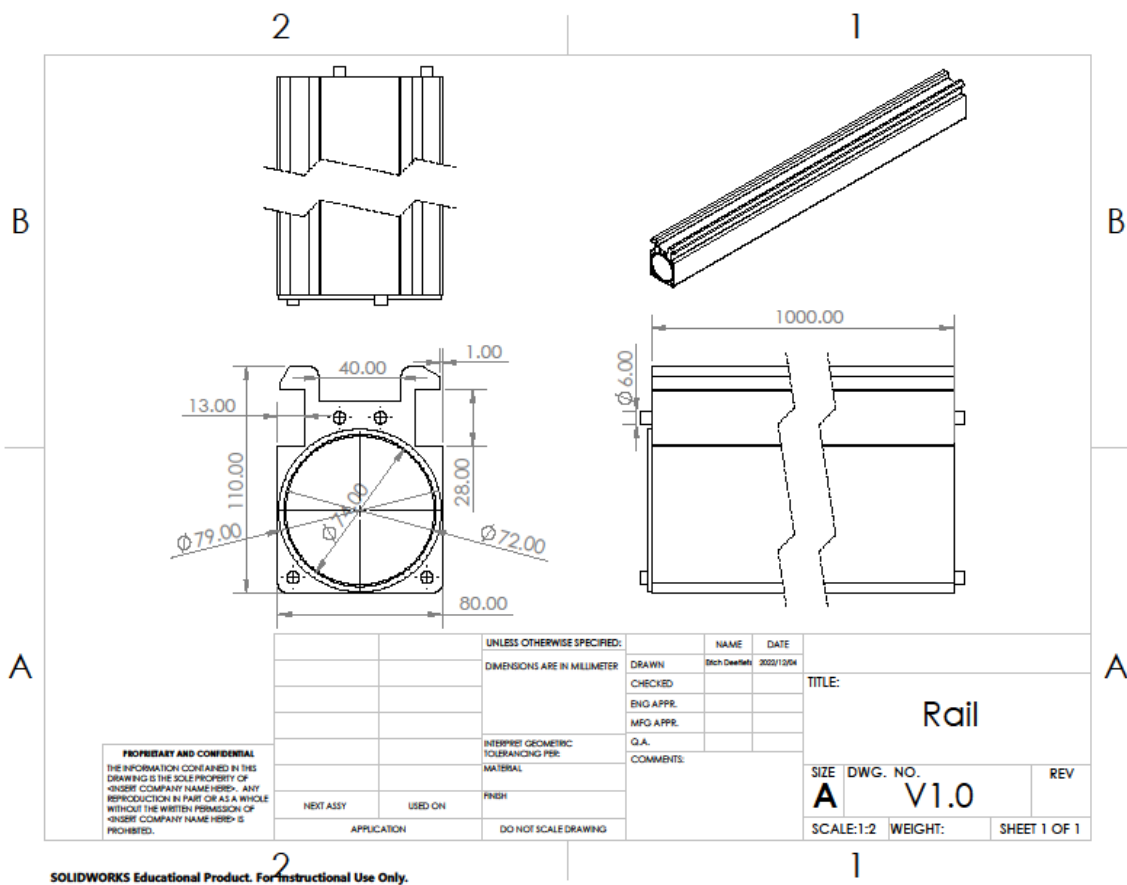


Figure 46: Rail

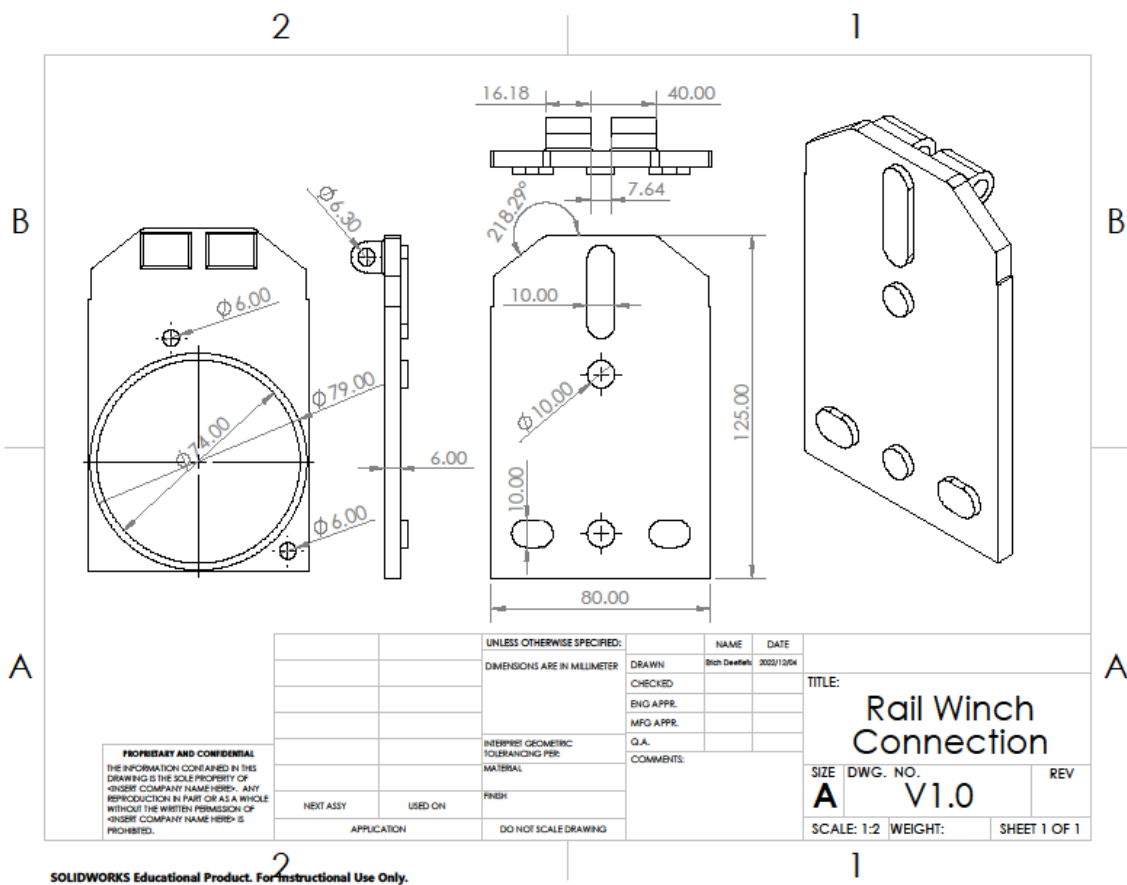


Figure 47: Rail winch connection

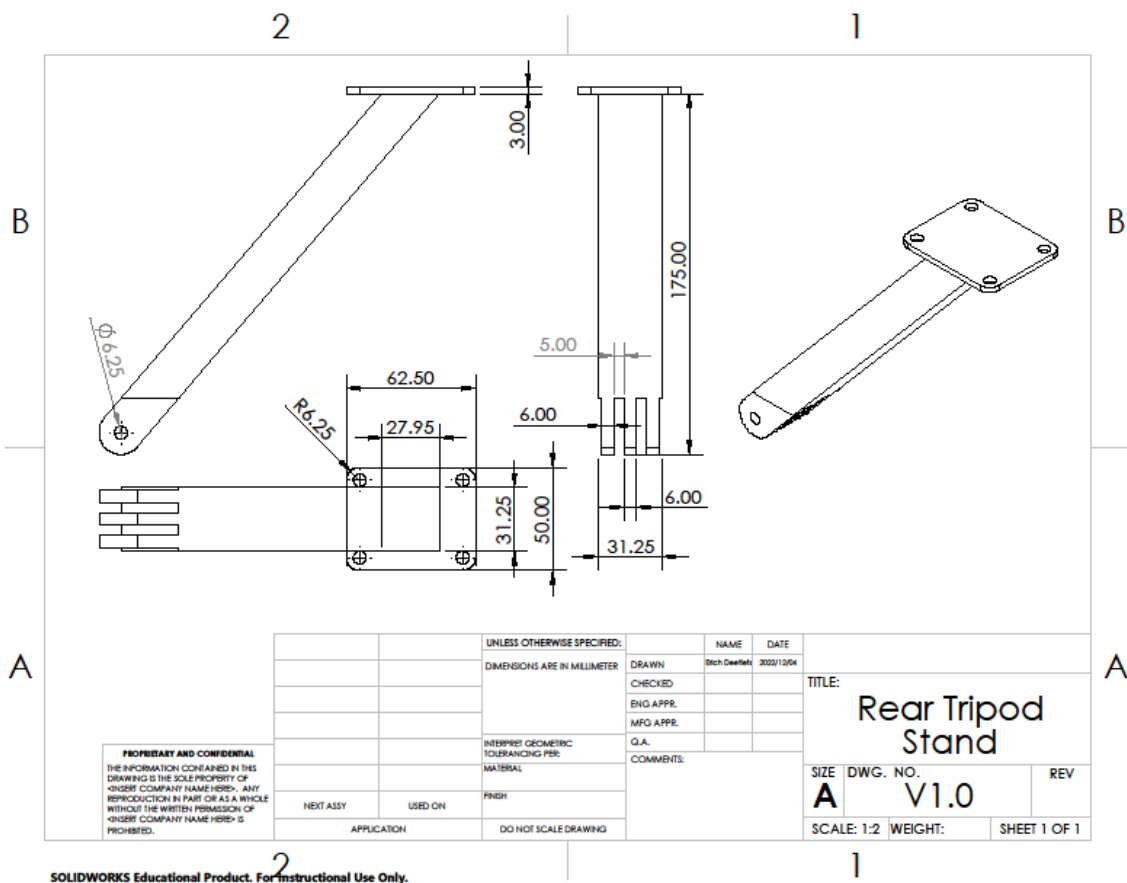


Figure 48: Rear tripod stand

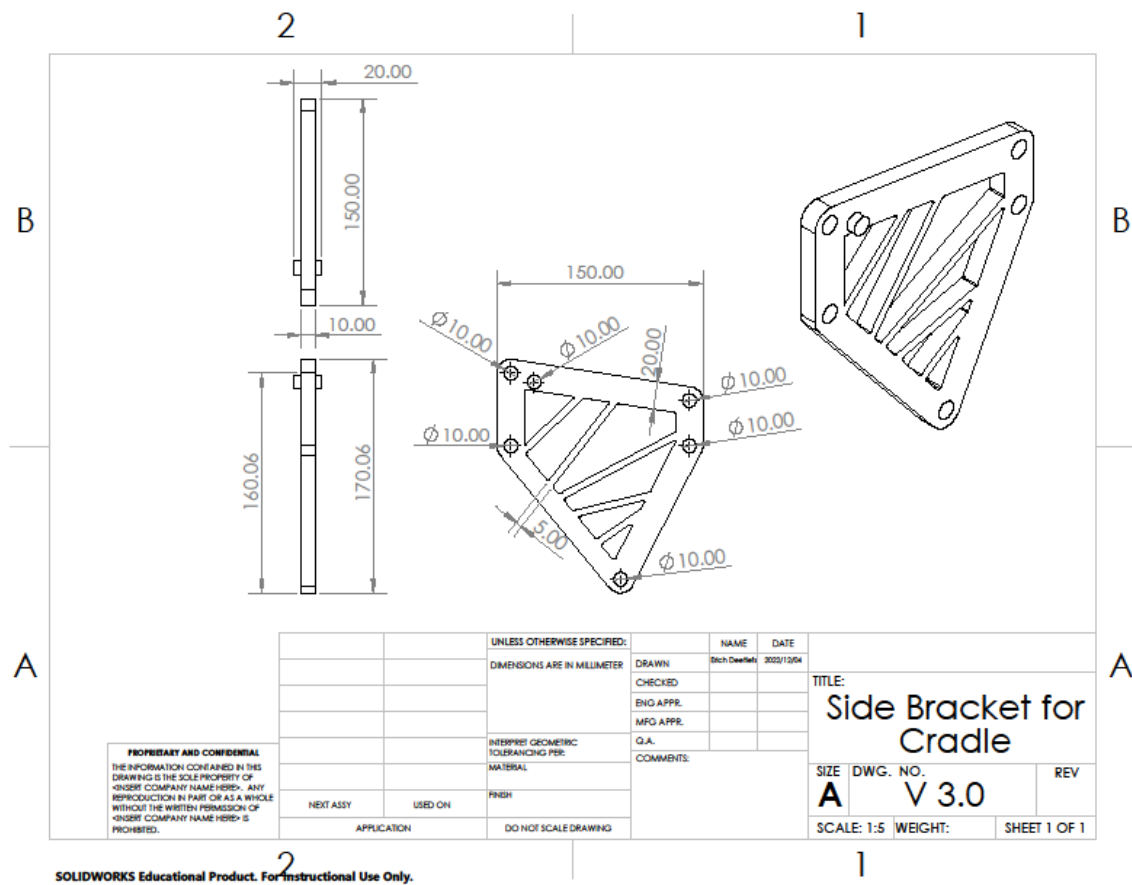


Figure 49: Side bracket for cradle

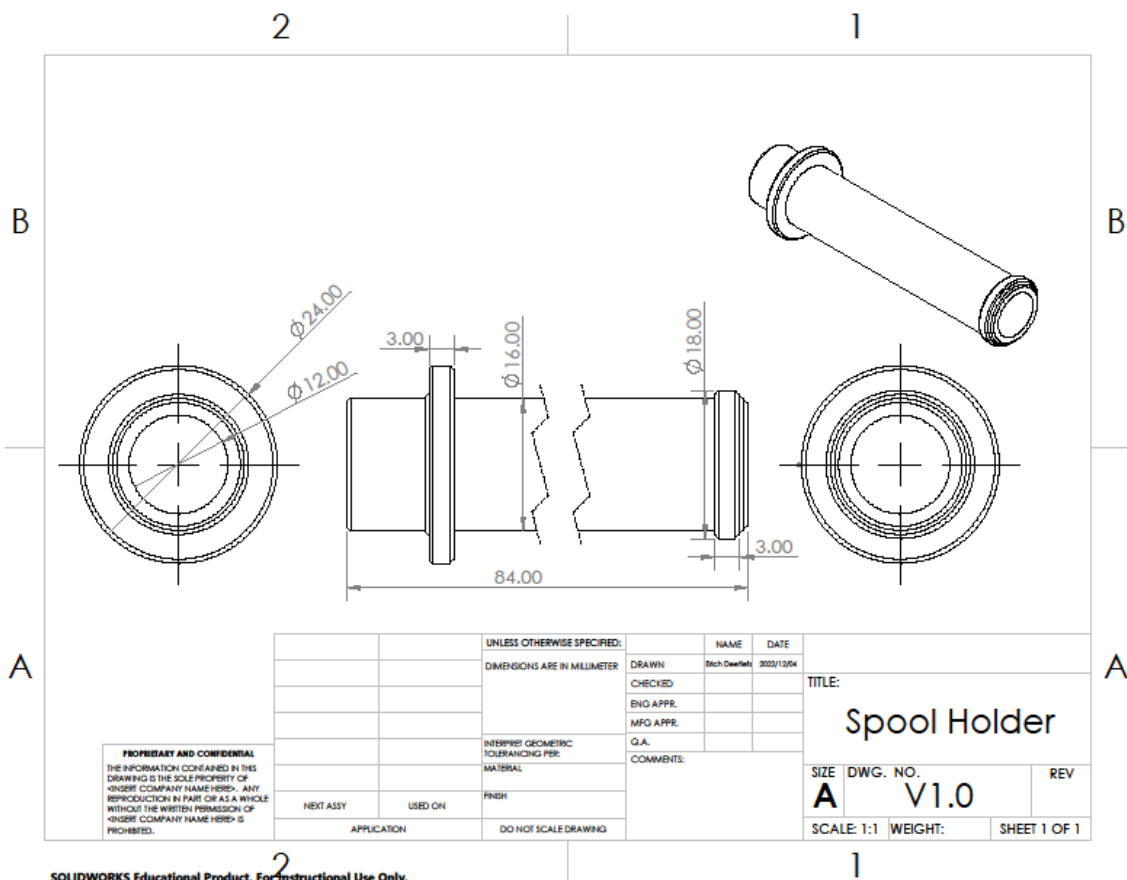


Figure 50: Spool holder

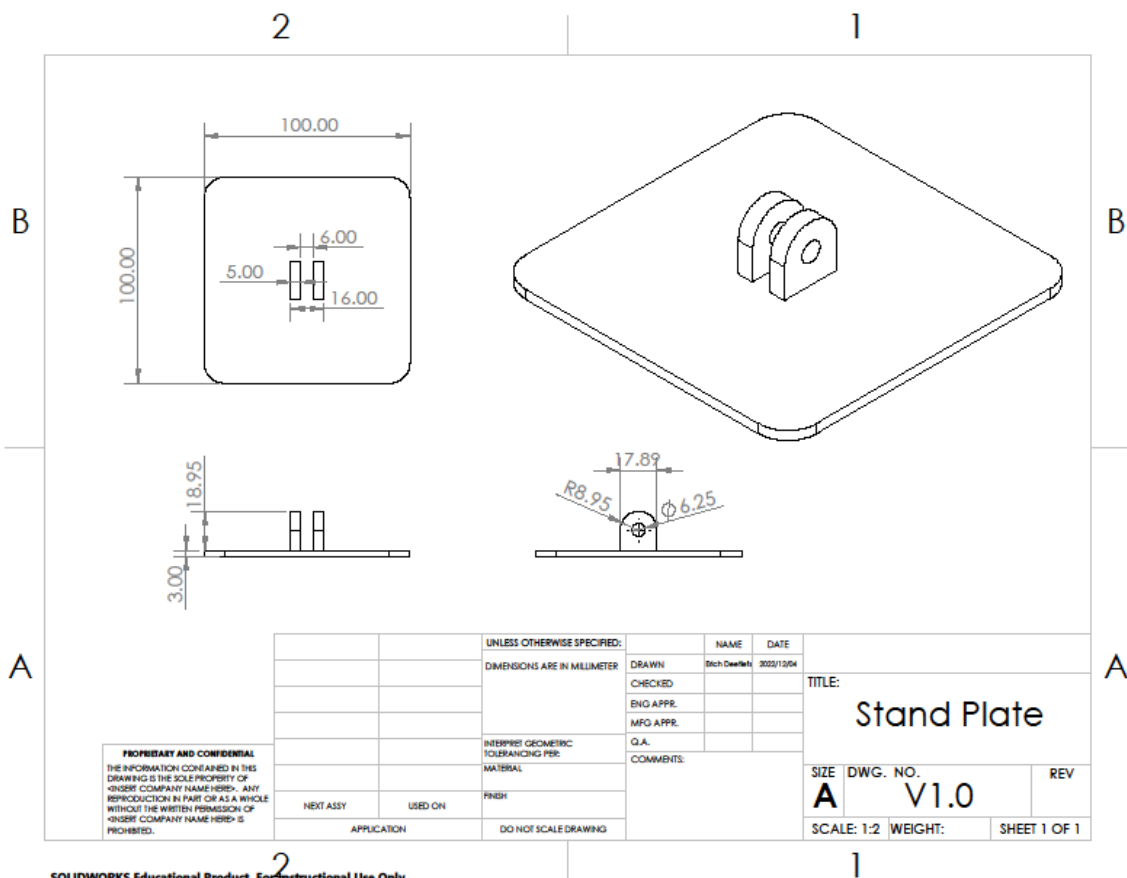


Figure 51: Stand plate

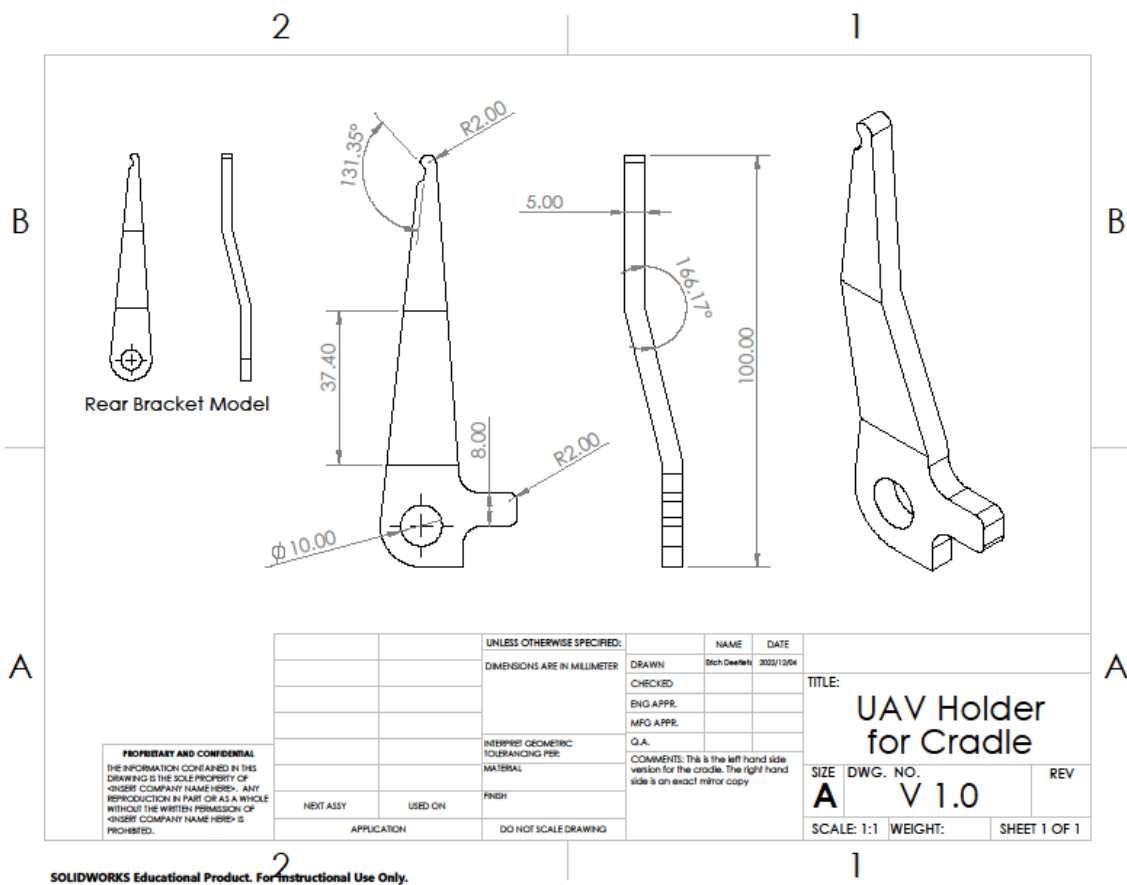


Figure 52: UAV holder for cradle

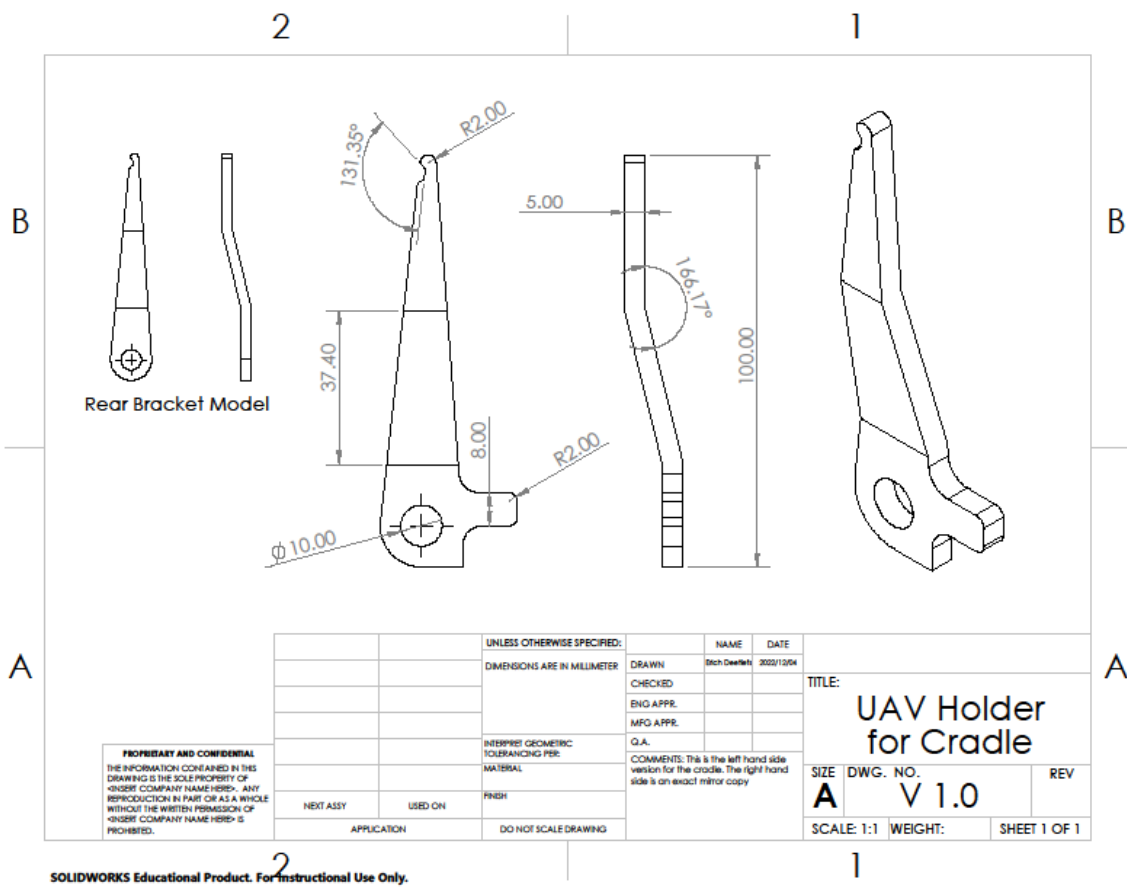


Figure 53: UAV holder for cradle

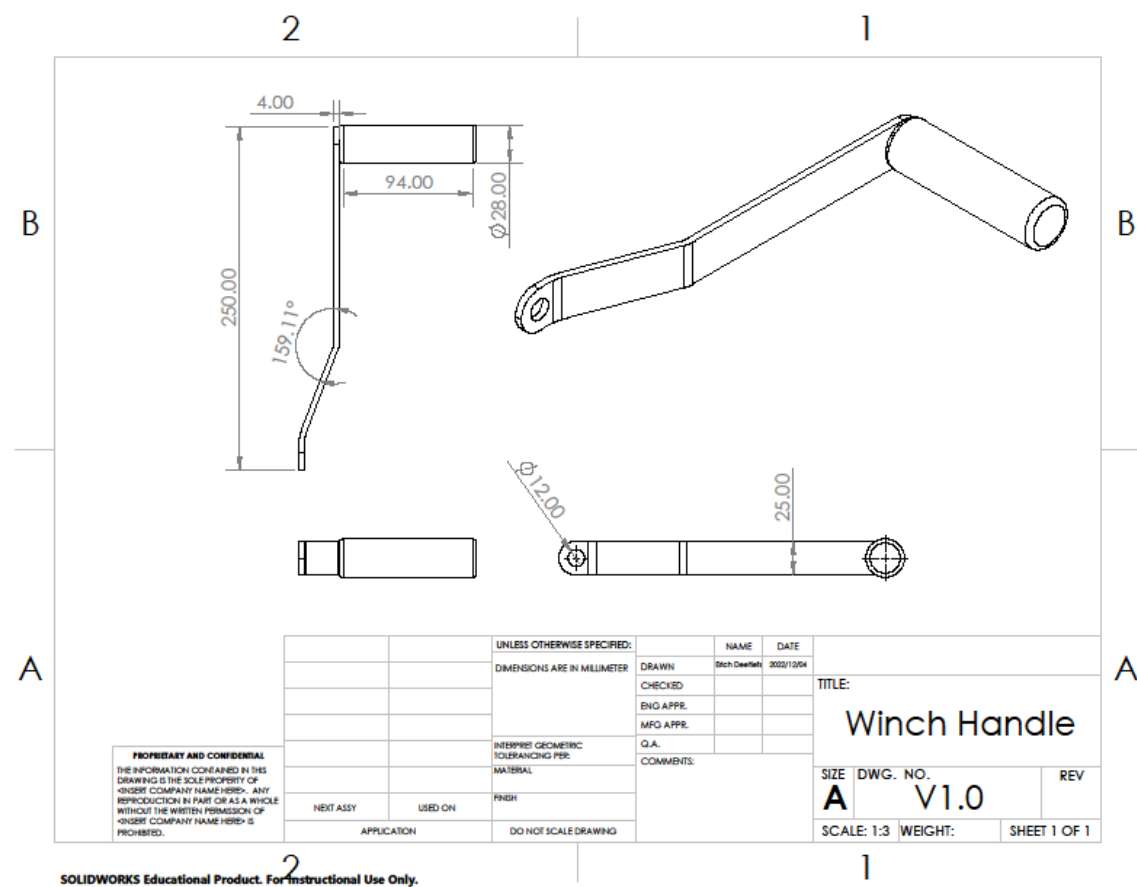


Figure 54: Winch handle

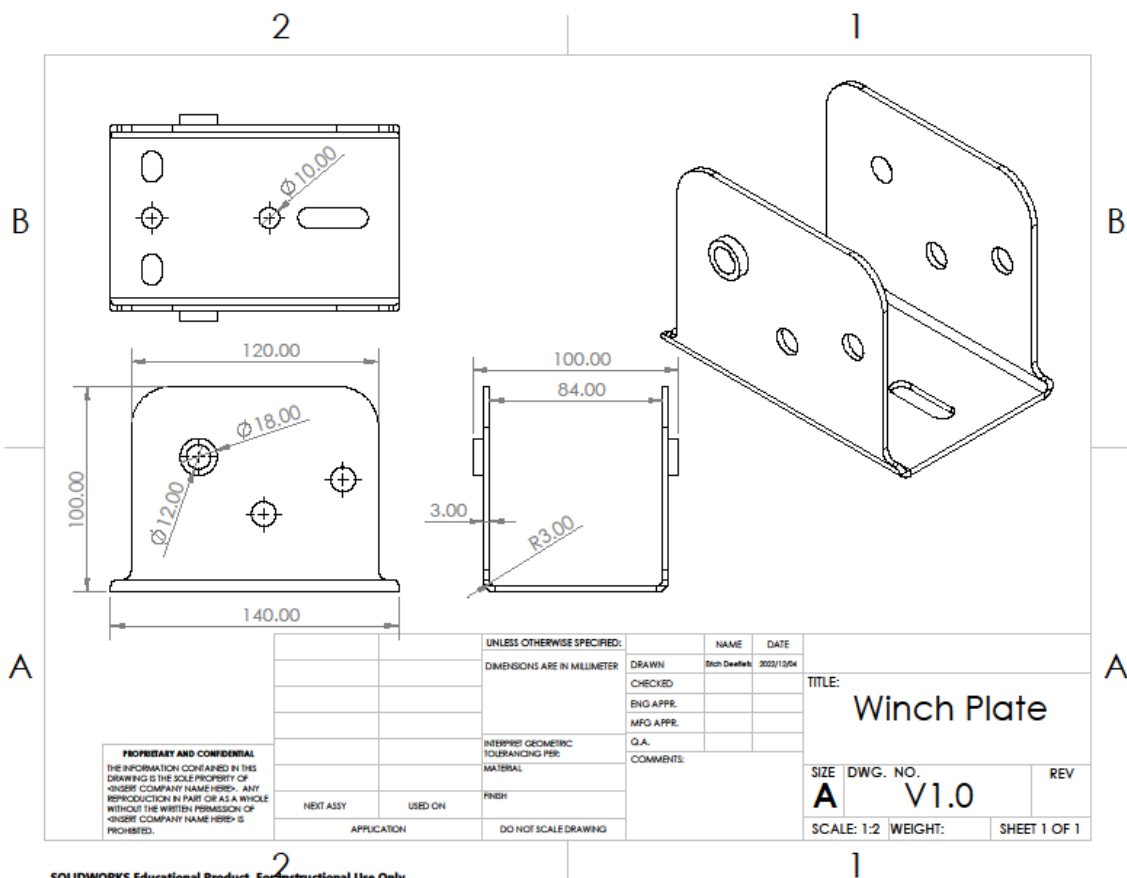


Figure 55: Winch plate

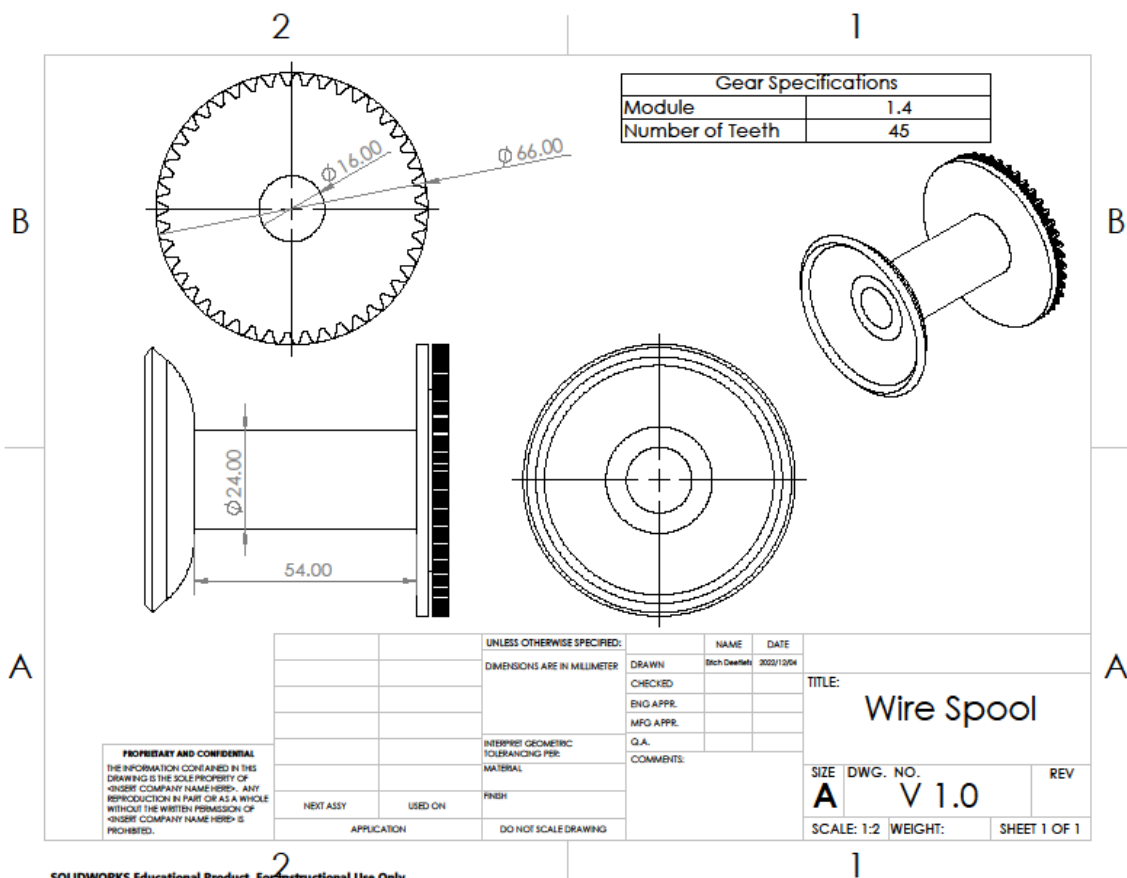


Figure 56: Wire spool

Appendix C: Nickel-chromium alloy - Data Sheet

General information

Designation i

Nickel-chromium alloy, INCONEL 718, solution treated & aged, wrought (Ni-Cr alloy)	
Condition	i Solution treated & aged
UNS number	i N07718
US name	i ASTM Grade N07718; AMS 5662, 5663, 5664, 5832, 5914, 5962, 5596, 5597, 5950
EN name	i NiCr19NbMo
EN number	i 2.4668
ISO name	i ISO 9723-9725

Tradenames i

ALTEMP 718 Solution treated, ATI Allegheny Ludlum (USA); Altemp; C50TF89, B50T68, B50TF16A, GE (USA); CPW407, Pratt & Whitney (USA); DMD423.32, SNECMA (FRANCE); EMS 55458, Garrett (USA); HAYNES 718, Haynes International Inc. (USA); Haynes; INCONEL 718, Special Metals Corp. (USA); Inconel; LA213, Turbomeca (FRANCE); MSRR 7132, MSRR 7228, Rolls Royce (UK); Nicrofer; PWA 649, Pratt & Whitney (USA); PYROMET ALLOY 718, Carpenter Technology Corp. (USA); Pyromet; SUPERMET 718, Firth Rixson (USA); Supermet; Udimar; Unitemp; WA2225.3, MTU (GERMANY)

Typical uses i

Aerospace, high temperature applications, heating elements, furnace parts, resistors, electronic parts, combustion systems, after-burners, fuel nozzles, chemical processing equipment, pulp and paper manufacture, marine architecture, nuclear reactors

Included in Materials Data for Simulation	i ✓
Materials Data for Simulation name	i Nickel alloy, Inconel 718, solution treated & aged

Composition overview

Compositional summary i

Ni50-55 / Cr17-21 / Fe11-25 / Mo2.8-3.3 / Nb2.4-2.8 / Ta2.4-2.8 / Ti0.65-1.2 / Al0.2-0.8 (impurities: Co<1, Mn<0.35, Si<0.35, Cu<0.3, C<0.08, P<0.015, S<0.015, B<0.006)
Nb + Ta = 4.75 to 5.5

Material family	i Metal (non-ferrous)
Base material	i Ni (Nickel)

Composition detail (metals, ceramics and glasses)

Al (aluminum)	i 0.2	-	0.8	%
B (boron)	i 0	-	0.006	%
C (carbon)	i 0	-	0.08	%
Co (cobalt)	i 0	-	1	%
Cr (chromium)	i 17	-	21	%
Cu (copper)	i 0	-	0.3	%
Fe (iron)	i 11.1	-	24.6	%
Mn (manganese)	i 0	-	0.35	%
Mo (molybdenum)	i 2.8	-	3.3	%
Nb (niobium)	i 2.38	-	2.75	%
Ni (nickel)	i 41.5	-	63.5	%
P (phosphorus)	i 0	-	0.015	%
S (sulfur)	i 0	-	0.015	%
Si (silicon)	i 0	-	0.35	%

Ta (tantalum)	(i)	2.38	-	2.75	%
Ti (titanium)	(i)	0.65	-	1.15	%

Price

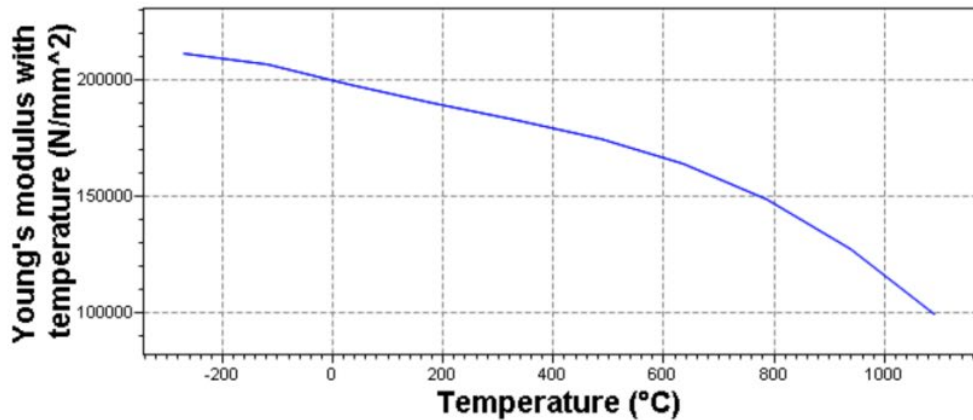
Price	(i)	* 2.01e4	-	2.48e4	CAD/tonne
Price per unit volume	(i)	* 1.64e-4	-	2.05e-4	CAD/mm ³

Physical properties

Density	(i)	8.18e-9	-	8.26e-9	tonne/mm ³
---------	-----	---------	---	---------	-----------------------

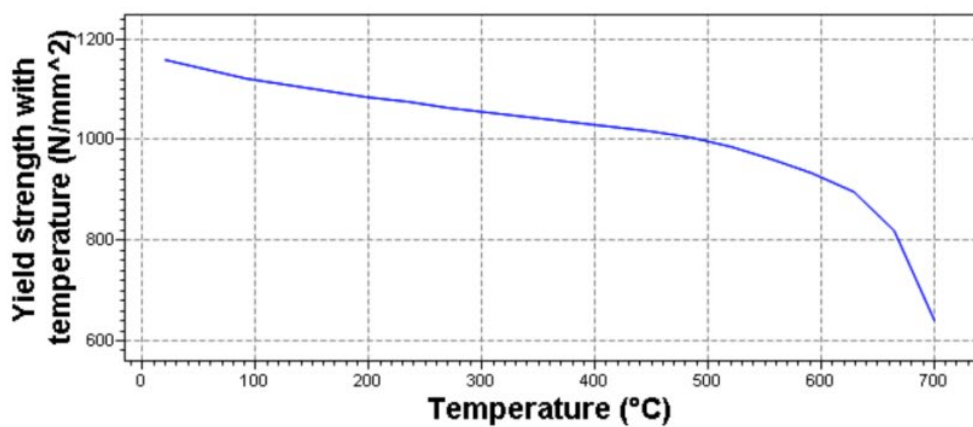
Mechanical properties

Young's modulus	(i)	1.98e5	-	2.08e5	N/mm ²
Young's modulus with temperature	(i)	1.98e5	-	1.98e5	N/mm ²

Parameters: Temperature = 23°C

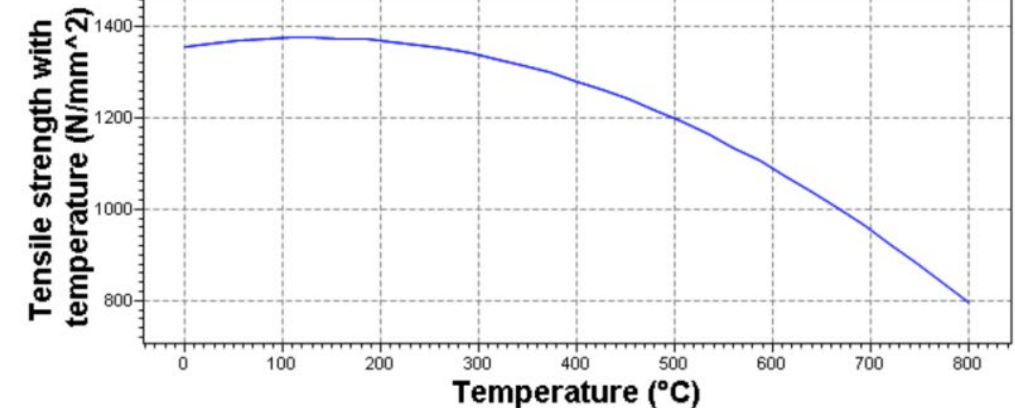
↗

Specific stiffness	(i)	2.41e13	-	2.53e13	N.mm/tonne
Yield strength (elastic limit)	(i)	1e3	-	1.11e3	N/mm ²
Yield strength with temperature	(i)	1.16e3	-	1.16e3	N/mm ²

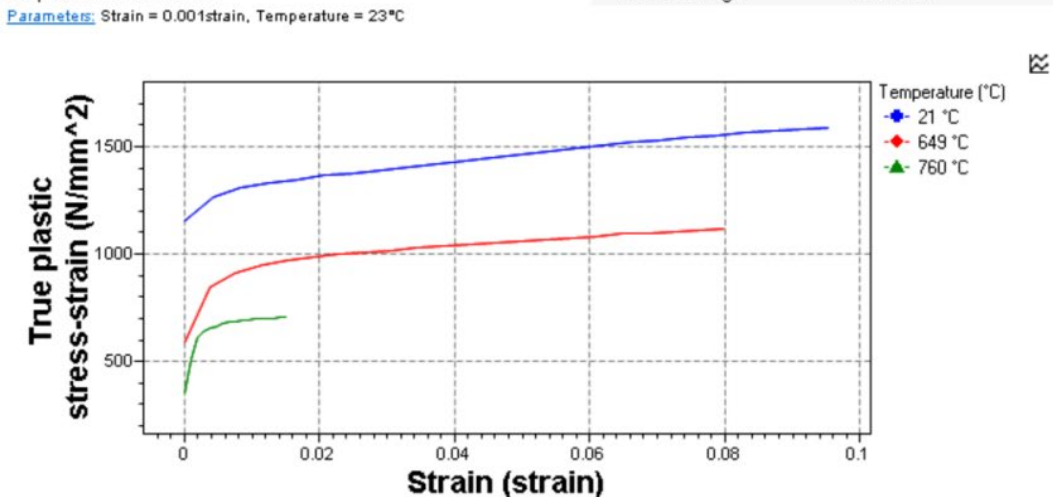
Parameters: Temperature = 23°C

↗

Tensile strength	(i)	1.17e3	-	1.32e3	N/mm ²
Tensile strength with temperature	(i)	1.36e3	-	1.36e3	N/mm ²



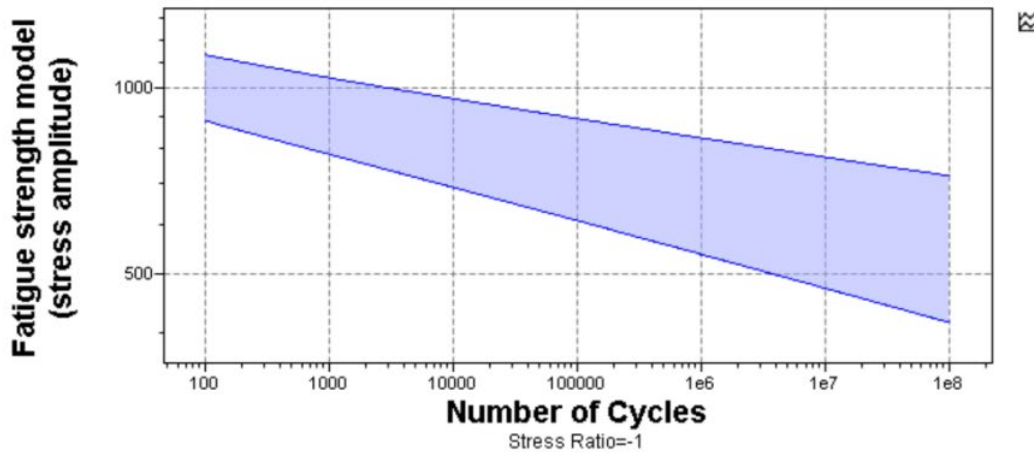
Specific strength	(i)	1.22e11	-	1.34e11	N.mm/tonne
Elongation	(i)	0.1	-	0.15	strain
Tangent modulus		2.64e3			N/mm ²
True plastic stress-strain		Out Of Range			N/mm ²



Compressive strength	(i)	* 931	-	1.15e3	N/mm ²
Flexural modulus	(i)	* 1.98e5	-	2.08e5	N/mm ²
Flexural strength (modulus of rupture)	(i)	1e3	-	1.11e3	N/mm ²
Shear modulus	(i)	7.7e4	-	8.09e4	N/mm ²
Bulk modulus	(i)	1.57e5	-	1.73e5	N/mm ²
Poisson's ratio	(i)	0.29	-	0.302	
Shape factor	(i)	16			
Hardness - Vickers	(i)	400	-	500	HV
Hardness - Rockwell B	(i)	* 112	-	117	HRB

Elastic stored energy (springs)	(i)	2.46	-	3.01	N.mm/mm ³
Fatigue strength at 10 ⁷ cycles	(i)	* 485	-	755	N/mm ²
Fatigue strength model (stress amplitude)	(i)	* 474	-	773	N/mm ²

Parameters: Stress Ratio = -1, Number of Cycles = 1e7cycles



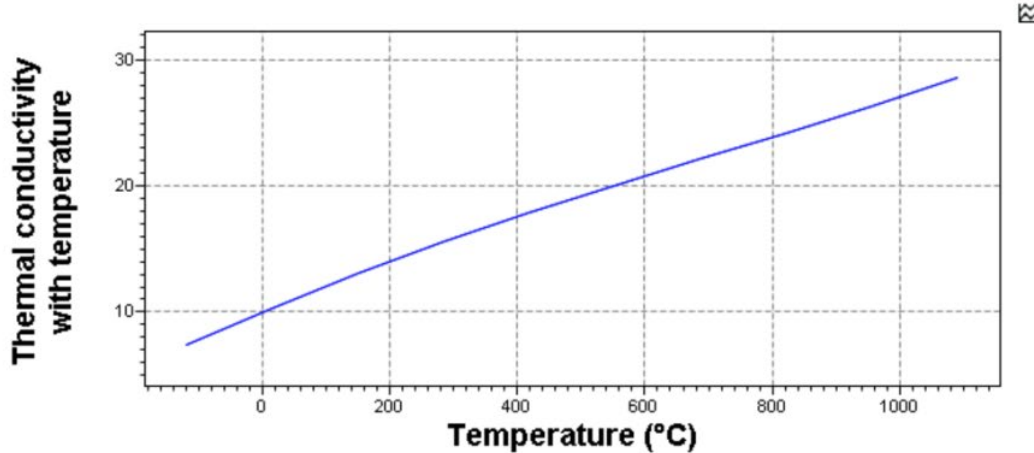
Impact & fracture properties

Fracture toughness	(i)	3.75e3	-	4.12e3	N/mm ^{1.5}
Toughness (G)	(i)	69.2	-	83.6	N.mm/mm ²

Thermal properties

Melting point	(i)	1.26e3	-	1.34e3	°C
Maximum service temperature	(i)	632	-	705	°C
Minimum service temperature	(i)	-273	-		°C
Thermal conductivity	(i)	11.1	-	12	N.mm/s/mm.°C
Thermal conductivity with temperature	(i)	10.5	-	10.5	N.mm/s/mm.°C

Parameters: Temperature = 23°C



Appendix D: Fluorosilicone - Data Sheet

General information

Designation (i)

Fluorosilicone (FVMQ, heat cured, 10-30% fumed silica), Fluorosilicone elastomer / Trifluoropropyl vinyl methyl silicone (FVMQ / SI / FSi), heat cured

Tradenames (i)

Baysilone; Elastosil-R; GE LIM; Rhodorsil HCR; Shincor; Shincor LIM; Silastic; Tufel

Typical uses (i)

Similar to regular silicone but where oil and fuel resistance is required, smart watches, fitness trackers, VR headsets, gaming consoles, electric toothbrushes, electric scooters, robotics, electric cars, hybrid cars

Composition overview

Compositional summary (i)

Polymer of dimethyl silicone, formula -(OSi(CH₃)₂)-, with some methyl groups substituted by gamma-trifluoropropyl groups, formula -(OSiCH₃C₂H₄CF₃)-, and some by vinyl groups as cure sites (crosslinking sites), formula -(OSiCH₃CH=CH₂)-. Typically compounded with 10-30% fumed silica (SiO₂) with 100-325 m²/g surface area. Contains organic peroxide or platinum (addition) heat cure system for LIM (liquid injection molding) or HTV (high temperature vulcanization).

Material family	(i)	Elastomer (thermoset, rubber)		
Base material	(i)	SI-FVMQ (Silicone rubber, fluorovinylmethyl type)		
% filler (by weight)	(i)	10	-	30 %
Filler/reinforcement	(i)	Mineral		
Filler/reinforcement form	(i)	Particulate		
Polymer code	(i)	SI-FVMQ-MD20		

Composition detail (polymers and natural materials)

Polymer	(i)	70	-	90 %
Silica (fumed)	(i)	10	-	30 %

Price

Price	(i)	* 8.5e4	-	9.81e4 CAD/tonne
Price per unit volume	(i)	* 1.19e-4	-	1.47e-4 CAD/mm ³

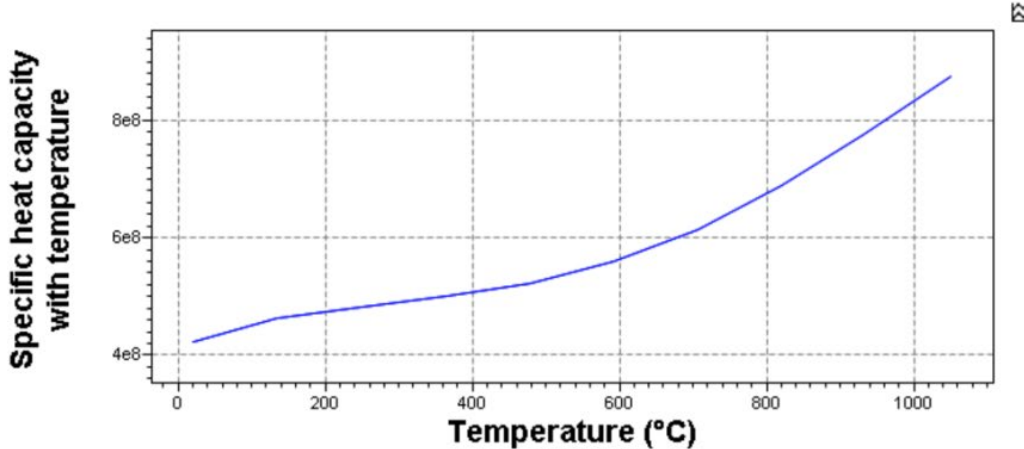
Physical properties

Density	(i)	1.4e-9	-	1.5e-9 tonne/mm ³
---------	--	--------	---	------------------------------

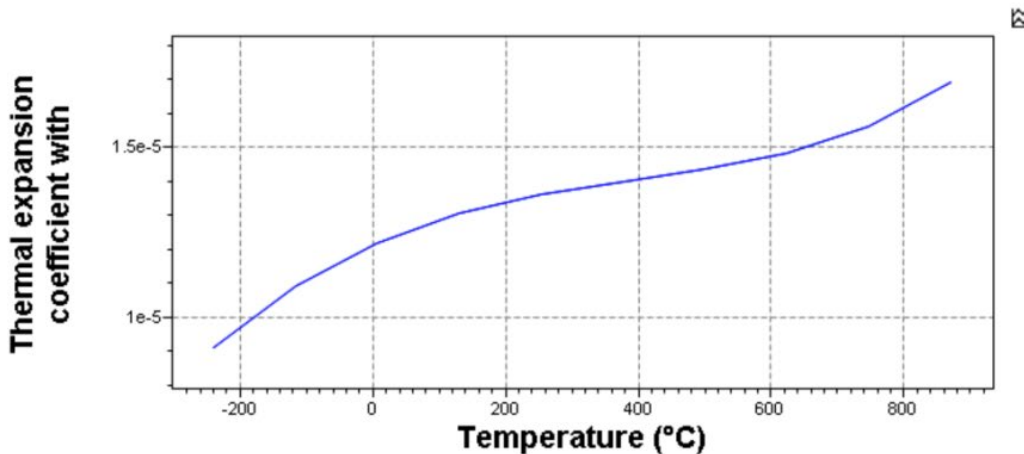
Mechanical properties

Young's modulus	(i)	5	-	50 N/mm ²
Specific stiffness	(i)	3.45e9	-	3.45e10 N.mm/tonne
Yield strength (elastic limit)	(i)	8.2	-	12.1 N/mm ²
Tensile strength	(i)	8.2	-	12.1 N/mm ²
Tensile stress at 100% strain	(i)	1.2	-	3.6 N/mm ²
Specific strength	(i)	5.65e9	-	8.37e9 N.mm/tonne
Elongation	(i)	2.7	-	6.75 strain
Elongation at yield	(i)	2.7	-	6.75 strain
Compressive modulus	(i)	* 5	-	50 N/mm ²
Compressive strength	(i)	* 9.84	-	14.5 N/mm ²

Specific heat capacity	(i)	4.4e8	-	4.58e8	N.mm/tonne.°C
Specific heat capacity with temperature <small>Parameters: Temperature = 23°C</small>	(i)	4.23e8	-	4.23e8	N.mm/tonne.°C



Thermal expansion coefficient	(i)	1.28e-5	-	1.34e-5	strain/°C
Thermal expansion coefficient with temperature <small>Parameters: Temperature = 23°C</small>	(i)	1.23e-5	-	1.23e-5	strain/°C



Reference temp	20	°C			
Thermal shock resistance	(i)	372	-	420	°C
Thermal distortion resistance	(i)	8.38e5	-	9.19e5	N.mm/s.mm
Latent heat of fusion	(i)	* 2.75e11	-	3e11	N.mm/tonne

Electrical properties

Electrical resistivity	(i)	0.00115	-	0.00125	ohm.mm
Electrical conductivity	(i)	800	-	870	Siemens/mm
Galvanic potential	(i)	* -0.05	-	0.03	V

Compression set at 23°C	(i)	5	-	10	%
Compression set at 70°C	(i)	5	-	10	%
Compression set at 100°C	(i)	5	-	10	%
Tear strength	(i)	17.5	-	46.4	N/mm

Impact & fracture properties

Fracture toughness	(i)	5.28	-	33.3	N/mm^1.5
Toughness (G)	(i)	2.36	-	52.4	N.mm/mm^2
Impact strength, notched 23 °C	(i)	590	-	600	N.mm/mm^2
Impact strength, notched -30 °C	(i)	590	-	600	N.mm/mm^2
Impact strength, unnotched 23 °C	(i)	590	-	600	N.mm/mm^2
Impact strength, unnotched -30 °C	(i)	590	-	600	N.mm/mm^2

Thermal properties

Glass temperature	(i)	-70	-	-60	°C
Maximum service temperature	(i)	200	-	250	°C
Minimum service temperature	(i)	-57	-	-47	°C
Thermal conductivity	(i)	0.2	-	0.3	N.mm/s/mm.°C
Specific heat capacity	(i)	1.05e9	-	1.1e9	N.mm/tonne.°C
Thermal expansion coefficient	(i)	* 2.5e-4	-	3e-4	strain/°C
Thermal shock resistance	(i)	* 725	-	7.3e3	°C
Thermal distortion resistance	(i)	* 719	-	1.11e3	N.mm/s.mm

Electrical properties

Electrical resistivity	(i)	3e14	-	5e15	ohm.mm
Electrical conductivity	(i)	2e-16	-	3.34e-15	Siemens/mm
Dielectric constant (relative permittivity)	(i)	2.3	-	3.1	
Dissipation factor (dielectric loss tangent)	(i)	0.003	-	0.024	
Dielectric strength (dielectric breakdown)	(i)	1.6e4	-	2e4	V/mm
Comparative tracking index	(i)	400	-	600	V

Magnetic properties

Magnetic type	(i)	Non-magnetic
---------------	-----	--------------

Optical, aesthetic and acoustic properties

Refractive index	(i)	1.4	-	1.44	
Transparency	(i)	Translucent			
Acoustic velocity	(i)	5.02e4	-	2.17e5	mm/s
Mechanical loss coefficient (tan delta)	(i)	* 0.2	-	0.4	

Critical materials risk

Contains >5wt% critical elements?	(i)	No
-----------------------------------	-----	----

Absorption & permeability

Water absorption @ 24 hrs	(i)	0.1	-	0.15	%
Water vapor transmission	(i)	* 1.78e-17	-	4.06e-17	tonne.mm/mm^2.s
Permeability (O ₂)	(i)	* 0.00126	-	0.00286	mm^2/s.N/mm^2

Processing properties

Polymer injection molding	(i)	Acceptable			
Polymer extrusion	(i)	Acceptable			
Polymer thermoforming	(i)	Unsuitable			
Linear mold shrinkage	(i)	2.4	-	4	%
Mold temperature	(i)	180	-	200	°C

Durability

Water (fresh)	(i)	Excellent			
Water (salt)	(i)	Excellent			
Weak acids	(i)	Excellent			
Strong acids	(i)	Excellent			
Weak alkalis	(i)	Excellent			
Strong alkalis	(i)	Excellent			
Organic solvents	(i)	Acceptable			
Oils and fuels	(i)	Excellent			
Oxidation at 500C	(i)	Unacceptable			
UV radiation (sunlight)	(i)	Good			
Flammability	(i)	Self-extinguishing			
Oxygen index	(i)	27	-	35	%

Primary production energy, CO₂ and water

Embodied energy, primary production (virgin grade)	(i)	* 1.18e14	-	1.3e14	N.mm/tonne
Embodied energy, primary production (typical grade)	(i)	* 1.18e14	-	1.3e14	N.mm/tonne
CO ₂ footprint, primary production (virgin grade)	(i)	* 6.2	-	6.84	tonne/tonne
CO ₂ footprint, primary production (typical grade)	(i)	* 6.2	-	6.84	tonne/tonne
Water usage	(i)	1.9e11	-	5.71e11	mm^3/tonne

Processing energy, CO₂ footprint & water

Polymer molding energy	(i)	* 1.41e13	-	1.55e13	N.mm/tonne
Polymer molding CO ₂	(i)	* 1.13	-	1.24	tonne/tonne
Polymer molding water	(i)	* 1.07e10	-	1.6e10	mm^3/tonne
Grinding energy (per unit wt removed)	(i)	* 2.04e12	-	2.26e12	N.mm/tonne
Grinding CO ₂ (per unit wt removed)	(i)	* 0.153	-	0.169	tonne/tonne

Recycling and end of life

Recycle	(i)	✗			
Downcycle	(i)	✓			
Combust for energy recovery	(i)	✓			
Heat of combustion (net)	(i)	* 1.06e13	-	1.11e13	N.mm/tonne
Combustion CO ₂	(i)	* 0.939	-	0.987	tonne/tonne

Appendix E: Bill of Materials

Item Number	Item	Supplier	Supplier Part Number	Material Description	Price	Quantity	Cost
001	Ball Bearing	MiMOTION	7408907	10 mm ID, 26 mm OD, 8 mm Width, Double Sealed, C3 Internal Clearance	\$ 28.54	6	\$ 171.24
002	Assorted O-Rings	KEWAYO	KEWAYO01	225 pieces included	\$ 16.47	1	\$ 16.47
003	C-Ring	Huyett	7318240000	ANSI B27.7-3CM1 (min order 7)	\$ 0.32	7	\$ 2.25
004	Draw Latch	D.B. Roberts Inc	R5-0074-07, R5-0079-07	Steel, zinc plated	\$ 39.97	4	\$ 159.88
005	Quick Release Pin	VTurboWay	B07RJBGHNP	316 Stainless Steel: 3"x1/4" (Full Length 3.75")	\$ 13.99	2	\$ 27.98
006	Bungee	Primeline Industries	Custom	2m x 1": 296.3 N/m	Quote	6	Quote
007	Heavy Hex Bolt	ASMC Industrial	0000-124212	M12 x 1.75 x 110 (30N) (min order 10)	\$ 3.46	10	\$ 34.64
008	Heavy Hex Nut	ASMC Industrial	0000-251292	M12 x 1.75 (min order 50)	\$ 1.47	50	\$ 73.60
009	Damper Material	Polycomp UK	Mil-DTL-25988C	CAD/kg	\$ 9.81	0.7	\$ 6.87
010	Structural Metal	ALTEMP USA	UNS N07718 nickel alloy inconel 718	CAD/kg	\$ 20.01	93	\$ 1,860.93
Total:							\$ 2,353.85